

Göttingen, HASCO2012

July 20th, 2012

QCD and jets: experiment

Juan Terrón (Universidad Autónoma de Madrid, Spain)



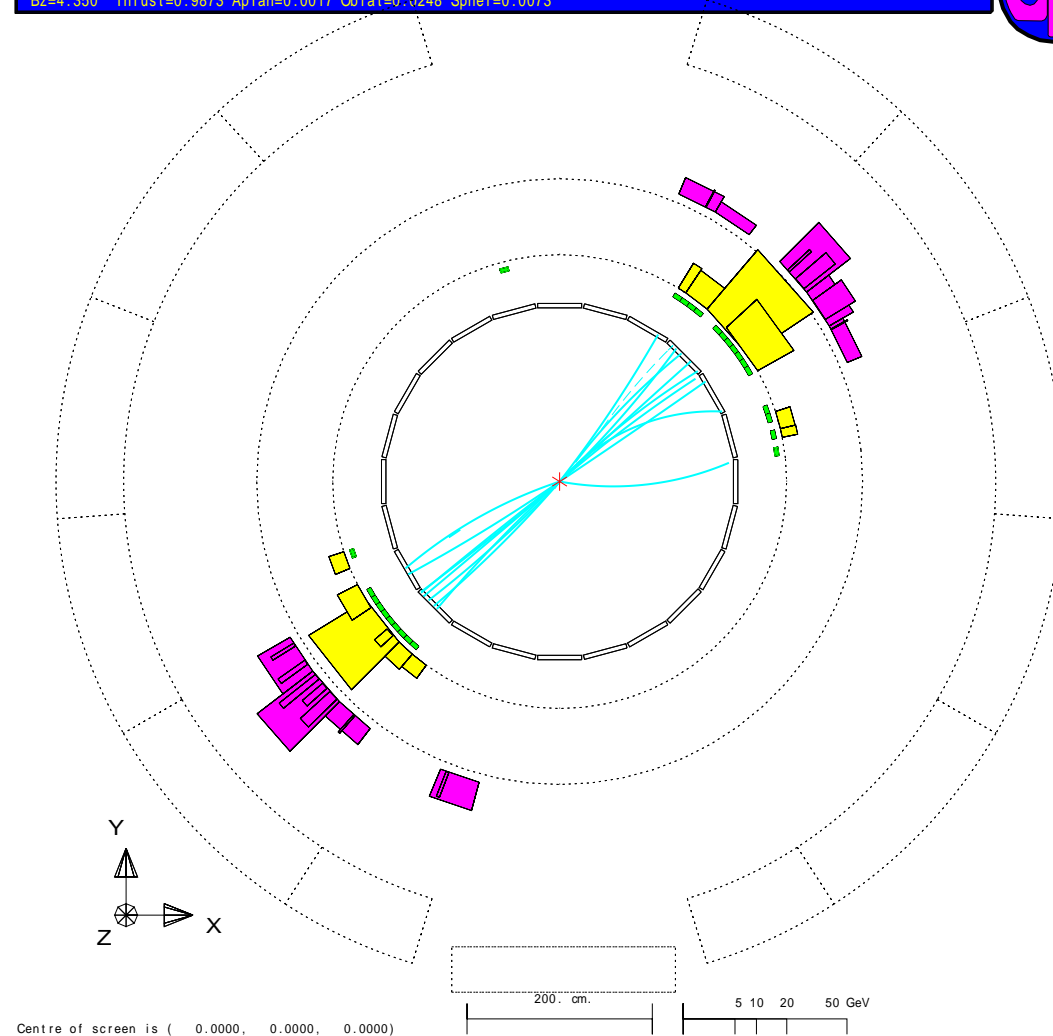
● Outline

- Jets and Jet Algorithms**
- Jets in e^+e^- collisions**
- Structure Functions**
- Jets in Neutral Current DIS**
- Jet Substructure in NC DIS**
- Jets in Photoproduction**

Jets

What is a jet?

```
Run:event 4093: 1000 Date 930527 Time 20716 Ctrk(N= 39 Sump= 73.3) Ecal(N= 25 SumE= 32.6) Hcal(N=22 SumE= 22.6)
Ebeam 45.658 Evis 99.9 Emiss -8.6 Vtx ( -0.07, 0.06, -0.80) Muon(N= 0) Sec Vtx(N= 3) Fdet(N= 0 SumE= 0.0)
Bz=4.350 Thrust=0.9873 Aplan=0.0017 Oblat=0.0248 Spher=0.0073
```

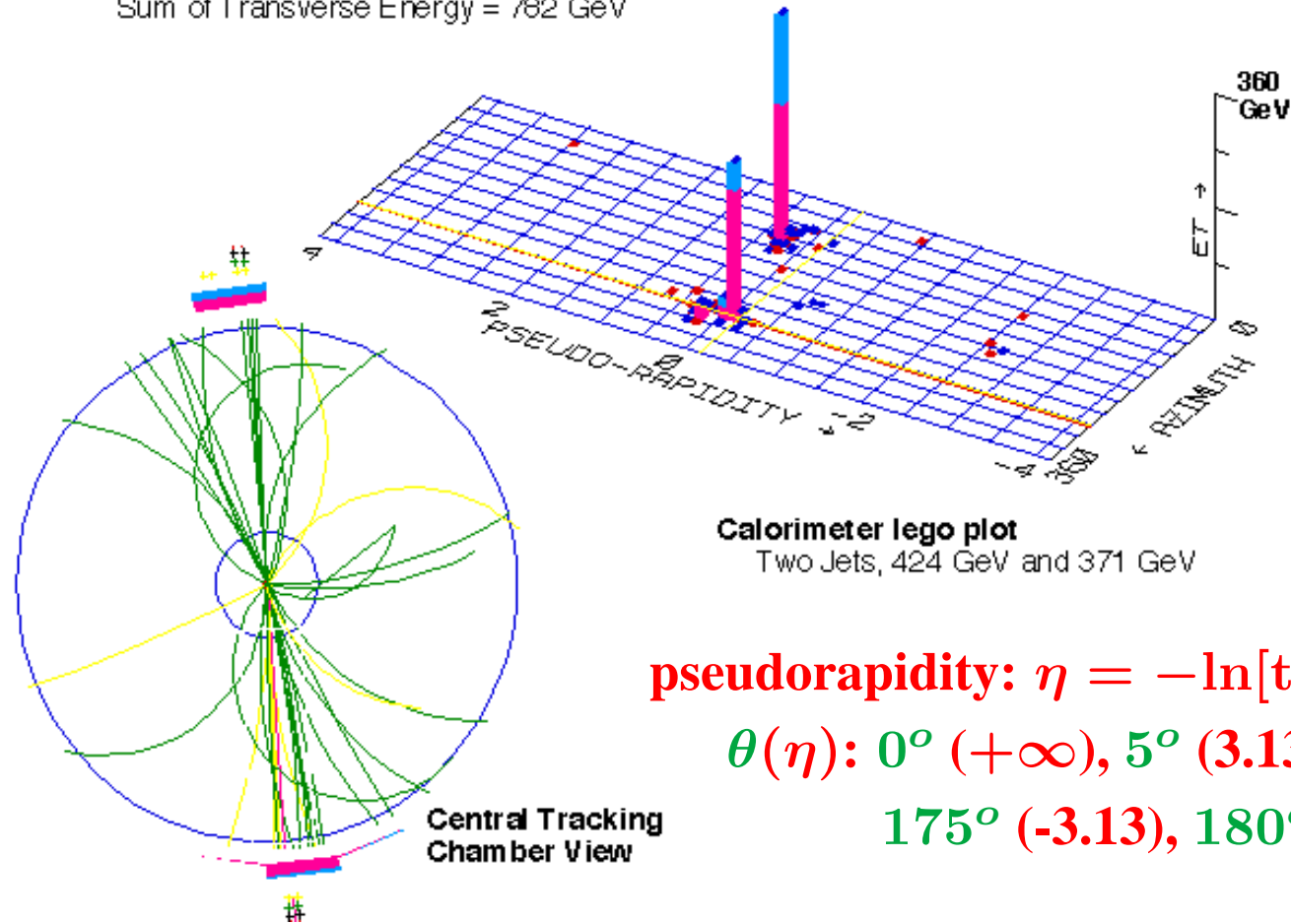


$$e^+e^- \rightarrow \text{jet} + \text{jet} \quad (e^+e^- \text{ annihilation})$$

What is a jet (II)?

CDF: Highest Transverse Energy Event from the 1988-89 Collider Run

Sum of Transverse Energy = 782 GeV



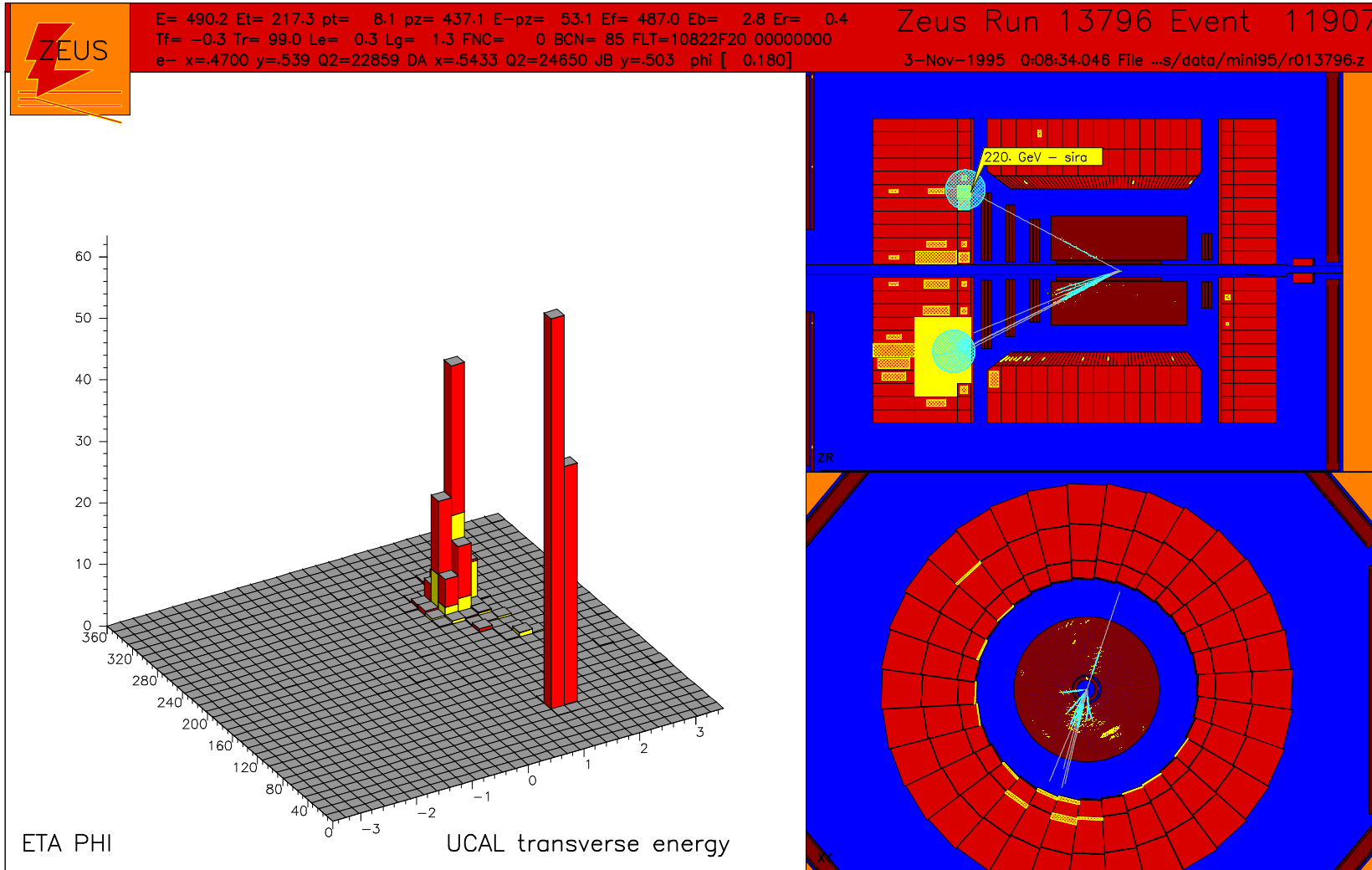
pseudorapidity: $\eta = -\ln[\tan(\theta/2)]$

$\theta(\eta)$: $0^\circ (+\infty)$, $5^\circ (3.13)$, $90^\circ (0)$

$175^\circ (-3.13)$, $180^\circ (-\infty)$

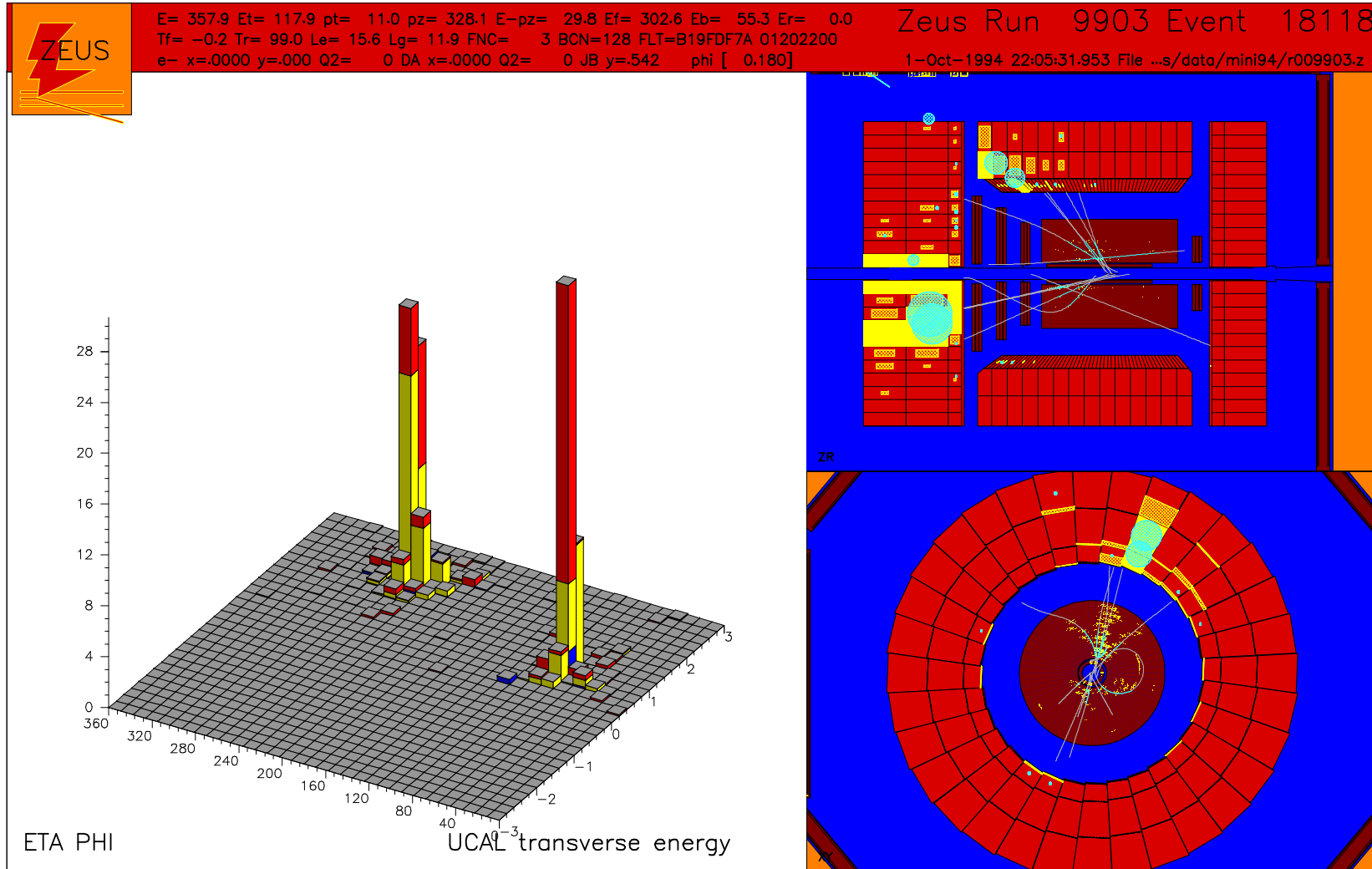
$p\bar{p} \rightarrow \text{jet} + \text{jet} + \text{Anything}$ ($p\bar{p}$ collision)

What is a jet (III)?



$$ep \rightarrow e + \text{jet} + \text{Anything} \quad (\text{NC DIS})$$

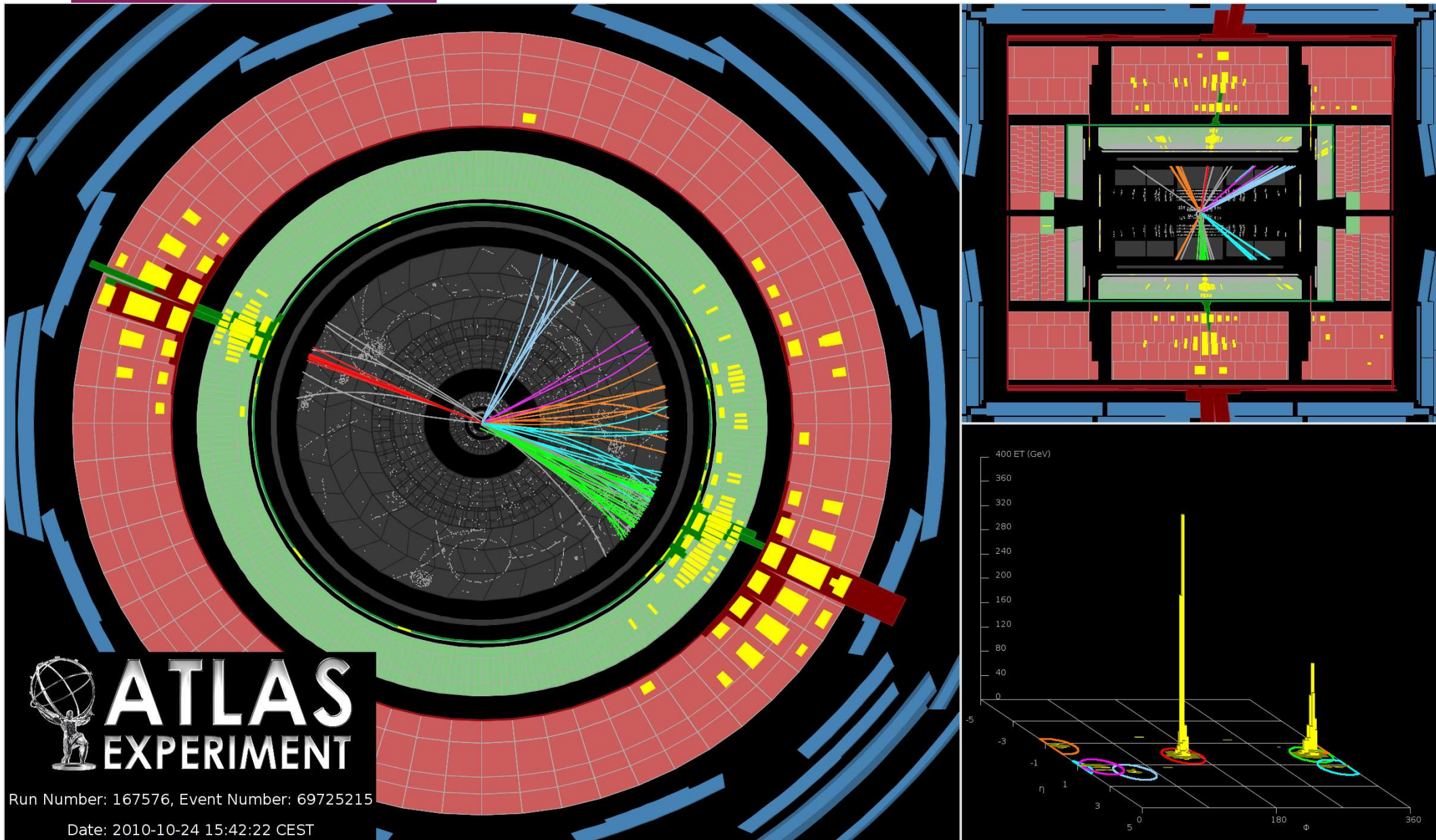
What is a jet (IV)?



$ep \rightarrow \text{jet} + \text{jet} + \text{Anything}$ (photoproduction)

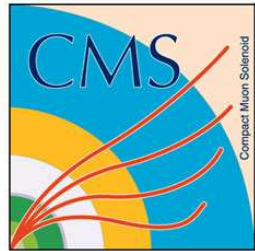
What is a jet (V)?

$pp \rightarrow \text{jet} + \text{jet} + \text{Anything}$

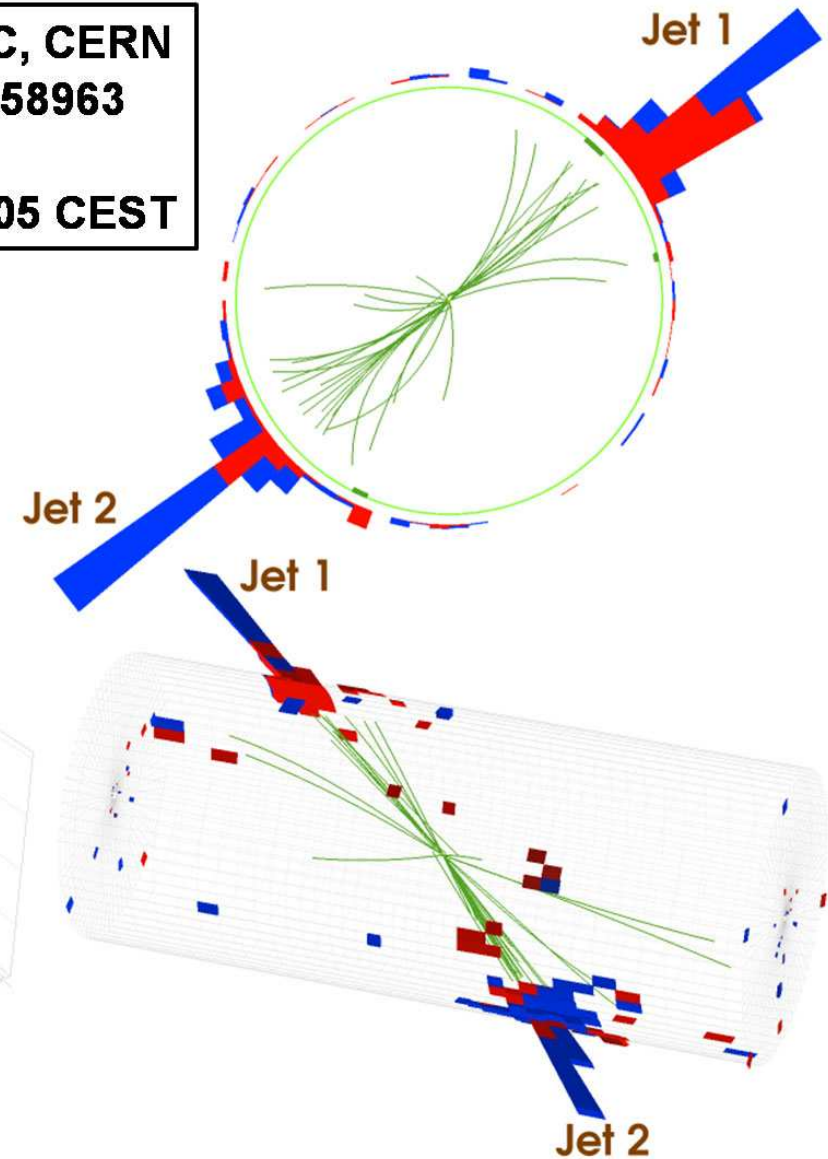
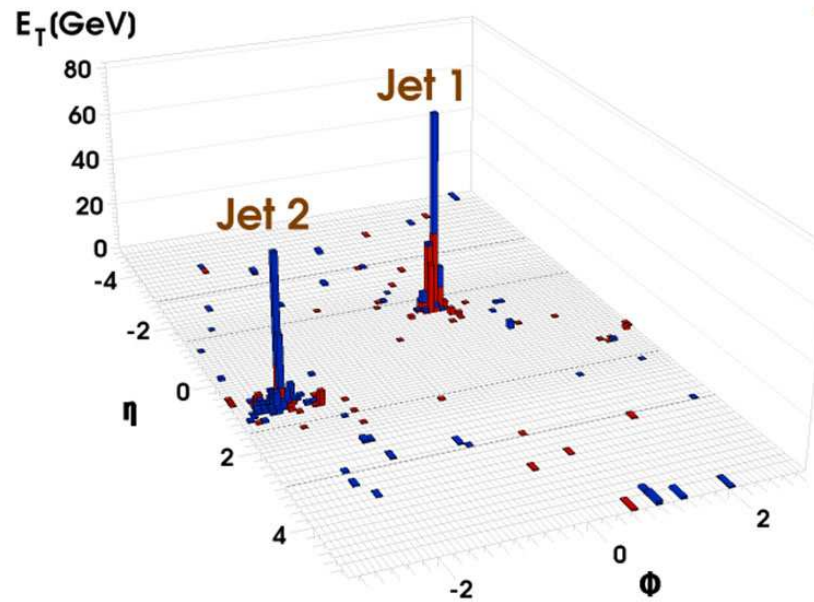


What is a jet (VI)?

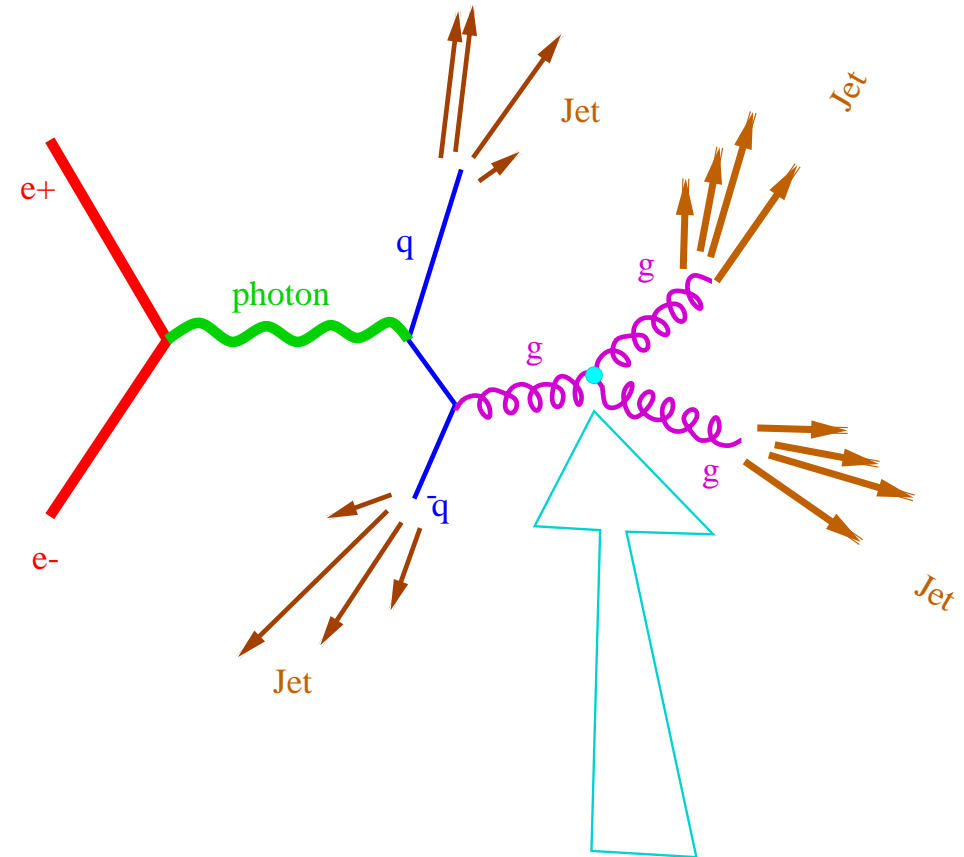
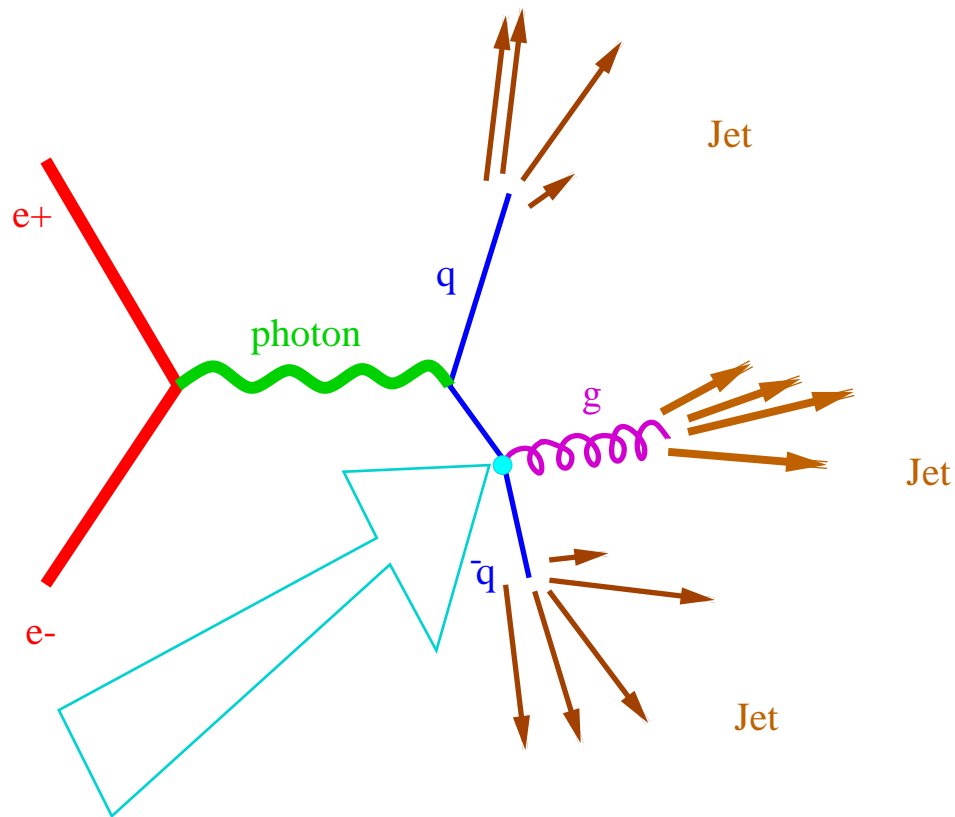
$$pp \rightarrow \text{jet} + \text{jet} + \text{Anything}$$



CMS Experiment at LHC, CERN
Run 133450 Event 16358963
Lumi section: 285
Sat Apr 17 2010, 12:25:05 CEST



Some good reasons to study jets

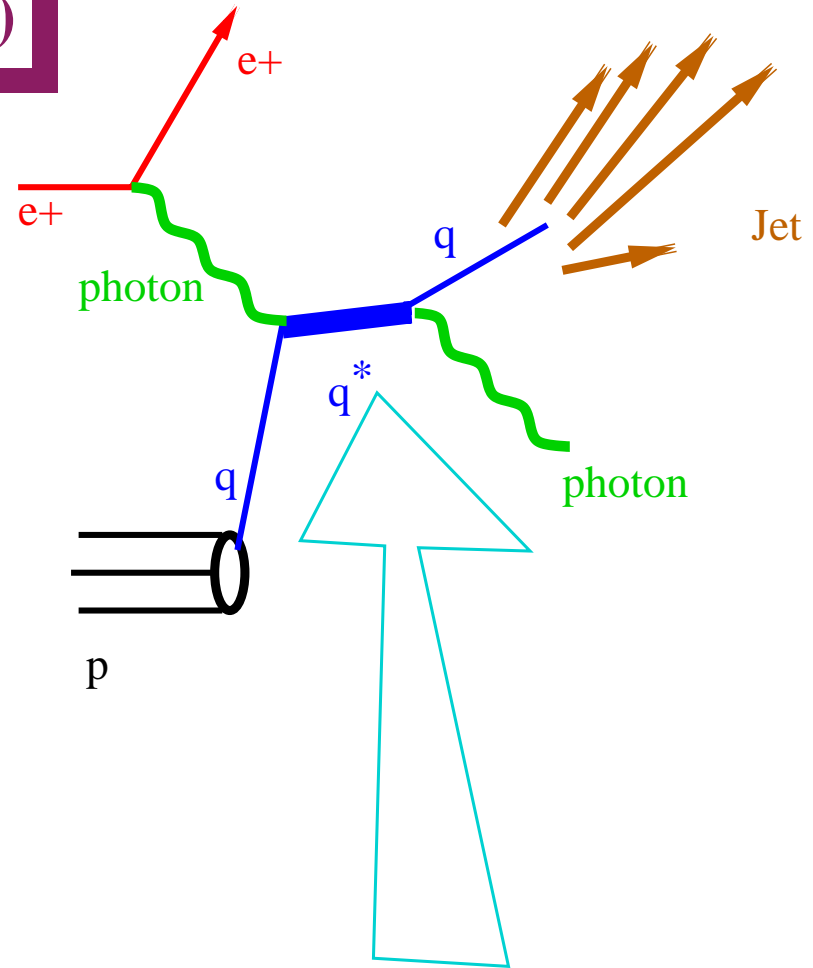
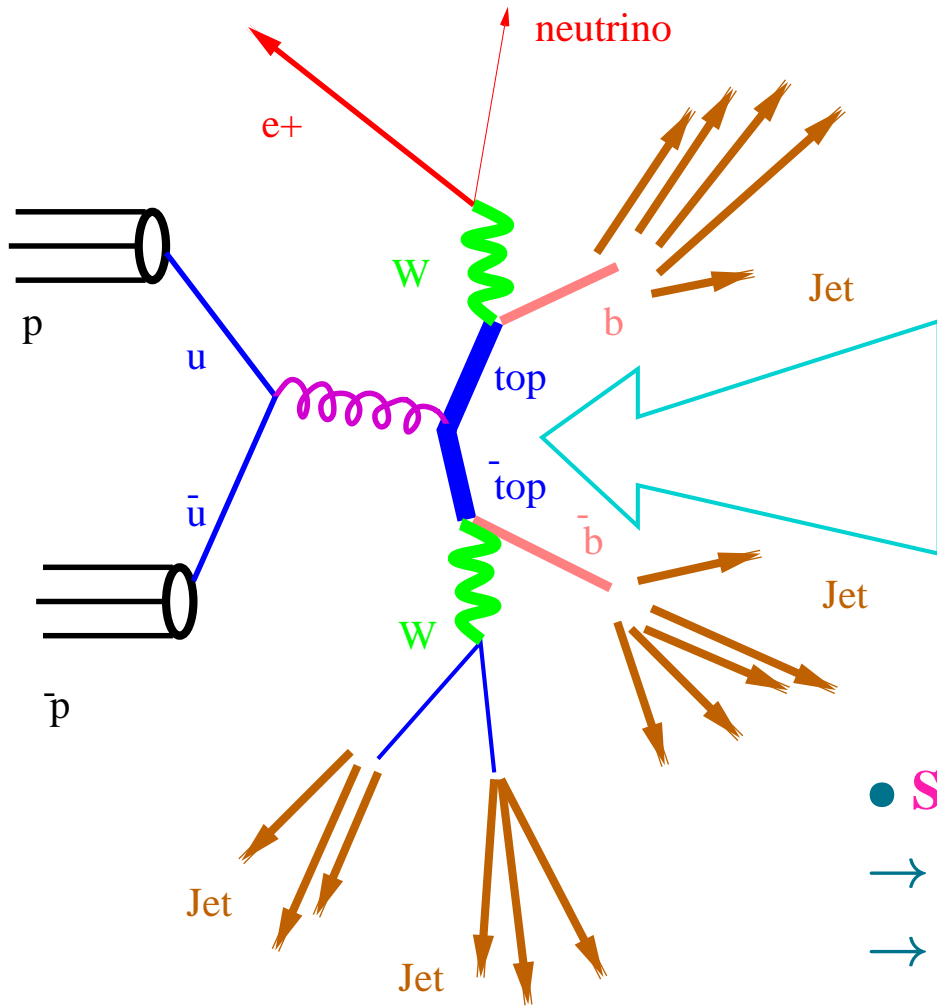


- **Studies of the strong interactions:**

- measurements of the strong coupling constant (α_S)

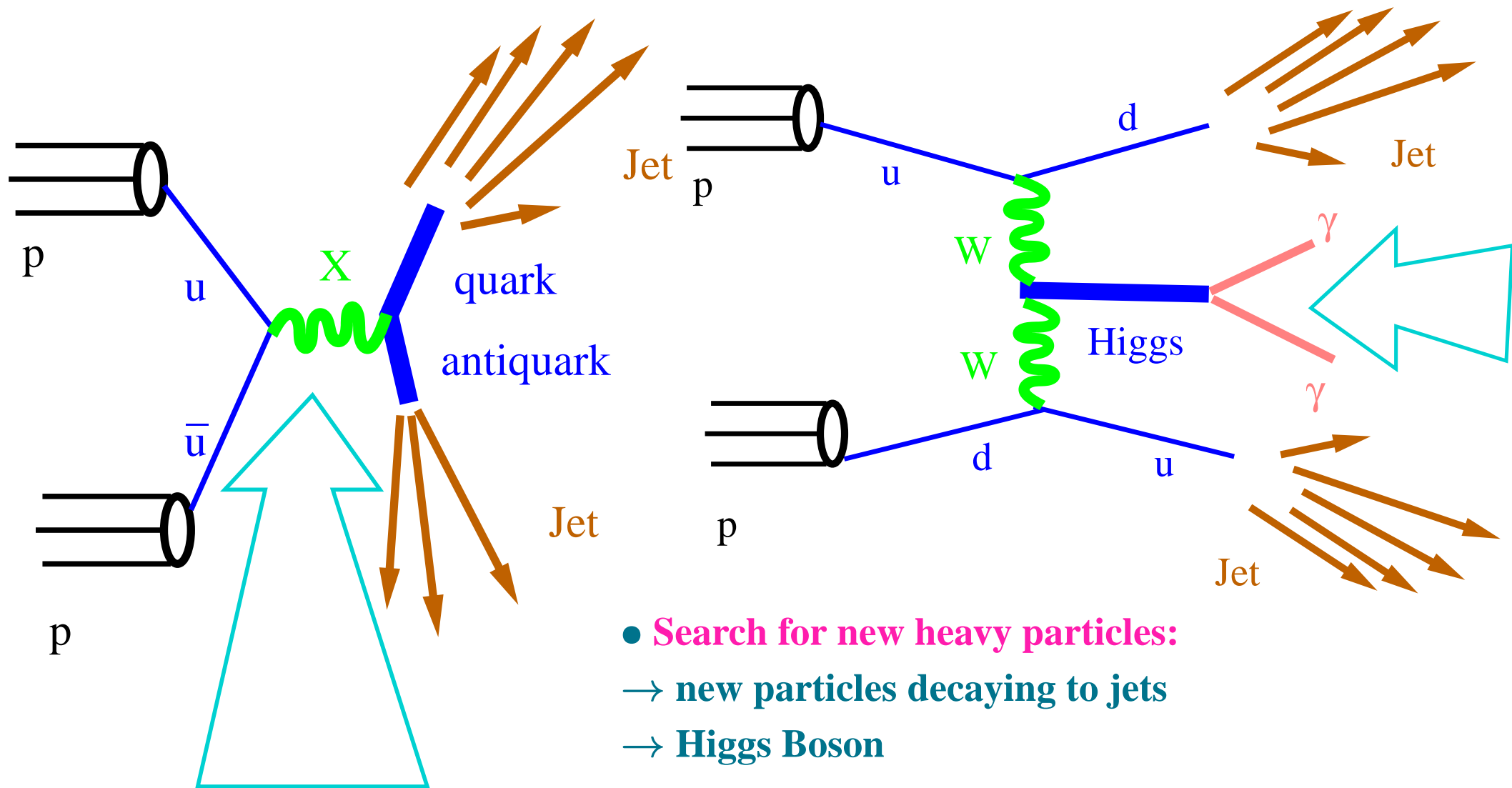
- colour dynamics (e.g. the self-coupling of the gluon)

Some good reasons to study jets (II)



- **Study of and search for new heavy particles:**
 - **measurements of top quark production**
 - **search for excited quarks**

Some good reasons to study jets (III)



- **Search for new heavy particles:**
 - new particles decaying to jets
 - **Higgs Boson**

Jet Algorithms

How to find jets?

- To reconstruct the final-state quarks and gluons

→ **Something more sophisticated than a bucket is needed!**

⇒ **JET ALGORITHM**

→ **MEASURABLE!**

→ **CALCULABLE!**

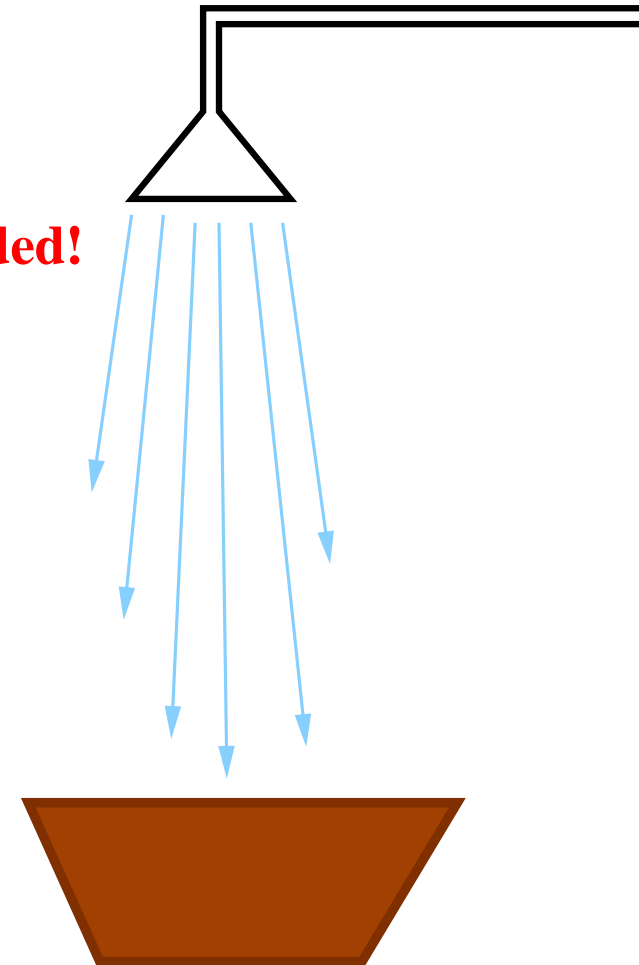
→ **ACCURATE!**

- Jet algorithm:

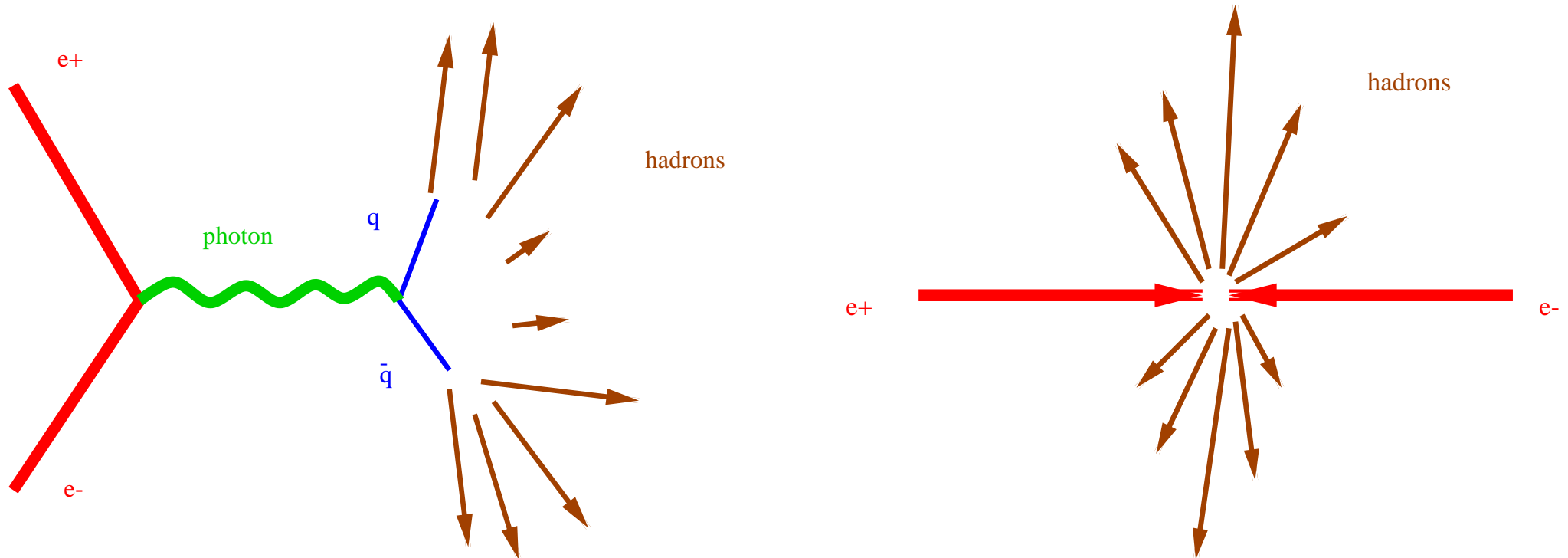
→ Reference frame

→ Variables of the hadron

→ Combining hadrons



Variables for Jet Search in e^+e^- annihilations



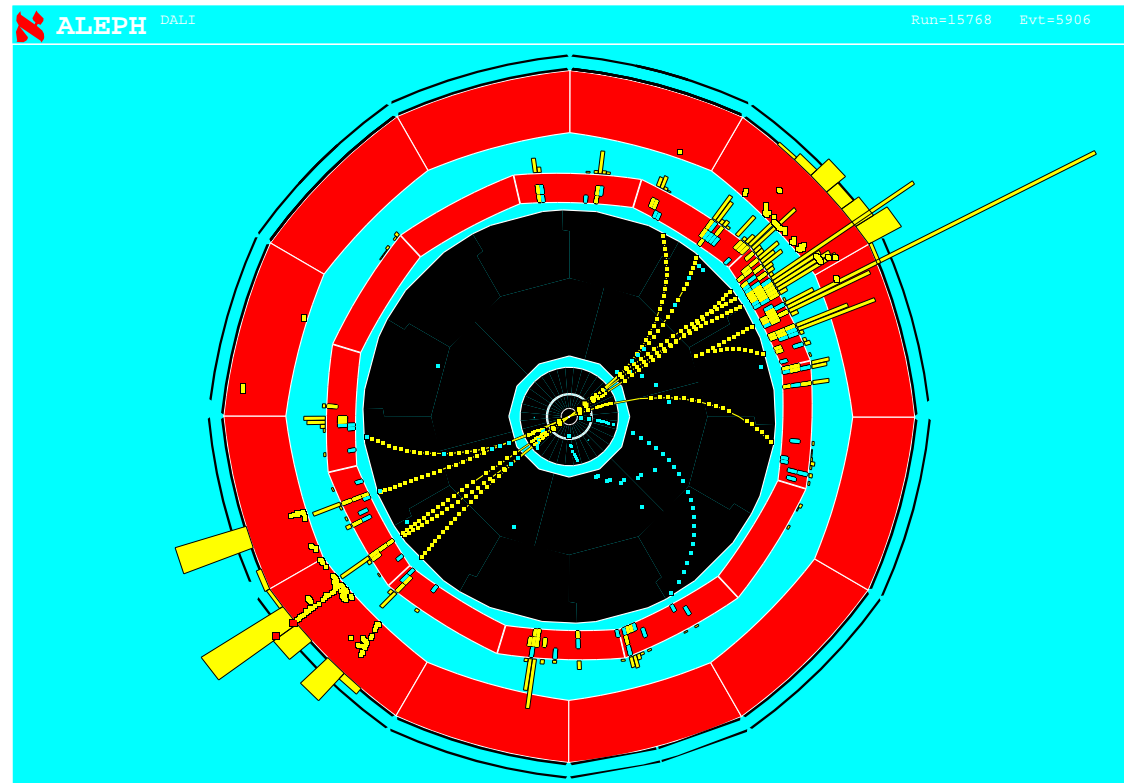
- e^+e^- annihilations in the centre-of-mass system
- Invariance under rotations \Rightarrow Energies and angles

\Rightarrow Input to the jet algorithm: E_i , θ_i and ϕ_i for every hadron i

\Rightarrow “distance” between hadrons i and j : their angular separation θ_{ij}

Combining the hadrons to build up jets: cluster algorithms

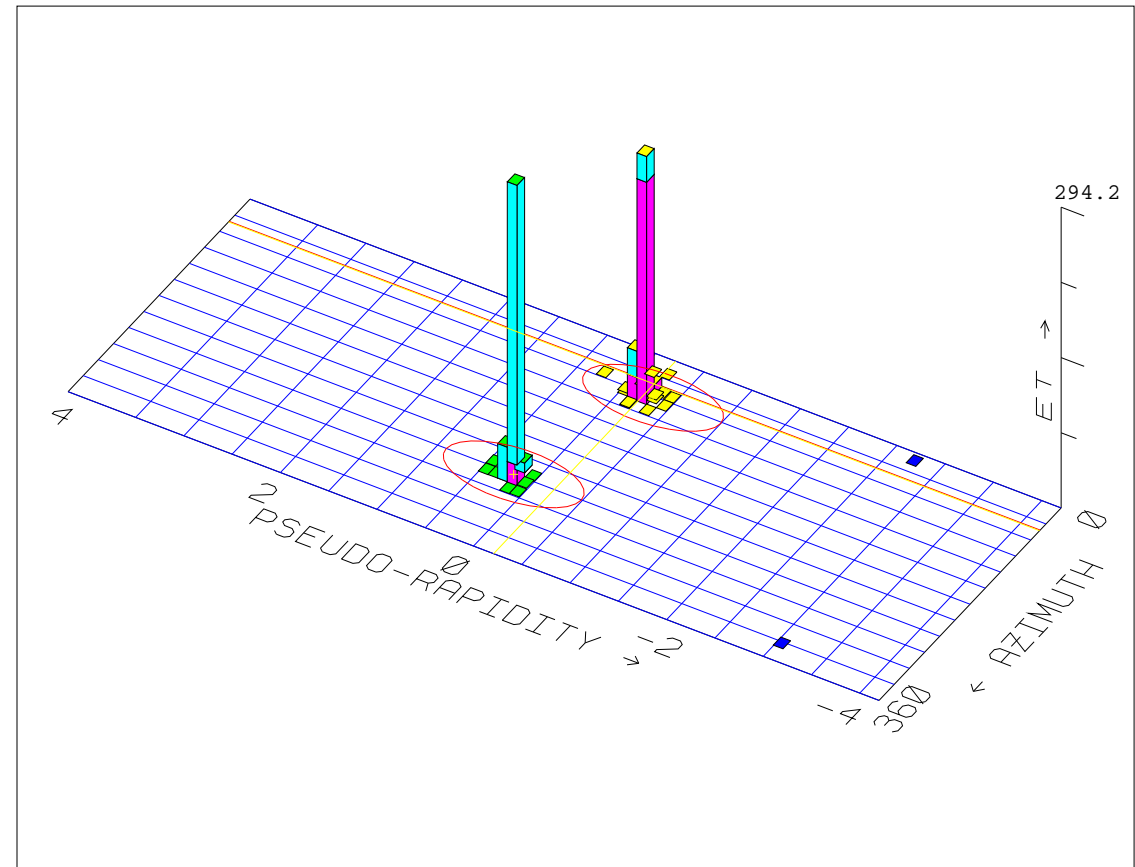
- **Hadrons are combined iteratively according to their “distance”**
- **Usually a binary decision**
- **Two-step procedure:**
 - **decision about combining hadrons i and j based on d_{ij}**
 - **momentum of the combined pseudo-particle (ij)**
(recombination procedure)
- **They have a long and successful history in e^+e^- annihilations**
- **The JADE algorithm has been the standard**
 - **distance definition: $d_{ij}^2 = 2E_i E_j (1 - \cos \theta_{ij})$**
 - **recombination procedure: $p_{(ij)} \equiv p_i + p_j$**



Made on 1-Oct-1993 10:56:54 by DREVERMANN with DALI.D1.

Combining the hadrons to build up jets: cone algorithms

- Maximizing the total transverse energy of the hadrons within a cone of fixed size
- Three-step procedure:
 - constructing the seeds (starting positions for the cone)
 - moving the cone around until a stable position is found
 - dealing with overlapping cones (to merge or not to merge)



- They have been applied mainly to $p\bar{p}$ collisions

- The iterative cone algorithm has been the standard

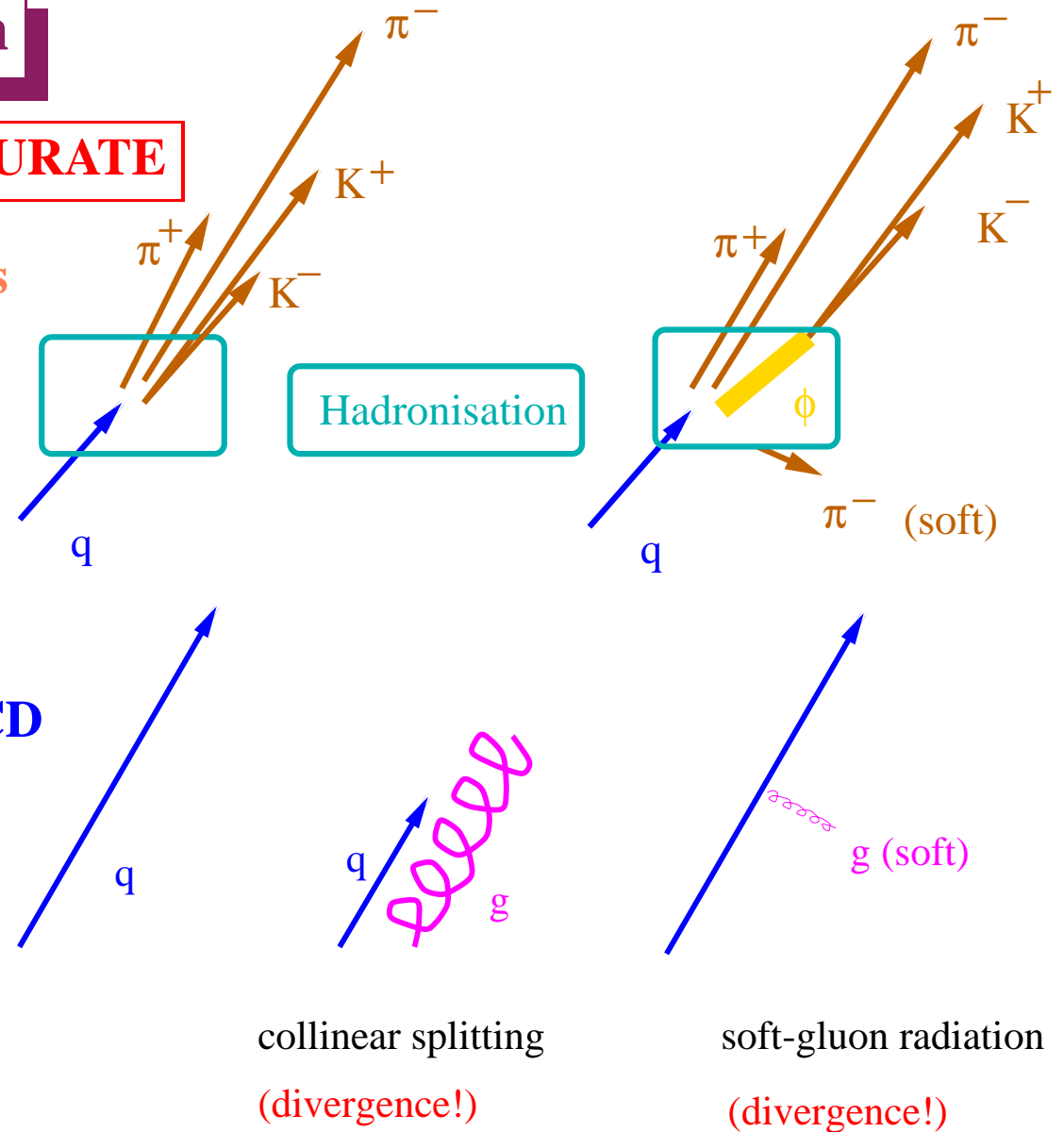
→ distance definition: $d_{iJ} \equiv \sqrt{(\eta_i - \eta_J)^2 + (\phi_i - \phi_J)^2}$

→ cone axis: $\eta_J \equiv \frac{1}{E_T} \sum_i E_{T,i} \cdot \eta_i$, $\phi_J \equiv \frac{1}{E_T} \sum_i E_{T,i} \cdot \phi_i$, $E_T = \sum_i E_{t,i}$

Requirements on a jet algorithm

MEASURABLE, CALCULABLE, ACCURATE

- Simple to use in experimental analyses and theoretical calculations
- Insensitive to the presence of soft particles or particle (strong) decays
 - infrared and collinear safe, so that it can be calculated order-by-order in perturbative QCD
- Close correspondence with the final state quarks and gluons
 - small hadronisation corrections
- Suppression of beam remnant jet contributions



Fulfilling the requirements

- The JADE algorithm is infrared and collinear safe

→ First situation: two particles (partons)

with equal and opposite momenta

$$d_{12}^2 = 4E_1(\bar{q})E_2(q) = s_{cm}$$

For $d_{cut}^2 < s_{cm} \Rightarrow$ Two jets

→ Second situation: three particles (partons)

the two collinear partons will be combined

$$d_{2'3'}^2 = 2E'_2(q)E'_3(g)(1 - \cos 0) = 0 !!$$

$p_{(2'3')} = p'_2 + p'_3 = p_2 !!$ (it wouldn't be the case if the p were added quadratically)

$d_{1(2'3')}^2 = 4E_1(\bar{q})E_{(2'3')}(qg) = s_{cm}$ and for $d_{cut}^2 < s_{cm} \Rightarrow$ Two jets

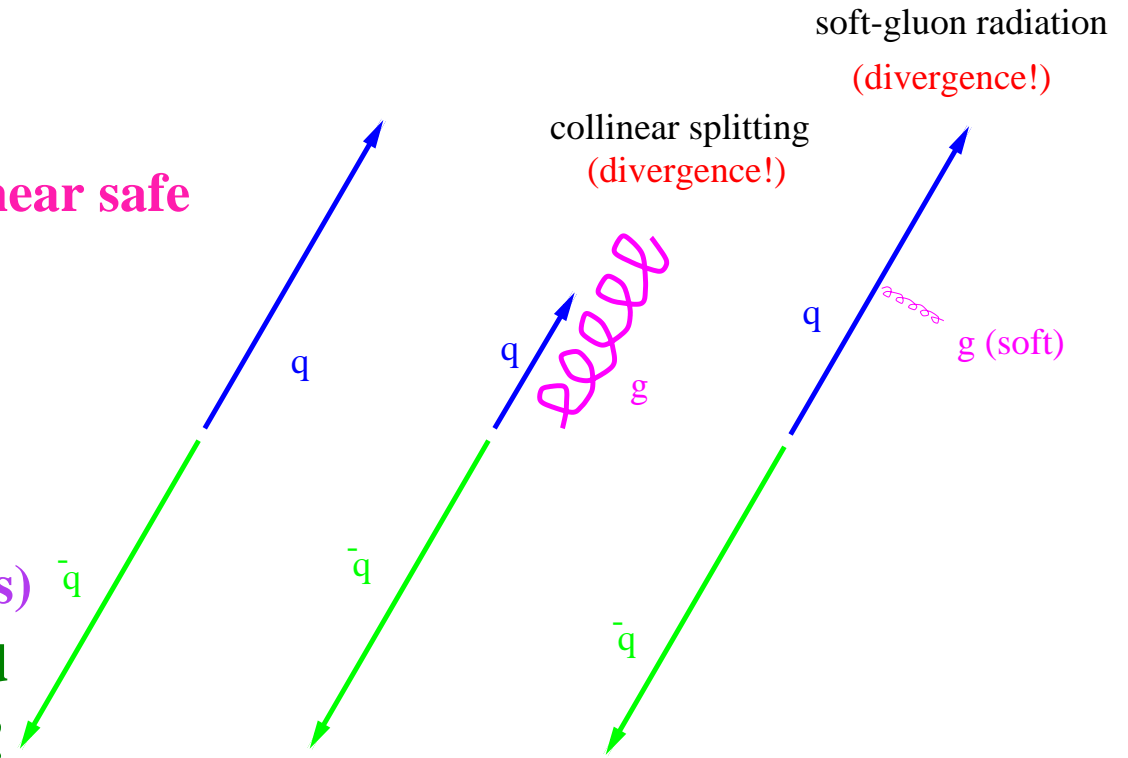
→ Third situation: the soft gluon will be combined with the closest (in angle) quark

$$\text{e.g. } d_{2'3'}^2 = 2E'_2(q)E'_3(g)(1 - \cos \theta_{2'3'}) < 2E_1(\bar{q})E'_3(g)(1 - \cos \theta_{13'})$$

$$p_{(2'3')} = p'_2 + p'_3 = p_2 !!$$

$d_{1(2'3')}^2 = 4E_1(\bar{q})E_{(2'3')}(qg) = s_{cm}$ and for $d_{cut}^2 < s_{cm} \Rightarrow$ Two jets

- The final result is the same in each configuration!



Fulfilling the requirements (II)

- **The cone algorithm is infrared and collinear safe at NLO**

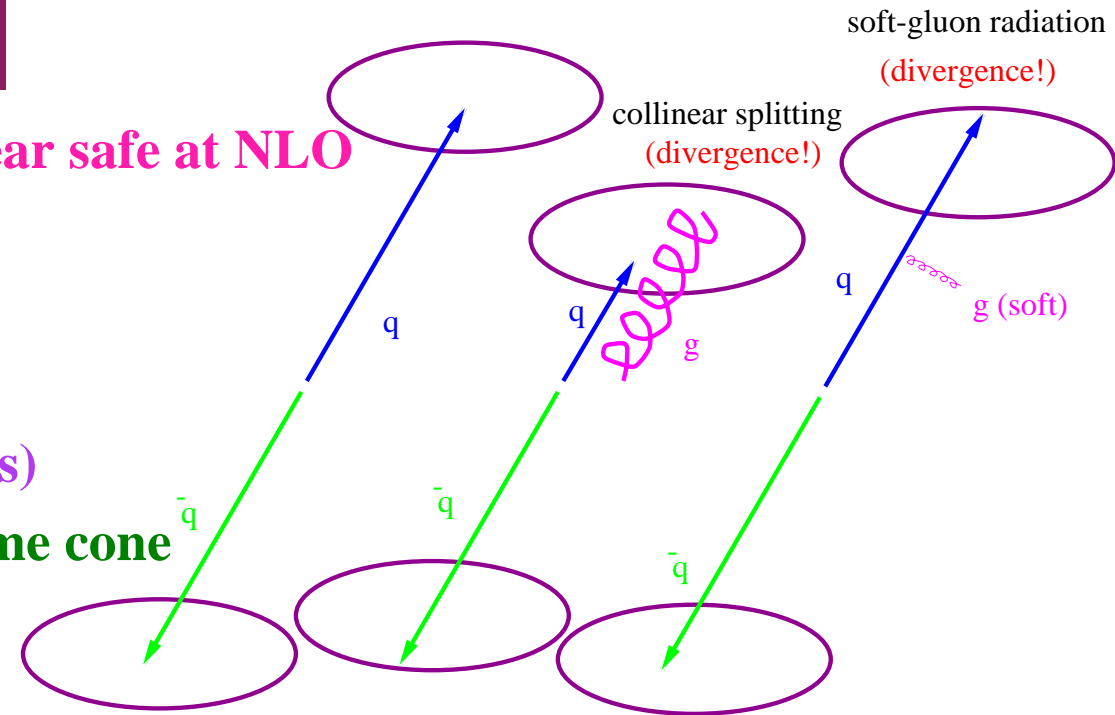
→ **First situation: two particles (partons) with equal and opposite momenta**

Each of them defines a cone \Rightarrow Two jets

→ **Second situation: three particles (partons)**

the two collinear partons will lie in the same cone

\Rightarrow Two jets



→ **Third situation: if the soft gluon is far from the other partons ($\sqrt{\Delta\eta^2 + \Delta\phi^2} > R$) it won't be lumped with any of them**

\Rightarrow Two jets

The jet axes and transverse energies will differ from the the values found in the 1st or 2nd situation by a quantity that $\rightarrow 0$ as $E(g) \rightarrow 0$!

- **The final result is the same in each configuration!**

Jets in e^+e^- collisions

Observation of jets in e^+e^- collisions

- First evidence for jets arising from quarks in $e^+e^- \rightarrow q\bar{q}$ events was obtained at the **SPEAR** e^+e^- collider in 1975
- Since jets could not be discerned simply by looking at the pattern of outgoing tracks, a method to define the jet axis was devised: the direction in which the sum of the squares of the momenta transverse to the axis was minimal:

$$\rightarrow S = \frac{3 \sum_i p_{\perp i}^2}{2 \sum_i p_i^2} \text{ (sphericity)}$$

\rightarrow jet-like event: $S = 0$
 \rightarrow isotropic event: $S \approx 1$

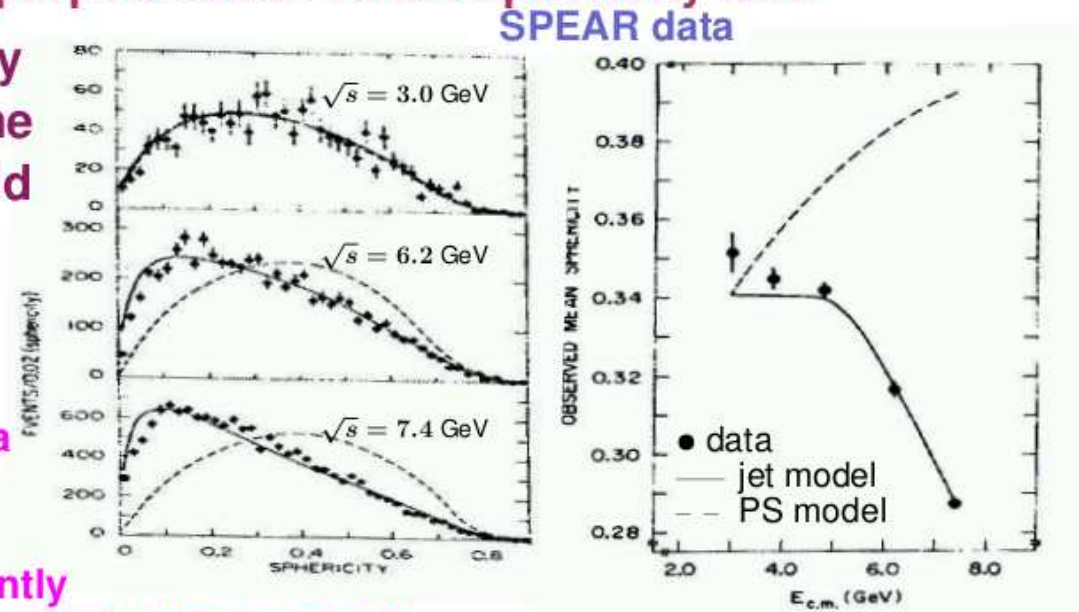
- $p_{\perp i}$: momentum of the i th particle perpendicular to the sphericity axis

- QCD predicts that as the cms energy increases, the events should become more jet-like so the sphericity should decrease

- Comparison to isotropic phase-space (PS) and jet models:

\rightarrow both models are consistent with the data for $\sqrt{s} = 3.0$ GeV

\rightarrow for $\sqrt{s} = 6.2$ and 7.4 GeV, the data are peaked toward low S and have significantly lower mean S than the PS model and agree with the jet model



Observation of jets in e^+e^- collisions

- The quark spin can also be inferred from the angular distribution of the thrust axis in hadronic Z decays \rightarrow **the angular distribution has the form**

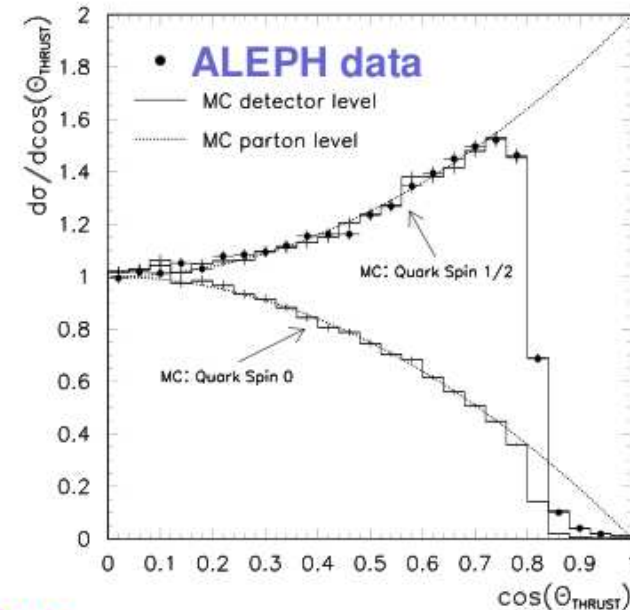
$$\frac{d\sigma}{d\cos\theta_{th}} \propto 1 + \alpha \cos^2\theta_{th}$$

where θ_{th} : polar angle of thrust axis

- \rightarrow **spin-1/2 quarks:** $\alpha = +1$
- \rightarrow **spin-0 quarks:** $\alpha = -1$

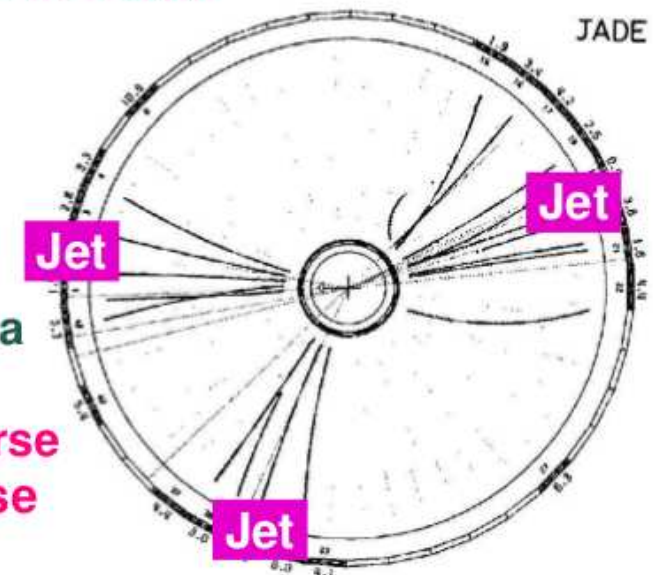
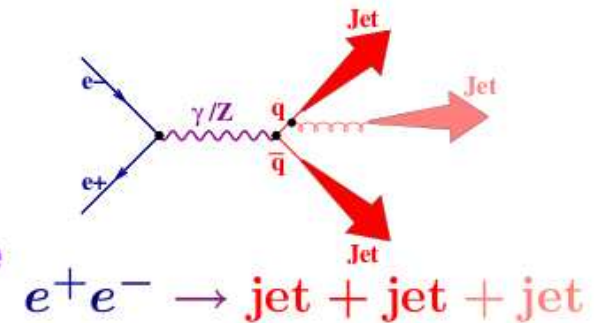
- Comparison to the predictions**

- \rightarrow **the spin-0 curve is clearly incompatible the data**
- \rightarrow **the spin-1/2 curve is in excellent agreement with the measurements**
- \Rightarrow **Confirmation that quarks are fermions with spin 1/2**



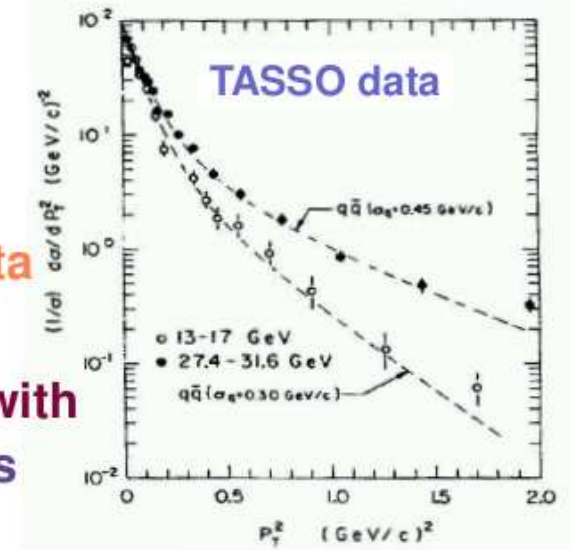
Observation of gluon jets in e^+e^- collisions

- In e^+e^- , **gluons** first appear as the $\mathcal{O}(\alpha_s)$ correction to the $e^+e^- \rightarrow q\bar{q}$ process
- **First observation of three-jet events in $e^+e^- \rightarrow q\bar{q}g$ at the PETRA e^+e^- collider in 1979** → direct evidence for the existence of gluons by looking for deviations from the quark-parton model predictions
- The quark-parton model for the process $e^+e^- \rightarrow q\bar{q}$ predicts **back-to-back jets of hadrons with typical transverse momentum of ~ 0.3 GeV**
- **In QCD,**
 - gluons will be radiated from the quarks and so the jets will no longer be back-to-back
 - the p_T distribution of the final-state hadrons will broaden with increasing energy
 - the $q\bar{q}g$ state must be coplanar since the momenta should sum 0 by momentum conservation
 - **the final-state hadrons will have small transverse momentum wrt the plane and large transverse momentum in the plane**
 - if the gluon is radiated with a large transverse momentum, the events will have a three-jet topology



Observation of gluon jets in e^+e^- collisions

- Two methods were used to determine the jet axis from the final-state hadrons:
 - minimising $\sum p_T^2$ (sphericity axis)
 - maximising $\sum |p_{||}|$ (thrust axis)
- Normalised transverse momentum distribution $\sigma^{-1} d\sigma/dp_T^2$ evaluated wrt the sphericity axis as a function of p_T^2 at $\sqrt{s} = 13 - 17$ and $24.7 - 31.6$ GeV:
 - the data at both energies are in reasonable agreement for $p_T^2 < 0.2 \text{ GeV}^2$
 - the high-energy data are well above the low energy data for $p_T^2 > 0.2 \text{ GeV}^2$
- The low-energy data have been fitted for $p_T^2 < 1.0 \text{ GeV}^2$ with the jet model: the value of the parameter σ_q (it determines the width of the p_T distribution) obtained was 0.30 GeV
- For the high-energy data, $\sigma_q = 0.45 \text{ GeV}$ in contradiction with the quark-parton model which assumes the quark to fragment into hadrons with an energy-independent p_T distribution
- QCD predicts the p_T to increase with the energy due to gluon bremsstrahlung



Observation of gluon jets in e^+e^- collisions

$$\langle p_T^2 \rangle_{\text{out}} = \frac{1}{N} \sum_{j=1}^N (\vec{p}_j \cdot \vec{n}_1)^2 \quad (\text{momentum component normal to the event plane})$$

$$\langle p_T^2 \rangle_{\text{in}} = \frac{1}{N} \sum_{j=1}^N (\vec{p}_j \cdot \vec{n}_2)^2 \quad (\text{momentum component in the event plane perpendicular to the jet axis})$$

where \vec{n}_3 : direction of sphericity axis, \vec{n}_1 : direction which maximises $\sum p_T^2$, \vec{n}_2 : direction orthogonal to \vec{n}_1 and \vec{n}_3

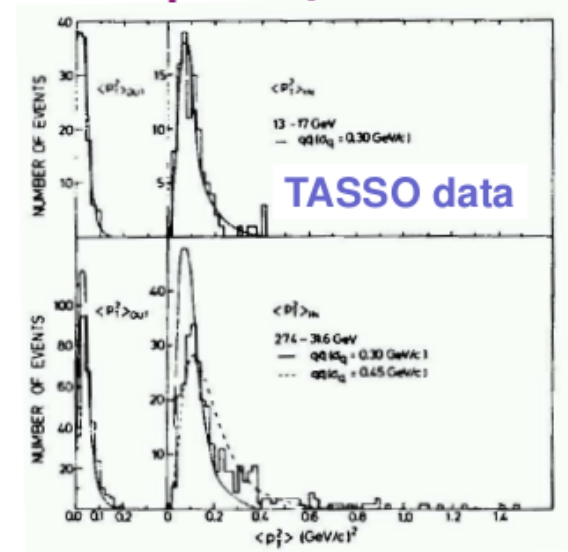
→ $\vec{n}_2 - \vec{n}_3$: event plane

→ the data show only little increase in $\langle p_T^2 \rangle_{\text{out}}$ between the low-energy and the high-energy data

→ the distribution of $\langle p_T^2 \rangle_{\text{in}}$ becomes much wider at high energies and a long tail is observed

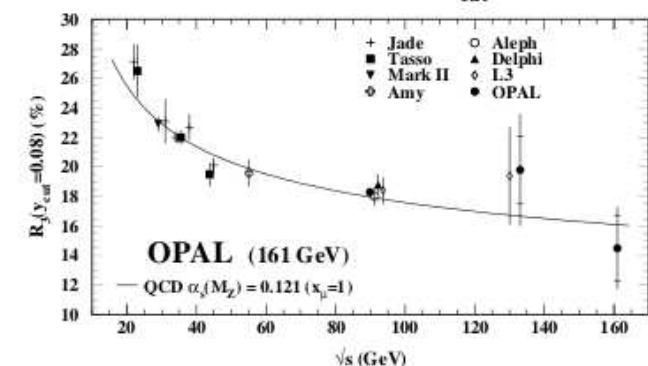
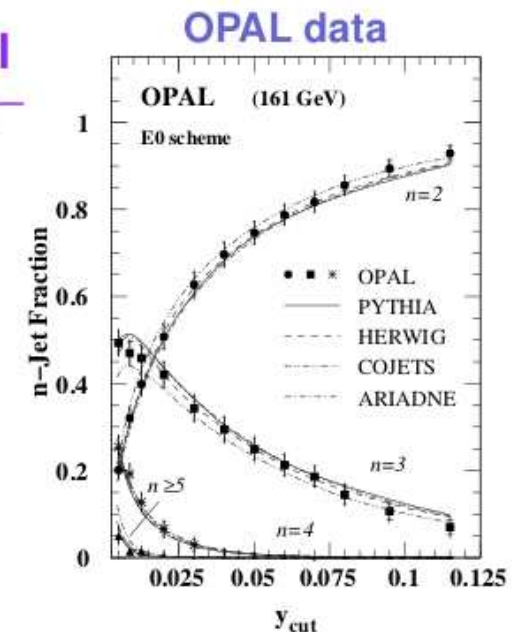
● Comparison to the jet-model predictions:

- hadrons resulting from pure $q\bar{q}$ events will be on average distributed uniformly around the jet axis
- fair agreement with the $q\bar{q}$ model is found both for $\langle p_T^2 \rangle_{\text{in}}$ and $\langle p_T^2 \rangle_{\text{out}}$ for the low-energy data
- at high energy, there is a fair agreement between $\langle p_T^2 \rangle_{\text{out}}$ and the $q\bar{q}$ model with $\sigma_q = 0.3$ GeV
- the long tail in $\langle p_T^2 \rangle_{\text{in}}$ is not reproduced by the model → **this discrepancy cannot be removed by increasing σ_q**
- ⇒ the data include a number of planar events not reproduced by the $q\bar{q}$ model
 - **evidence for $q\bar{q}g$ events**



Jet rates in e^+e^- collisions

- The topology of hadronic events in e^+e^- collisions is modified by the effects of gluon radiation, giving rise to events which differ from the collimated two-jet topology coming from the fragmentation of $q\bar{q}$ events
- Since the amount of gluon radiation is directly proportional to α_s , the study of the topology of hadronic decays in e^+e^- provides a determination of $\alpha_s(M_Z)$
- The strategy consists of finding variables which characterize the “three-jetness” of the events \rightarrow the variables have to be infrared and collinear safe to be able to perform reliable calculations: **jet rates as a function of the resolution parameter y_{cut}**
- Comparison to Monte Carlo predictions: \rightarrow **the predictions show in general a good agreement with the data**
- The three-jet rate (R_3) at $y_{cut} = 0.08$ as a function of \sqrt{s} shows the running of α_s directly



Theoretical Uncertainties

- Being collinear and infrared safe does **NOT** mean small theoretical uncertainties

- Perturbative QCD calculations are performed to a certain order in α_S

→ the size of higher-order contributions constrains the **accuracy** with which (e.g.) α_S can be experimentally determined

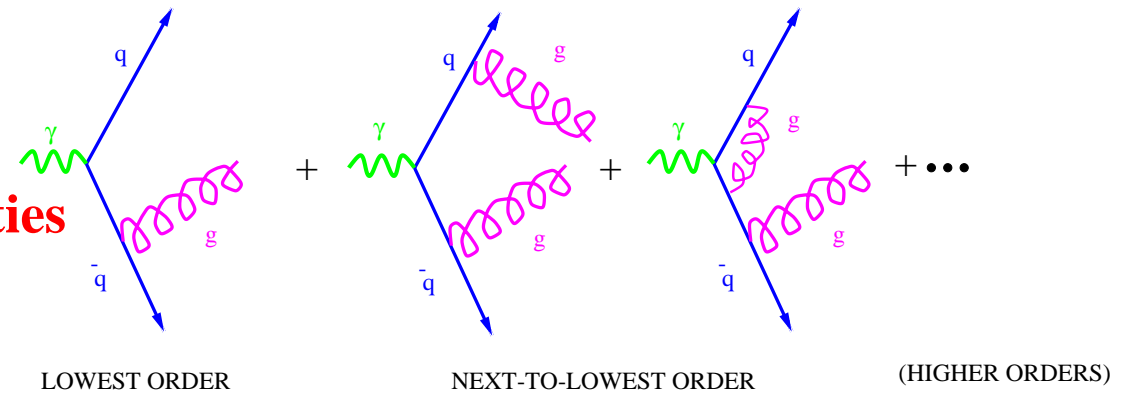
- The size of the higher-order contributions **DEPENDS** on the jet algorithm
- How can higher-order effects be estimated without computing them?

→ by investigating the renormalisation-scale dependence (μ_R)

$$A = A_1 \cdot \alpha_S(\mu_R) + A_2 \cdot \alpha_S^2(\mu_R) + \dots (\text{higher orders})$$

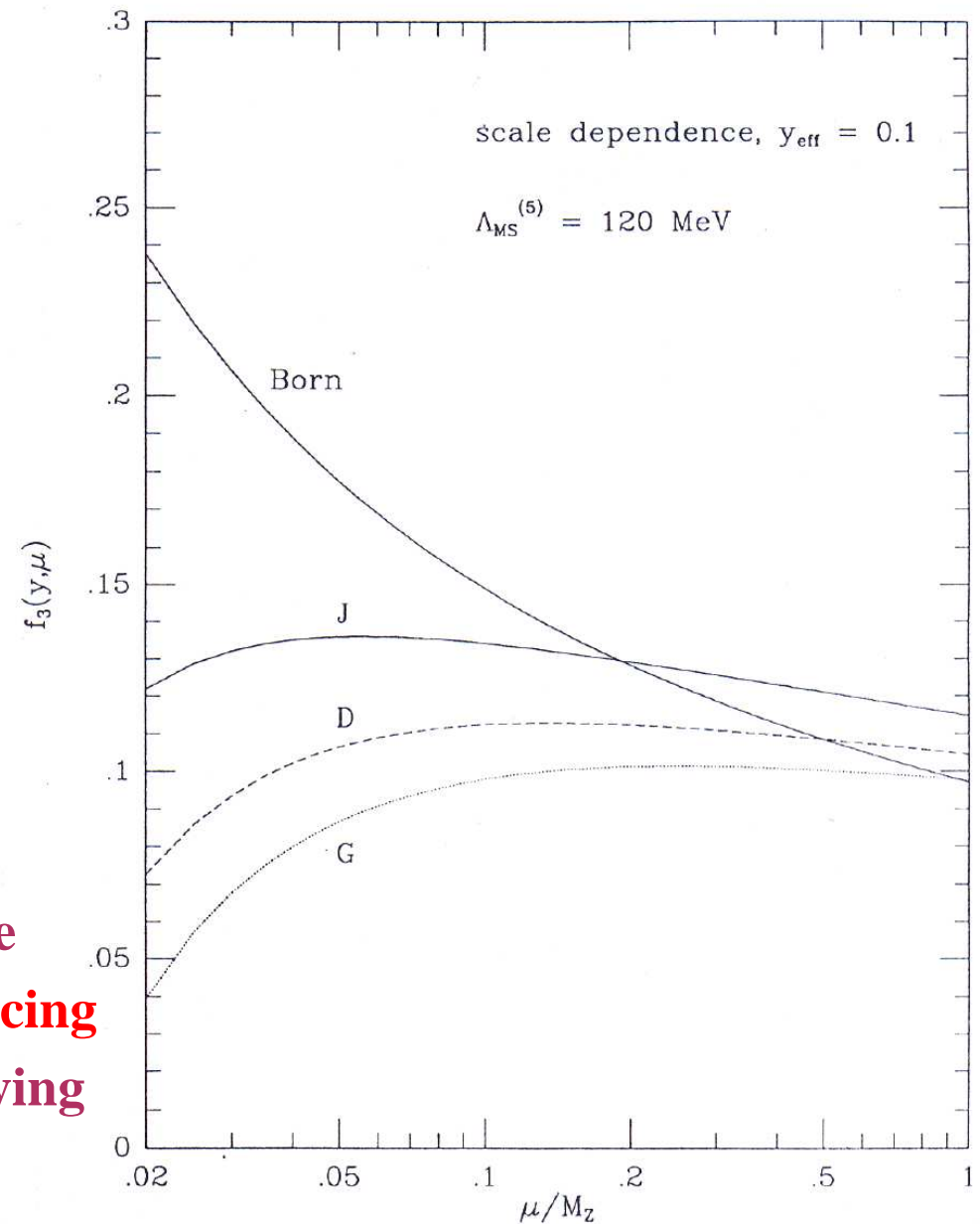
At all orders A does **NOT** depend on μ_R

⇒ The size of the “...” is such that it cancels the μ_R variation of the first two terms



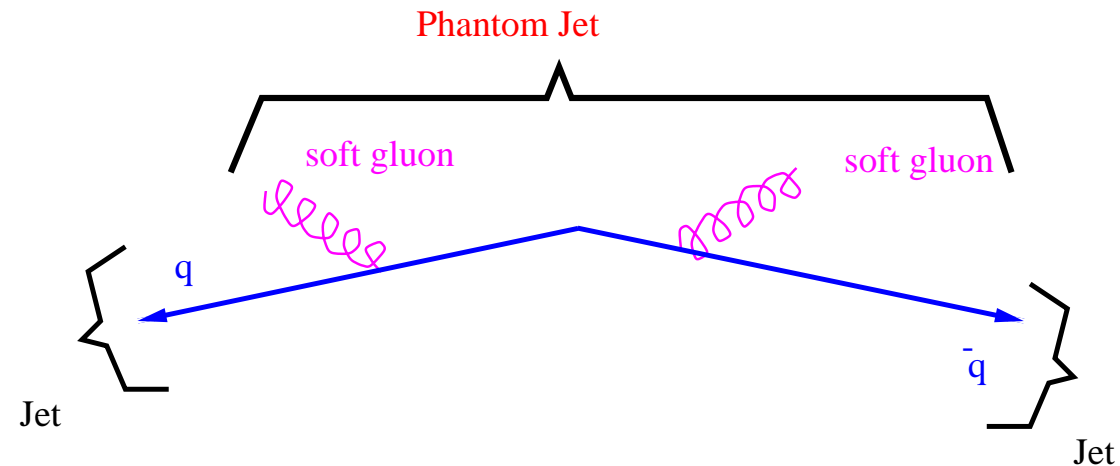
Theoretical Uncertainties (II)

- **NLO calculations for three-jet production in e^+e^- : → variation with μ_R to assess the size of higher-order contributions**
→ **Performance of various jet algorithms: variation of the observable f_3 over the range $0.1 < \mu_R/M_Z < 1.0$**
 - **JADE algorithm: 15%**
 - **Durham algorithm: 8%**
 - **Geneva algorithm: 3%**
- **The Durham and Geneva jet algorithms were specifically designed for the purpose of reducing the higher-order contributions upon identifying the limitations of the JADE algorithm**



Improving the jet algorithm

- **The limitation of the JADE algorithm:**
 - **soft gluons are copiously radiated**
 - **but soft gluons far apart can be combined into and a “phantom” jet**



- **This peculiar behaviour arises from the definition of “distance” in the JADE algorithm:**

$$d_{ij}^2 = 2E_i E_j (1 - \cos \theta_{ij}) \Rightarrow \text{two soft gluons can be very close } "d_{gg} \ll d_{gq}"$$

- **An improved definition of the distance:**

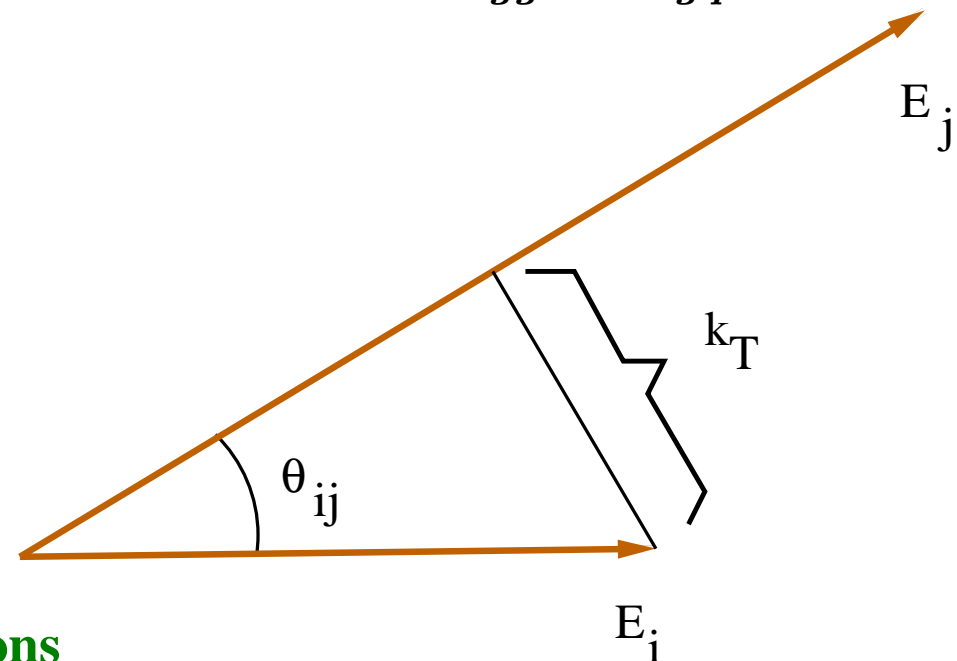
$$d_{ij}^2 = 2 \cdot \min(E_i^2, E_j^2) \cdot (1 - \cos \theta_{ij})$$

which amounts to replacing the invariant mass

→ by the minimum relative k_T of the pair

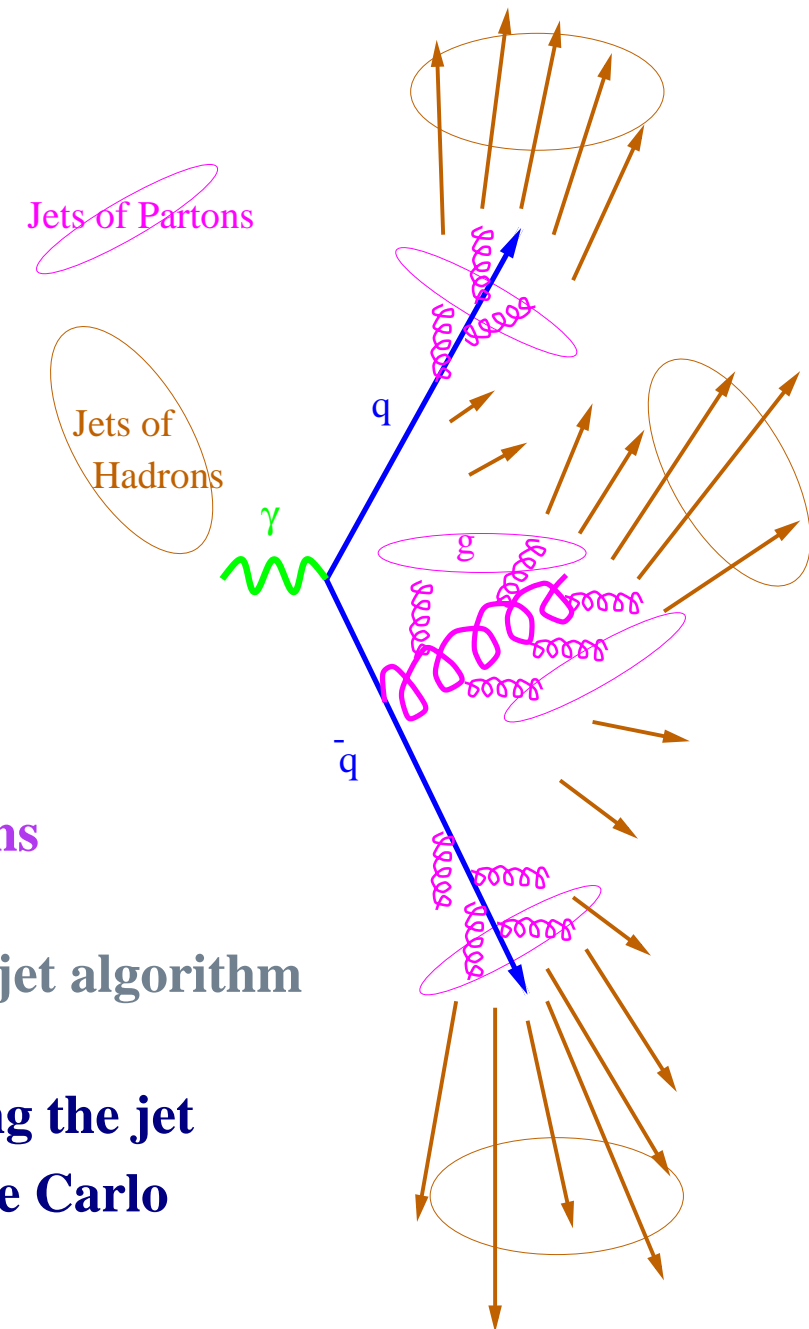
⇒ **Durham (or k_T) algorithm**

→ **it also allows the resummation of contributions from multiple-soft-gluon emissions**



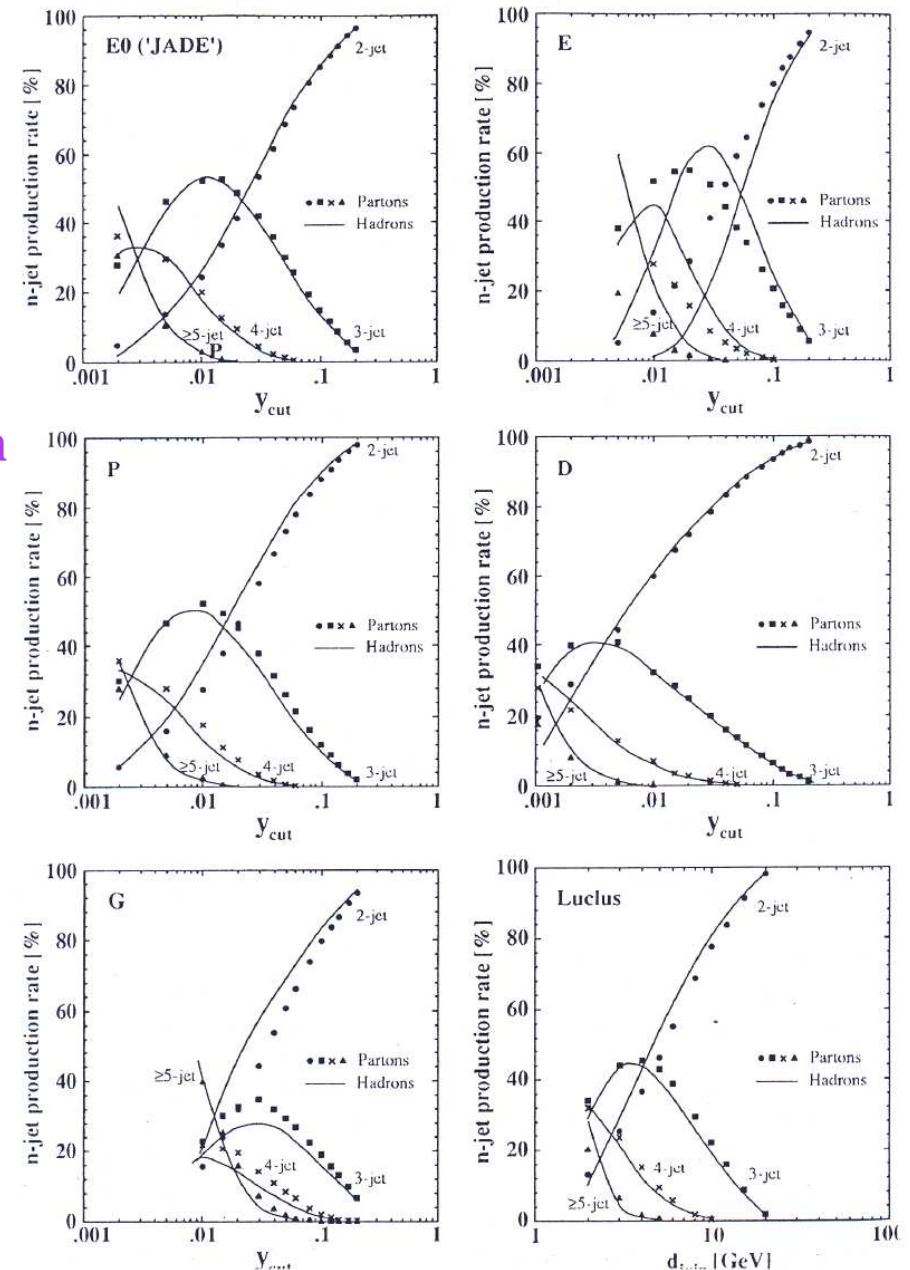
Hadronisation Effects

- Being collinear and infrared safe
does **NOT** mean small hadronisation uncertainties
- Parton-to-Hadron (hadronisation) effects are non-perturbative and are estimated with Monte Carlo simulations that include
 - q and g radiation in the parton-shower approach
 - fragmentation of the final-state partons into hadrons
- The size of the hadronisation effects **DEPENDS** on the jet algorithm
- They are estimated by comparing the results of applying the jet algorithm to the **parton** and **hadron** levels of the Monte Carlo simulated events



Hadronisation Effects (II)

- Jet rates in e^+e^- annihilations
as functions of the resolution parameter y_{cut}
- Comparison of hadron and parton level calculations using Monte Carlo simulations
- The size of the hadronisation effects depends upon
 - the distance definition
 - the recombination procedure
- The hadronisation effects are **LARGEST** for
 - the JADE algorithm with the E scheme
 - $(p_{ij} = p_i + p_j)$
 - the Geneva algorithm
- The hadronisation effects are **SMALLEST** for
 - the JADE algorithm with the $E0$ scheme
 - $(E_{ij} = E_i + E_j, \vec{p}_{ij} = \frac{E_{ij}}{|\vec{p}_i + \vec{p}_j|} (\vec{p}_i + \vec{p}_j))$
 - the Durham algorithm



Importance of the details of the jet algorithms

- The “details” of a jet algorithm are **RELEVANT** for
 - precise comparisons between **DATA** and **THEORY** to make accurate determinations of the fundamental parameters (e.g. $\alpha_S(M_Z)$)
 - precise identification and reconstruction of new heavy particles
- The decision on which algorithm to choose must be based on the size of the uncertainties
 - higher-order contributions
 - hadronisation corrections
 - hadronisation uncertainties
 - experimental uncertainties

Determination of $\alpha_s(M_Z)$ in e^+e^- collisions

- The QCD prediction for the differential two-jet rate as a function of the two-jet resolution parameter y_3 is given by

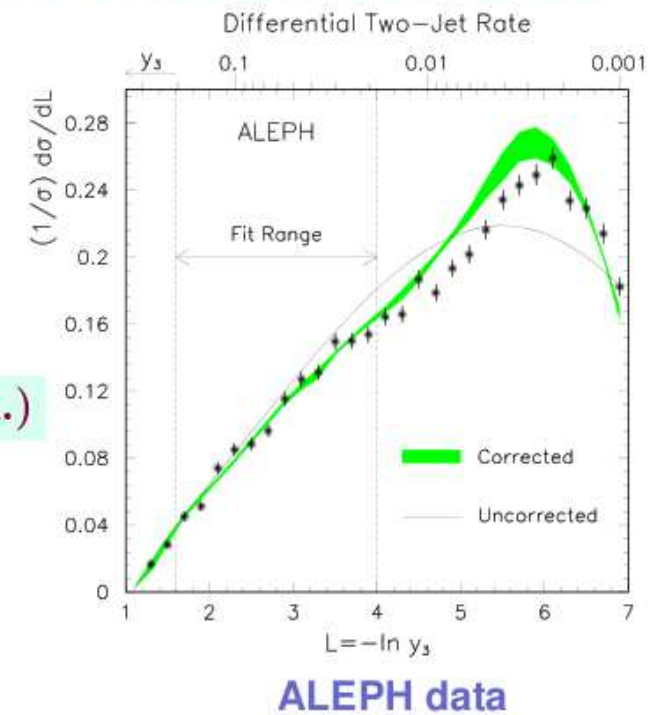
$$\frac{1}{\sigma} \frac{d\sigma}{dy_3} = \frac{\alpha_s(\mu)}{2\pi} A(y_3) + \left(\frac{\alpha_s(\mu)}{2\pi} \right)^2 \cdot \left[B(y_3) + 2\pi b_0 \ln \left(\frac{\mu^2}{s} \right) \cdot A(y_3) \right]$$

where $A(y_3)$ and $B(y_3)$ contain the full information of the second order matrix elements, μ : renormalisation scale

- Since the predictions correspond to a partonic final state with at most four partons \rightarrow need to apply hadronisation corrections
- A value of $\alpha_s(M_Z)$ of

$$\alpha_s(M_Z) = 0.121 \pm 0.002 \text{ (stat)} \pm 0.003 \text{ (exp.)} \pm 0.007 \text{ (th.)}$$

was obtained by fitting the measured differential two-jet rate distribution using the second order QCD prediction corrected for hadronisation effects



Determination of the spin of the gluon in e^+e^- collisions

- A study of three-jet events in e^+e^- collisions gives insight into the dynamics of perturbative QCD → three-jet events arise from hard non-collinear gluon radiation
- For massless jets, there are only four independent variables: two angular variables and two of the energy fractions, $x_i = 2E_i/\sqrt{s}$ since $x_1 + x_2 + x_3 = 2$ by energy conservation ($x_1 > x_2 > x_3$)
- The LO cross section for the process $e^+e^- \rightarrow q\bar{q}g$ with vector gluon (spin 1) is

$$\frac{1}{\sigma_0} \frac{d^2\sigma^V}{dx_1 dx_2} = \frac{2\alpha_s}{3\pi} \left[\frac{x_1^2 + x_2^2}{(1-x_1)(1-x_2)} + \text{permut} \right]$$

and for scalar gluon (spin 0),

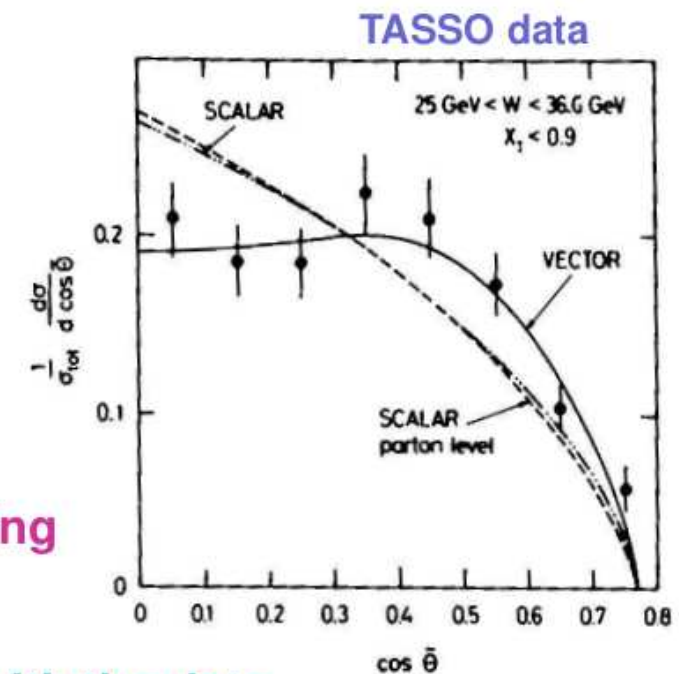
$$\frac{1}{\sigma_0} \frac{d^2\sigma^S}{dx_1 dx_2} = \frac{2\tilde{\alpha}_s}{3\pi} \left[\frac{x_3^2}{(1-x_1)(1-x_2)} + \text{permut} \right]$$

where $\tilde{\alpha}_s$: effective coupling in a theory with scalar gluons

- The spin of the gluon can be determined by comparing the data and predictions for the variable

$$|\cos \tilde{\theta}| = \frac{x_2 - x_3}{x_1} \quad (\text{Ellis-Karliner angle})$$

- the scalar gluon model is in clear disagreement with the data
- the vector gluon model provides a very good description of the data



Triple-gluon vertex

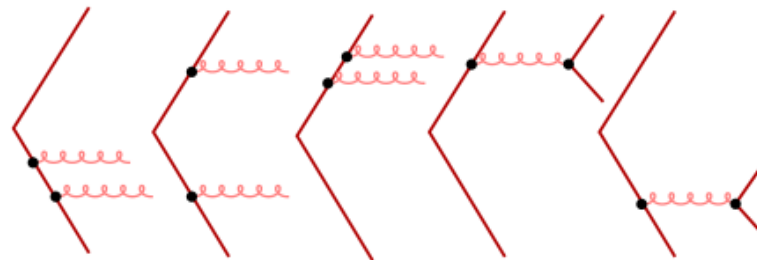
- QCD is based on the $SU(3)$ non-abelian group which induces the self-coupling of the gauge bosons whereas QED is based on the abelian $U(1)$ group (no self-coupling)

→ Due to the presence of the gluon self-coupling, the effects of the triple-gluon vertex should be observed

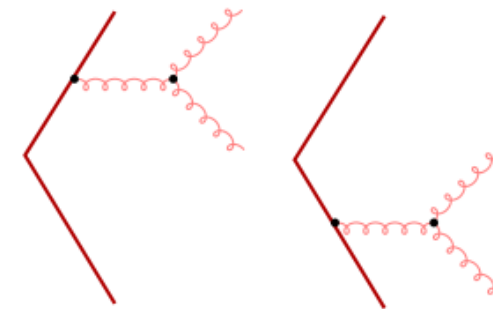
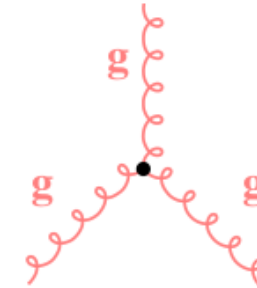
→ The events should contain at least four jets in the final state

- Events with at least four jets are needed since the diagrams that contain the triple-gluon vertex are

- The diagrams



also contribute to the four-jet cross section, but they are present in abelian theories as well



Four-jet events in e^+e^- : triple-gluon vertex

- Four-jet events have been observed at the e^+e^- collider LEP

→ QCD prediction confirmed by data!

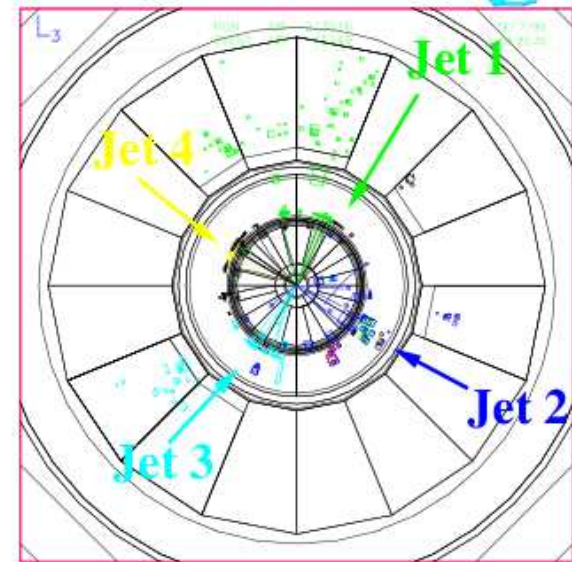
- The four-jet cross sections for $e^+e^- \rightarrow q\bar{q}gg$ and $e^+e^- \rightarrow q\bar{q}q\bar{q}$ can be expressed as

$$\frac{1}{\sigma_0} d\sigma_{q\bar{q}gg}(y_{ij}) = \left(\frac{\alpha_s C_F}{\pi} \right)^2 \left[A(y_{ij}) + \left(1 - \frac{1C_A}{2C_F} \right) B(y_{ij}) + \frac{C_A}{C_F} C(y_{ij}) \right] dY_{ij}$$

$$\frac{1}{\sigma_0} d\sigma_{q\bar{q}q\bar{q}}(y_{ij}) = \left(\frac{\alpha_s C_F}{\pi} \right)^2 \left[N_F \frac{T_F}{C_F} D(y_{ij}) + \left(1 - \frac{1C_A}{2C_F} \right) E(y_{ij}) \right] dY_{ij}$$

where

- $y_{ij} = (p_i + p_j)^\mu (p_i + p_j)_\mu / s$ is the normalised two-body invariant mass and i, j run over the four partons
- C_A, C_F and T_F are the color factors
- N_F is the number of active quark flavors
- A, \dots, E are group-independent kinematic functions
- σ_0 is the Born cross section for the process $e^+e^- \rightarrow q\bar{q}$
- dY_{ij} is the product of the differentials of any five of the six y_{ij} variables



Four-jet events in e^+e^- : triple-gluon vertex

- Variables have been devised to highlight the non-abelian character of QCD in contrast to abelian theories, eg the $SU(3)$ group of QCD could be replaced by the abelian $[U(1)]^3$ group
- These variables are
 - Bengtsson-Zerwas angle χ_{BZ} , the angle between the planes determined by the two lowest and the two highest energy jets:

$$\cos \chi_{BZ} = \left| \frac{(\vec{p}_1 \times \vec{p}_2) \cdot (\vec{p}_3 \times \vec{p}_4)}{|\vec{p}_1 \times \vec{p}_2| |\vec{p}_3 \times \vec{p}_4|} \right|$$

- Nachtmann-Reiter angle θ_{NR}^* , the angle between the momentum vector differences of jets 1,2 and jets 3,4:

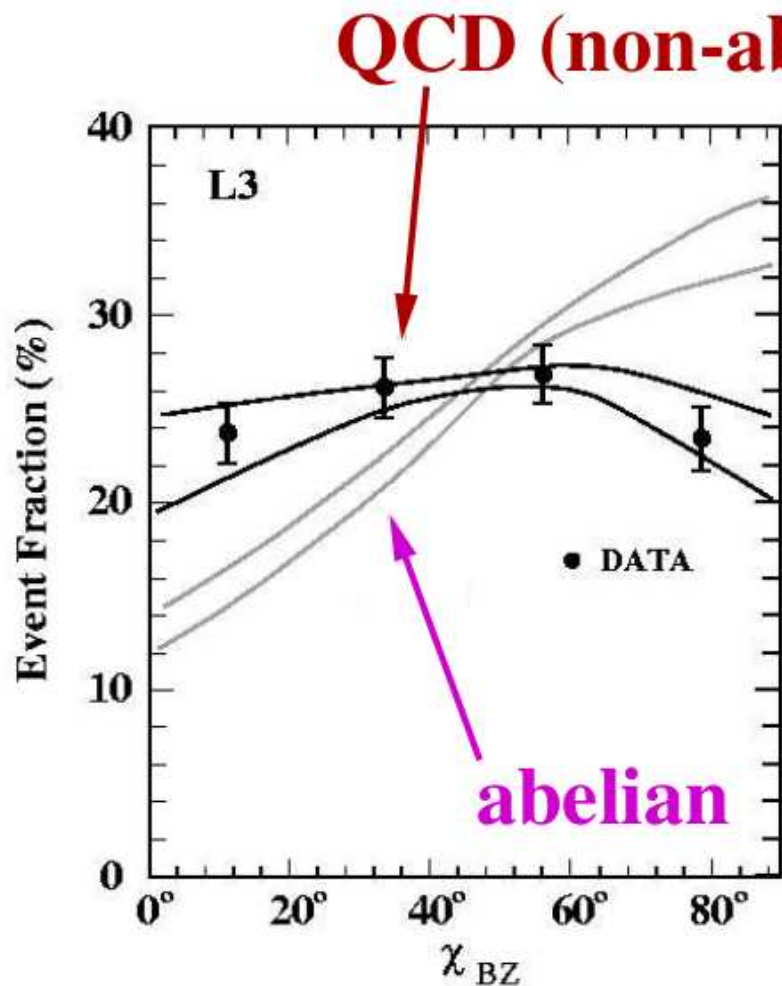
$$|\cos \theta_{NR}^*| = \left| \frac{(\vec{p}_1 - \vec{p}_2) \cdot (\vec{p}_3 - \vec{p}_4)}{|\vec{p}_1 - \vec{p}_2| |\vec{p}_3 - \vec{p}_4|} \right|$$

- α_{34} , the angle between the two lowest energy jets:

$$\cos \alpha_{34} = \frac{\vec{p}_3 \cdot \vec{p}_4}{|\vec{p}_3| |\vec{p}_4|}$$

Do the data favour an abelian or a non-abelian theory?

- These variables have been measured in four-jet events at LEP, eg



→ The data clearly favour a theory with non-abelian character: **QCD**

→ **QCD prediction confirmed by data!**

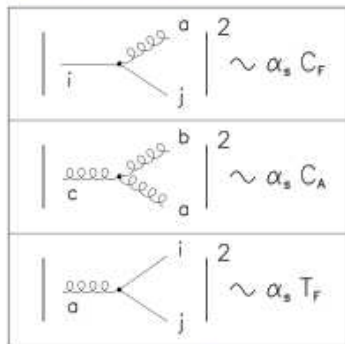
Four-jet events in e^+e^- : color factors

- A simultaneous measurement of the ratios C_A/C_F and T_F/C_F at e^+e^- colliders is possible through the study of angular correlations in four-jet events: the values are extracted from a fit of the theory to the data distributions on the angular variables

→ The results obtained are

$$C_A/C_F = 2.11 \pm 0.16 \text{ (stat)} \pm 0.28 \text{ (syst)}$$

$$T_F/C_F = 0.40 \pm 0.11 \text{ (stat)} \pm 0.14 \text{ (syst)}$$

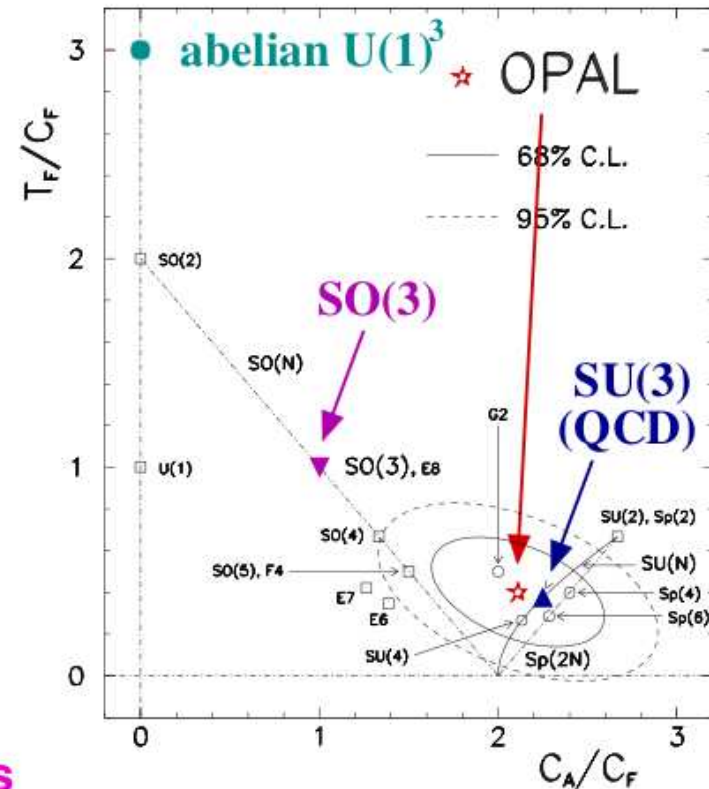


For $SU(N_C) \rightarrow C_A = N_C$

$$C_F = \frac{N_C^2 - 1}{2N_C}$$

$$T_F = 1/2$$

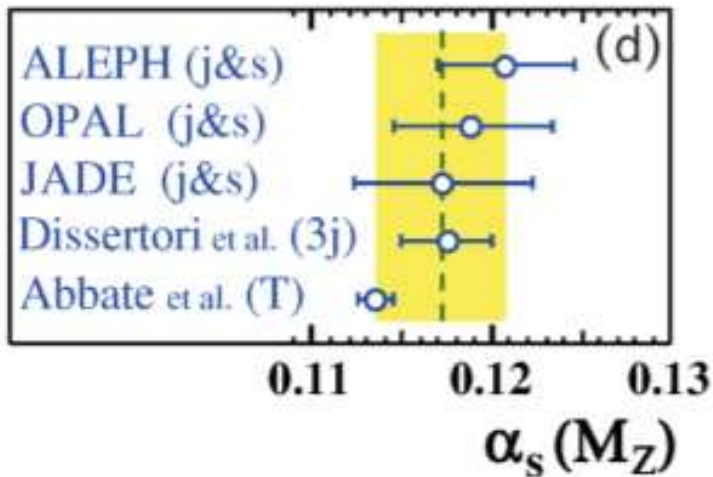
- The $U(1)^3$ and $SO(3)$ theories are clearly excluded by the measurements
- The results are in agreement with the predictions of the $SU(3)$ theory (QCD)



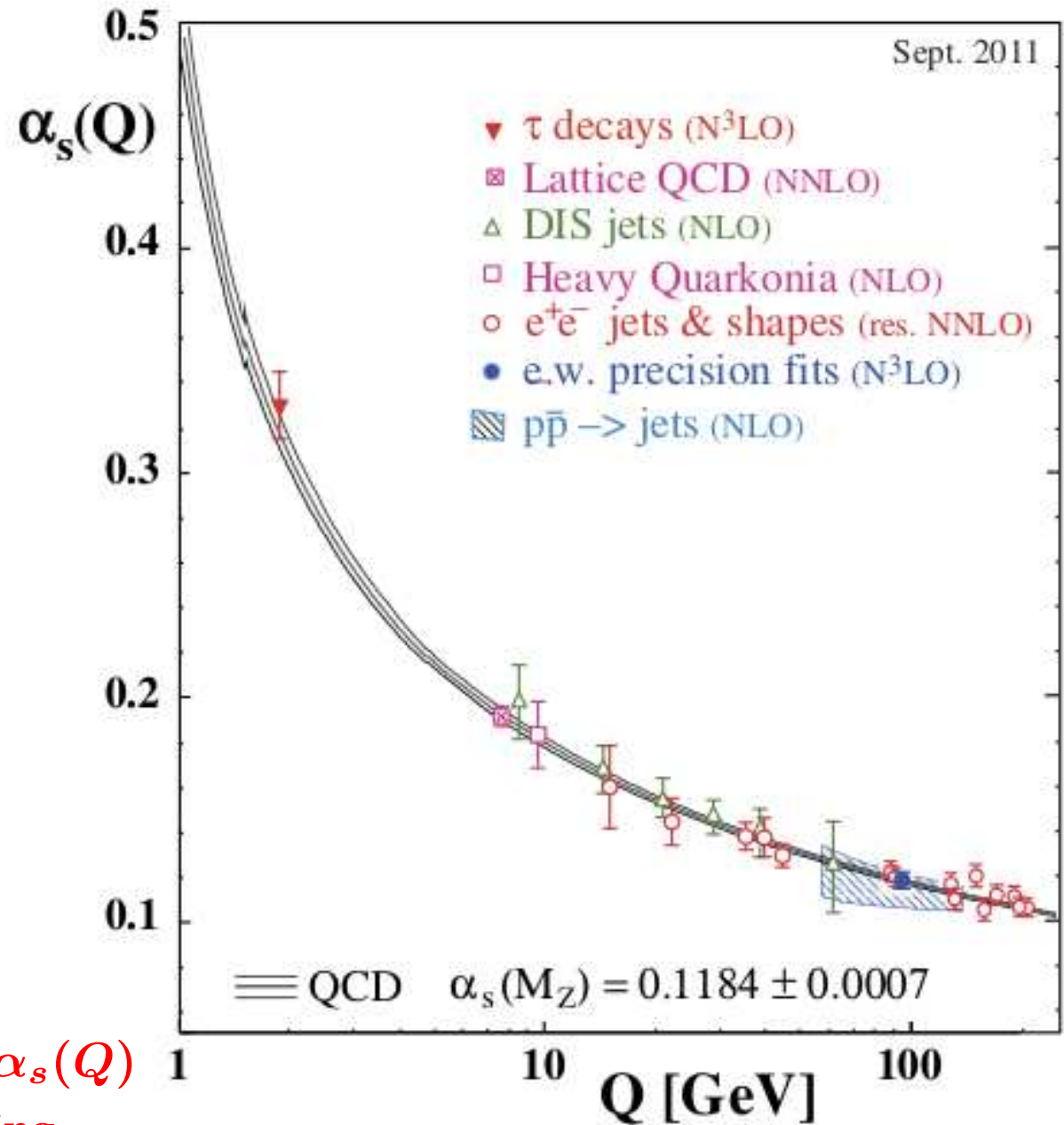
→ **QCD prediction confirmed by data!**

Measurements of α_s

Determinations of $\alpha_s(M_Z)$ in e^+e^- using measurements of event shapes and jet rates for which NNLO calculations are available



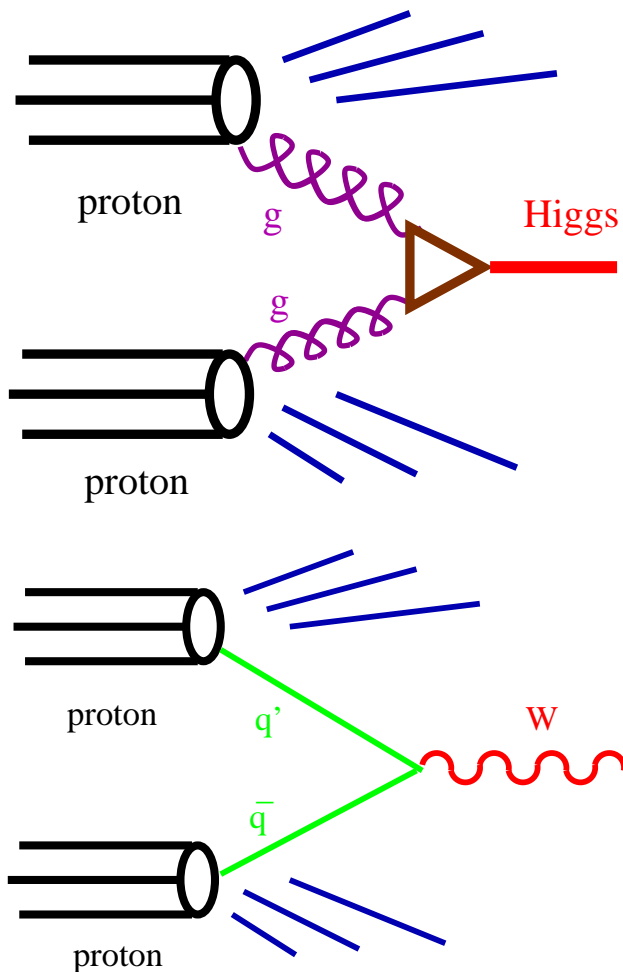
Determinations of $\alpha_s(Q)$
 → test of the running



Structure Functions

Universality (and usefulness) of Proton PDFs

$$\sigma_{pp \rightarrow H(W,Z,\dots)+X} = \sum_{a,b} \int_0^1 dx_1 f_{a/p}(x_1, \mu_F^2) \int_0^1 dx_2 f_{b/p}(x_2, \mu_F^2) \hat{\sigma}_{ab \rightarrow H(W,Z,\dots)}$$



σ_H sensitive to gluon distribution at

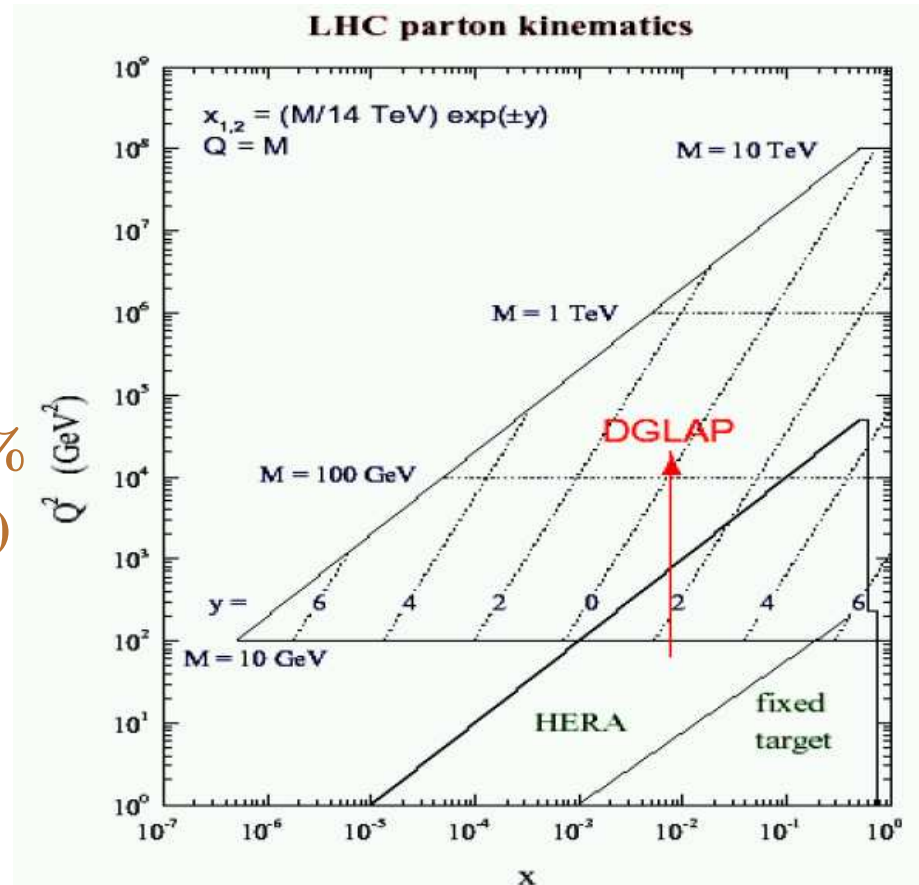
$x \sim \frac{M_H}{\sqrt{s}} \sim 8 \cdot 10^{-3}$
 and $\mu_F^2 \sim M_H^2 \sim 13000 \text{ GeV}^2$;

$\Delta\sigma_H^{PDF} / \sigma_H \sim \pm 3\%$
 (for $M_H = 115 \text{ GeV}$)

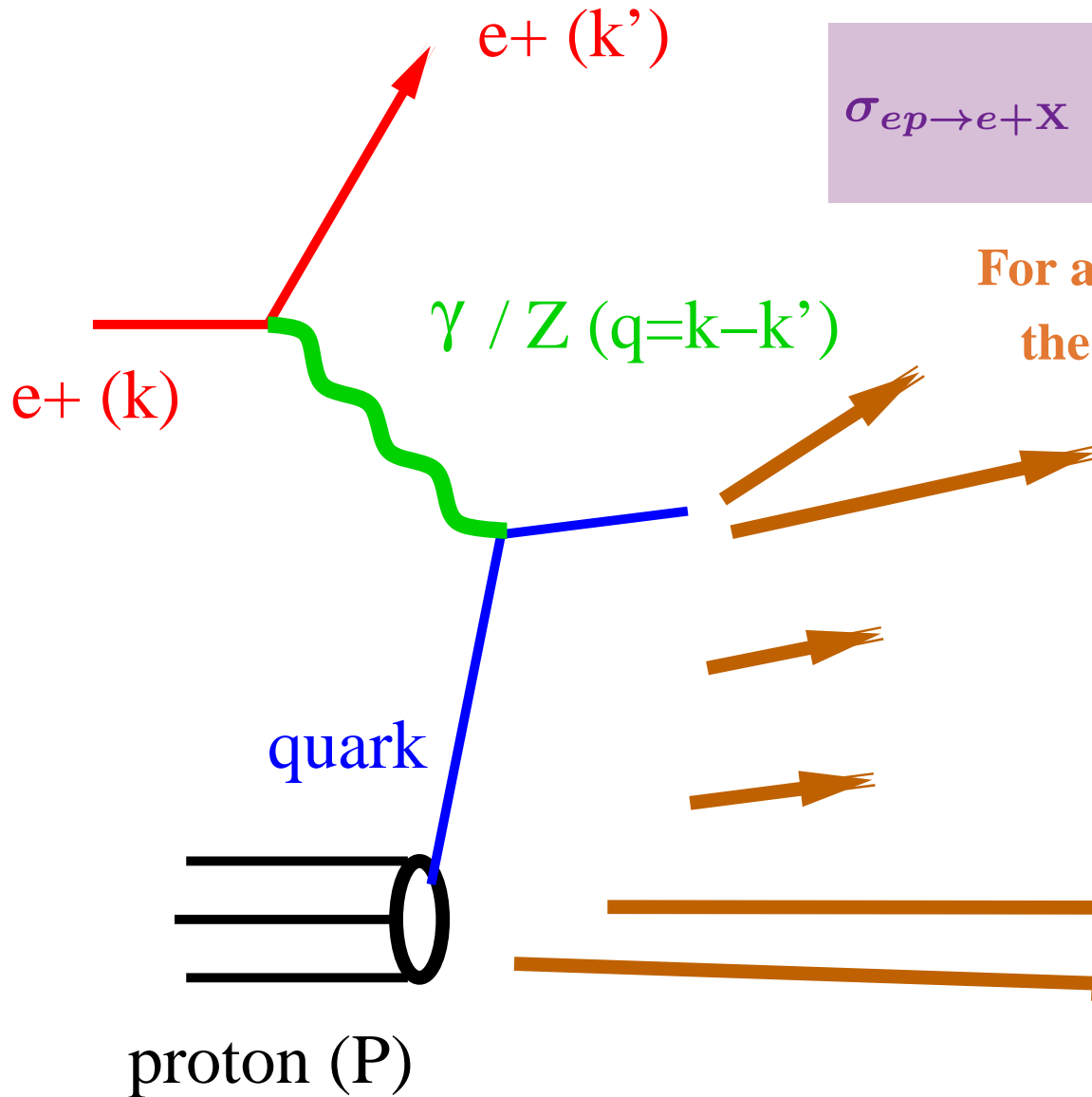
σ_W sensitive to sea distribution at

$x \sim \frac{M_W}{\sqrt{s}} \sim 6 \cdot 10^{-3}$

and $\mu_F^2 \sim M_W^2 \sim 6400 \text{ GeV}^2$; $\Delta\sigma_W^{PDF} / \sigma_W \sim \pm 3\%$



Kinematics of Neutral Current Deep Inelastic Scattering



$$\sigma_{ep \rightarrow e+X} = \sum_a \int_0^1 dx_1 f_{a/p}(x_1, \mu_F^2) \hat{\sigma}_{ea \rightarrow ea}$$

For a given ep centre-of-mass energy, \sqrt{s} ,
the (fully) inclusive cross section for

$$ep \rightarrow e + X$$

can be described by two independent kinematic variables, e.g.

$$Q^2 = -(k - k')^2$$

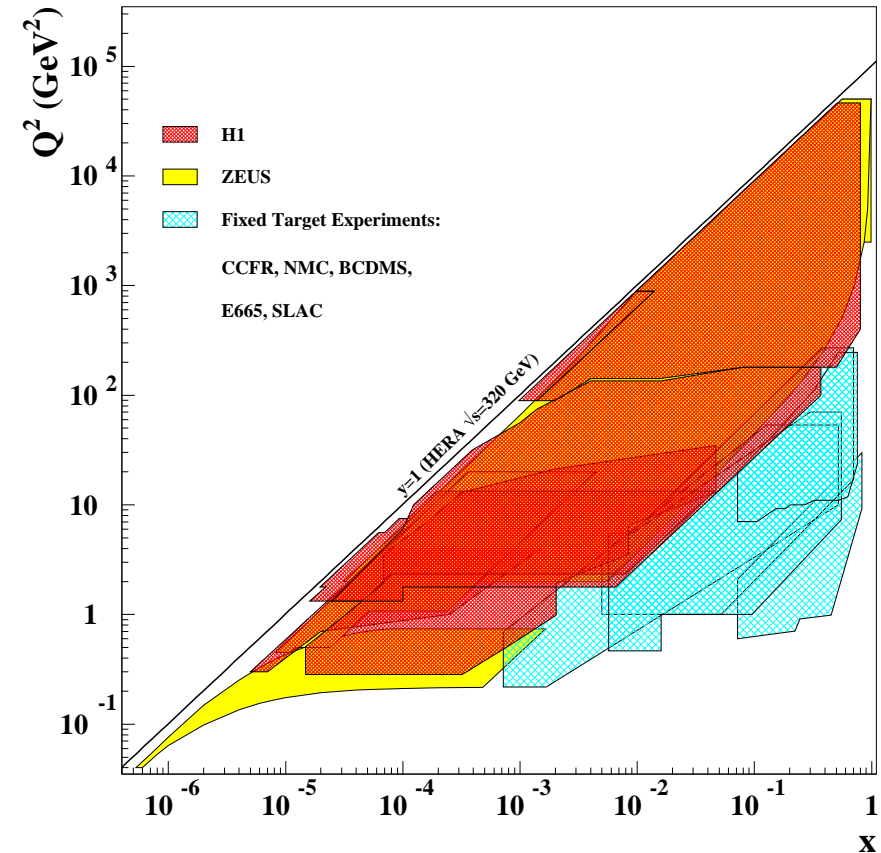
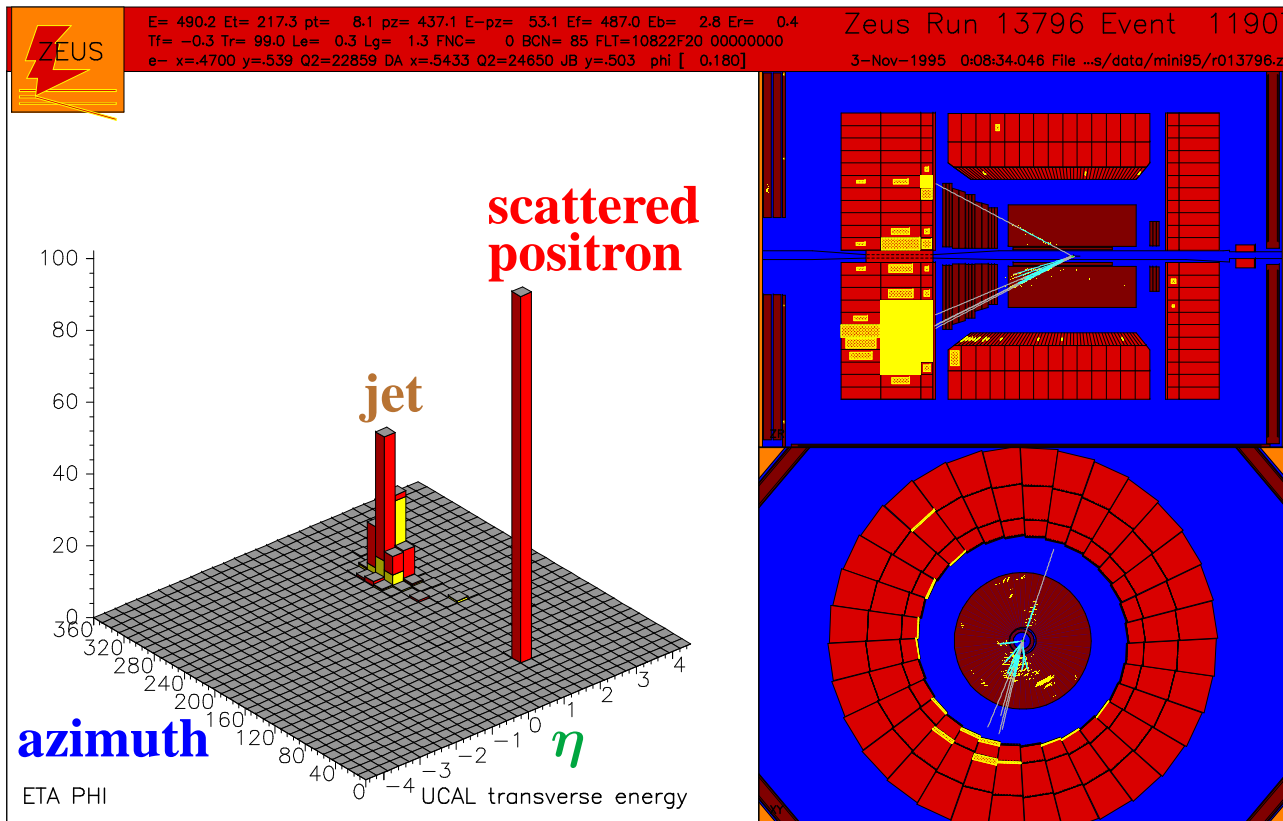
$$x_{Bj} = Q^2 / (2P \cdot q)$$

Neutral Current Deep Inelastic Scattering

- Neutral Current DIS event candidate

$Q^2 \sim 24000 \text{ GeV}^2$ and $x_{Bj} \sim 0.5$

- Coverage of kinematic plane (Q^2, x_{Bj})



Neutral Current Deep Inelastic Scattering

- Inclusive process $e^\pm p \rightarrow e^\pm + X$

$$\frac{d\sigma(e^\pm p)}{dx dQ^2} = \frac{2\pi\alpha^2}{xQ^4} \cdot (\underbrace{Y_+ \cdot F_2(x, Q^2)}_{\text{Dominant}} - \underbrace{y^2 \cdot F_L(x, Q^2)}_{\text{High } y} \mp \underbrace{Y_- \cdot x F_3(x, Q^2)}_{\text{High } Q^2})$$

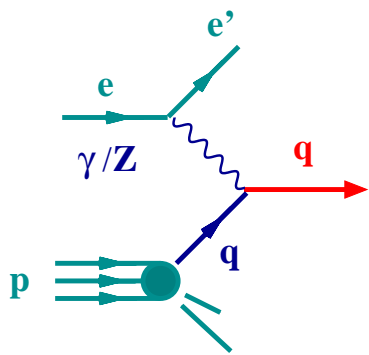
where $Y_\pm = 1 \pm (1 - y)^2$ and $y = Q^2 / (sx)$ (inelasticity parameter)

- Structure functions of the proton (F_2, F_L, F_3) and QCD

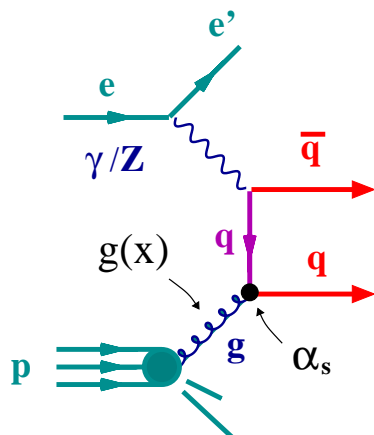
→ $F_2 \sim x \sum_i e_i^2 \cdot (q_i(x, Q^2) + \bar{q}_i(x, Q^2))$ for $Q^2 \ll M_Z^2$

→ the longitudinal structure function $F_L = 0$ in the quark-parton model

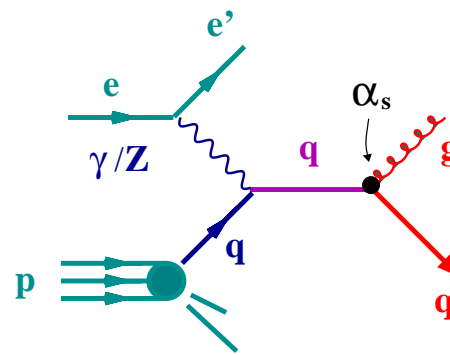
→ parity-violating term F_3 is small for $Q^2 \ll M_Z^2$



Quark-Parton Model



Boson-Gluon Fusion



QCD Compton

Clean probe of the Parton Distribution Functions in the Proton $q_i(x, Q^2), \bar{q}_i(x, Q^2), g(x, Q^2)$

Determination of $F_2^{\text{em}}(x, Q^2)$

- Measurement of the doubly-differential cross section $d\sigma(e^+p)/dx dQ^2$ for the reaction $e^+p \rightarrow e^+ + X$ over a large range $2.7 < Q^2 < 30000 \text{ GeV}^2, 6 \cdot 10^{-5} < x < 0.65$

- Extraction of $F_2^{\text{em}}(x, Q^2)$ from the reduced cross section (corrected for QED effects):

$$\tilde{\sigma}(e^+p) = (2\pi\alpha^2 Y_+ / xQ^4)^{-1} d\sigma_{\text{Born}} / dx dQ^2$$

$$F_2 = F_2^{\text{em}} + F_2^{\text{int}} \cdot \eta_{\gamma Z} + F_2^{\text{wk}} \cdot \eta_Z^2$$

$$= F_2^{\text{em}}(1 + \Delta_{F_2})$$

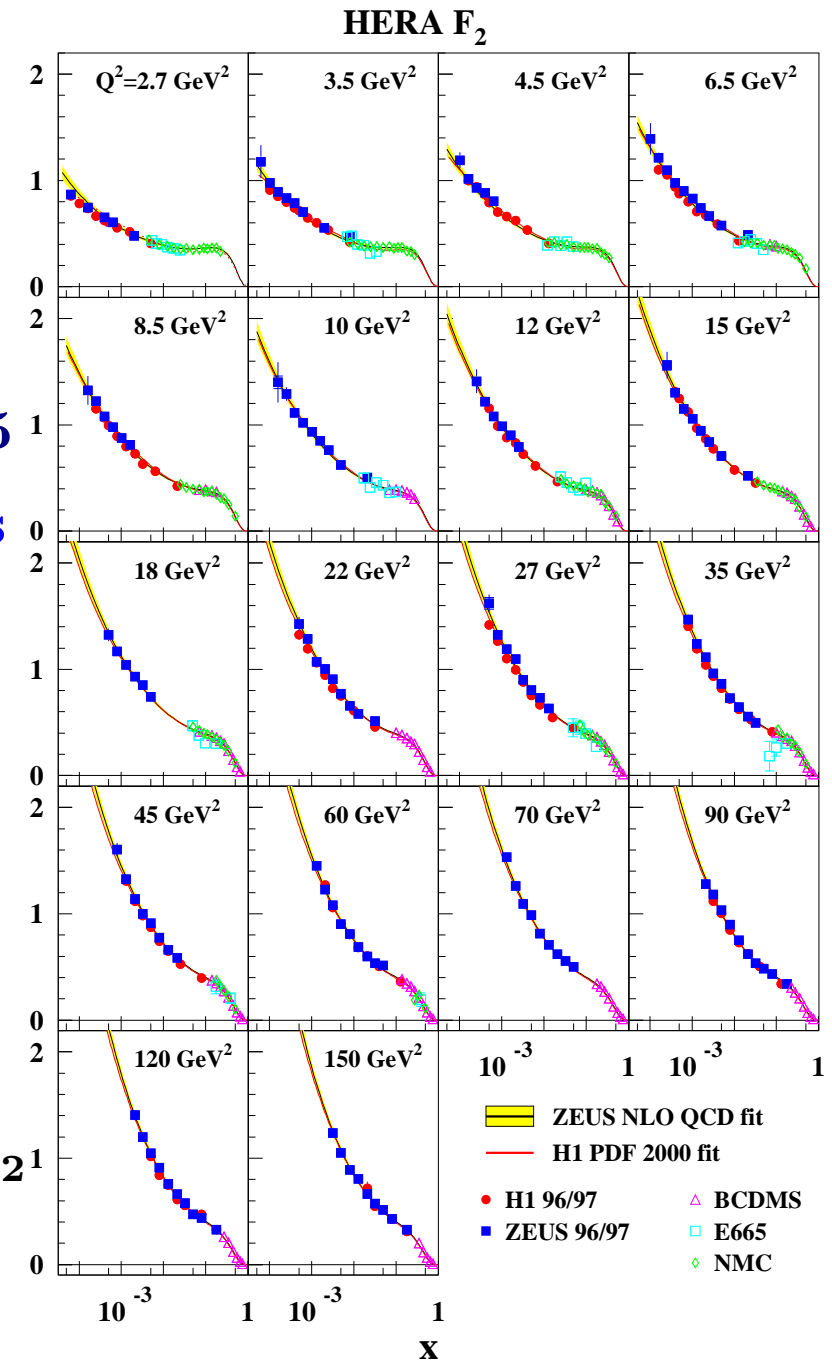
where $\eta_{\gamma Z} = Q^2 / (Q^2 + M_Z^2)$

$$\Rightarrow \tilde{\sigma}(e^+p) = F_2^{\text{em}}(1 + \Delta_{F_2} + \Delta_{F_3} + \Delta_{F_L})$$

- Typical precision 2-3%

→ systematic uncertainties dominate $Q^2 < 800 \text{ GeV}^2$

- Striking rise of F_2^{em} as x decreases



$F_2^{\text{em}}(x, Q^2)$ provides...

→ direct information on quark densities

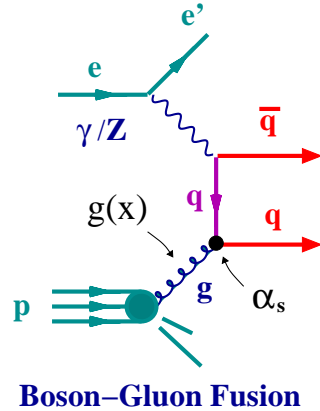
$$F_2 \sim x \sum_i e_i^2 \cdot (q_i + \bar{q}_i)$$

→ indirect information on gluon density

● Large and positive scaling violations at low x

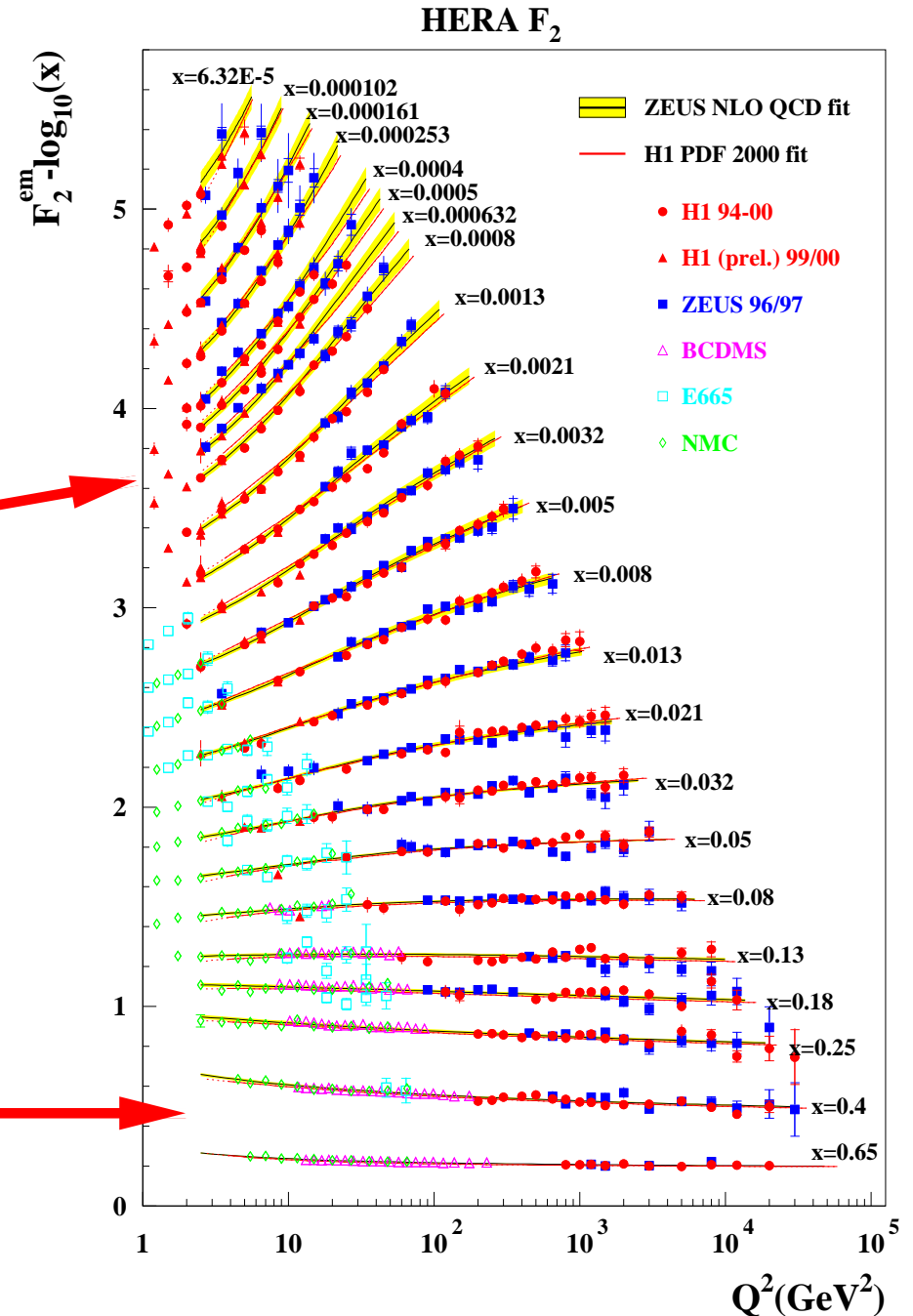
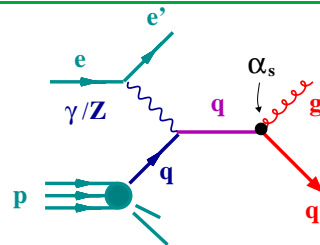
dominance of BGF

$$\partial F_2 / \partial \ln Q^2 \sim \alpha_s \cdot xg$$



● Aproximate scaling for $x \sim 0.1$

● Mild and negative scaling violations at high x



Determination of the Parton Distribution Functions in the Proton

- In order to determine the proton PDFs additional experimental information is needed on
 - quark densities at high x
 - **flavour composition of the sea**
- Additional data sets
 - F_2 data on μp scattering from BCDMS, NMC and E665 \Rightarrow mid/high- x
 - **Deuterium-target data from NMC and E665 $\Rightarrow \bar{u}, \bar{d}$**
 - NMC data on the ratio $F_2^D / F_2^P \Rightarrow$ high- x d/u
 - $x F_3$ data from CCFR (ν -Fe interactions) \Rightarrow high- x

- Global analysis using DGLAP evolution equations at next-to-leading order (NLO) in α_s

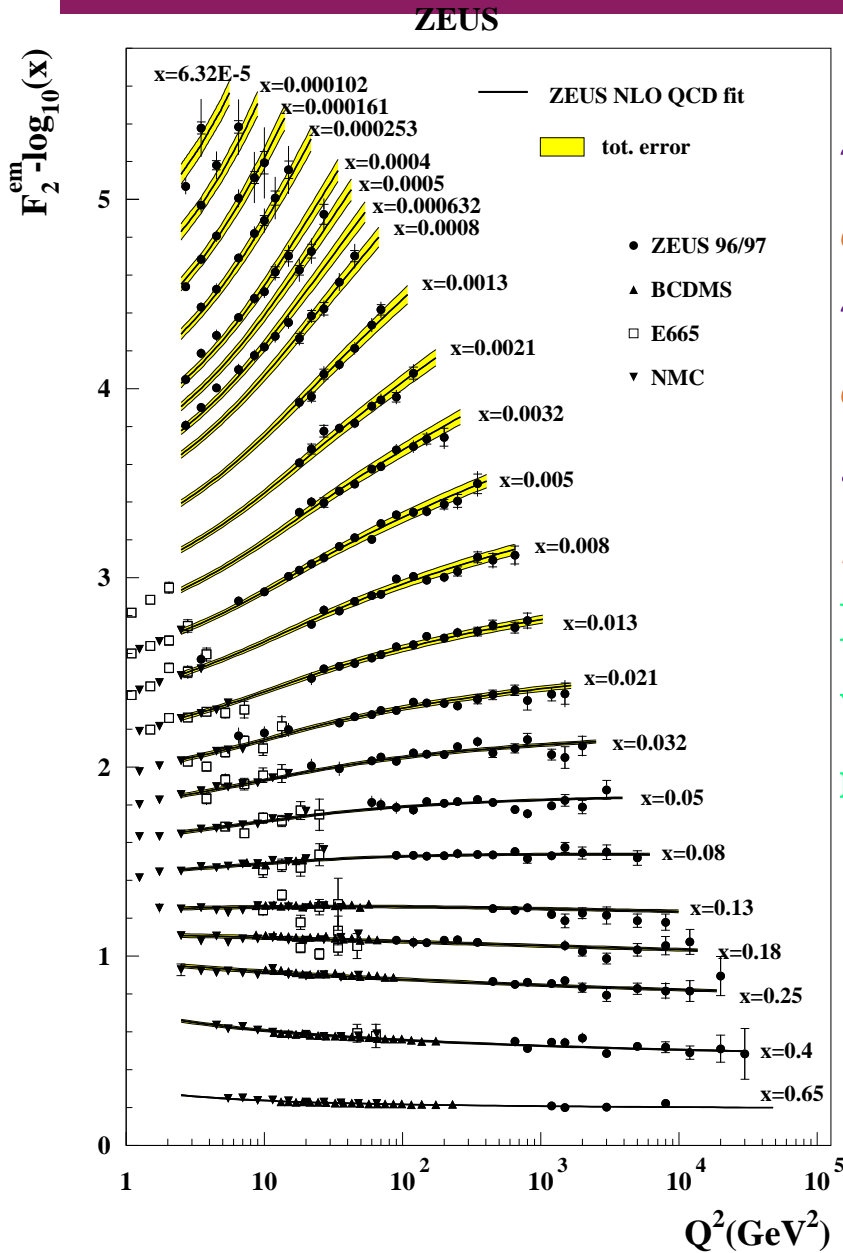
$$\frac{\partial q_i(x, \mu^2)}{\partial \ln \mu^2} = \frac{\alpha_s(\mu^2)}{2\pi} \int_x^1 \frac{dz}{z} \left(\sum_j P_{q_i q_j} \cdot q_j(x/z, \mu^2) + P_{q_i g} \cdot g(x/z, \mu^2) \right)$$

$$\frac{\partial g(x, \mu^2)}{\partial \ln \mu^2} = \frac{\alpha_s(\mu^2)}{2\pi} \int_x^1 \frac{dz}{z} \left(\sum_j P_{g q_j} \cdot q_j(x/z, \mu^2) + P_{g g} \cdot g(x/z, \mu^2) \right)$$

The DGLAP equations yield the proton PDFs at any value of Q^2 provided they are input as functions of x at some input scale Q_0^2

→ number sum rules and the momentum sum rule are imposed

Determination of the Parton Distribution Functions in the Proton



$$u = u_V + u_{sea}$$

$$d = d_V + d_{sea}$$

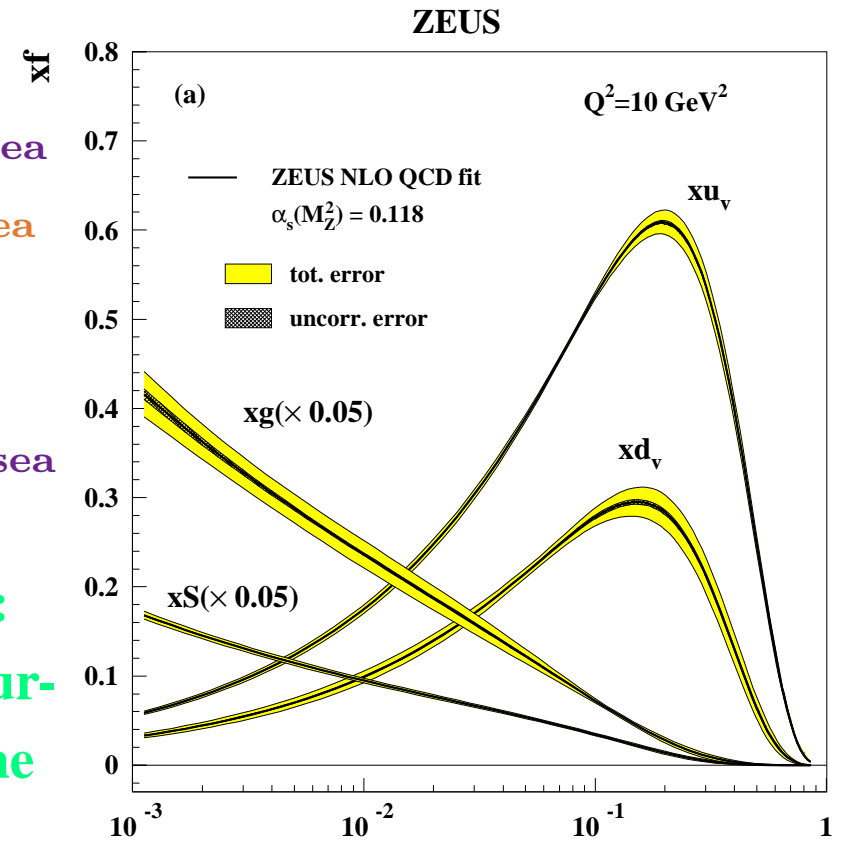
$$\bar{u} = \bar{u}_{sea}$$

$$\bar{d} = \bar{d}_{sea}$$

$$s = s_{sea} = \bar{s}_{sea}$$

$$S = \text{total sea}$$

Heavy quarks:
variable-flavour-
number scheme



Fit of ZEUS data and fixed-target data in the region $2.5 < Q^2 < 30000 \text{ GeV}^2$, $6.3 \cdot 10^{-5} < x < 0.65$ and $W^2 > 20 \text{ GeV}^2$ (1263 data points)

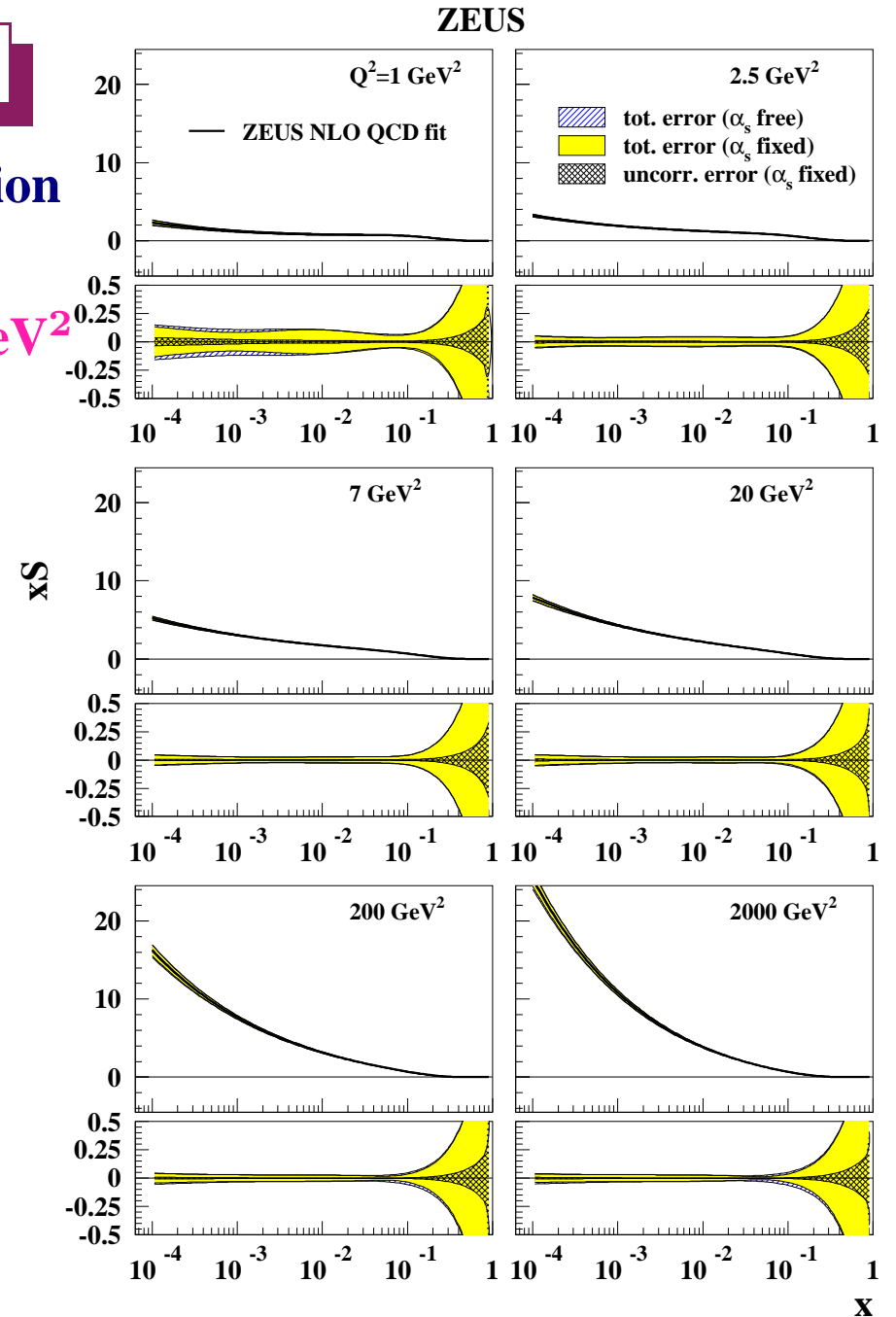
Full account of correlated exp. uncertainties

→ Good description of Struct. Func. data

⇒ Determination of proton PDFs

Determination of the Sea Distribution

- The total sea distribution $xS(x, Q^2)$ as a function of x for different Q^2 values \Rightarrow
- Its uncertainty is below $\sim 5\%$ for $Q^2 > 2.5 \text{ GeV}^2$ and $10^{-4} < x < 0.1$



Determination of the Gluon Distribution

- The gluon distribution $xg(x, Q^2)$ as a function of x for different Q^2 values \Rightarrow
- Its uncertainty is $\sim 10\%$ for $Q^2 \sim 20 \text{ GeV}^2$ and $10^{-4} < x < 0.1$
- \rightarrow the uncertainty decreases as Q^2 increases

Determination of α_s

- Inclusion of low- x data allows a simultaneous (and precise) determination of PDFs and α_s :

$$\alpha_s(M_Z) = 0.1166 \pm 0.0008(\text{uncorr})$$

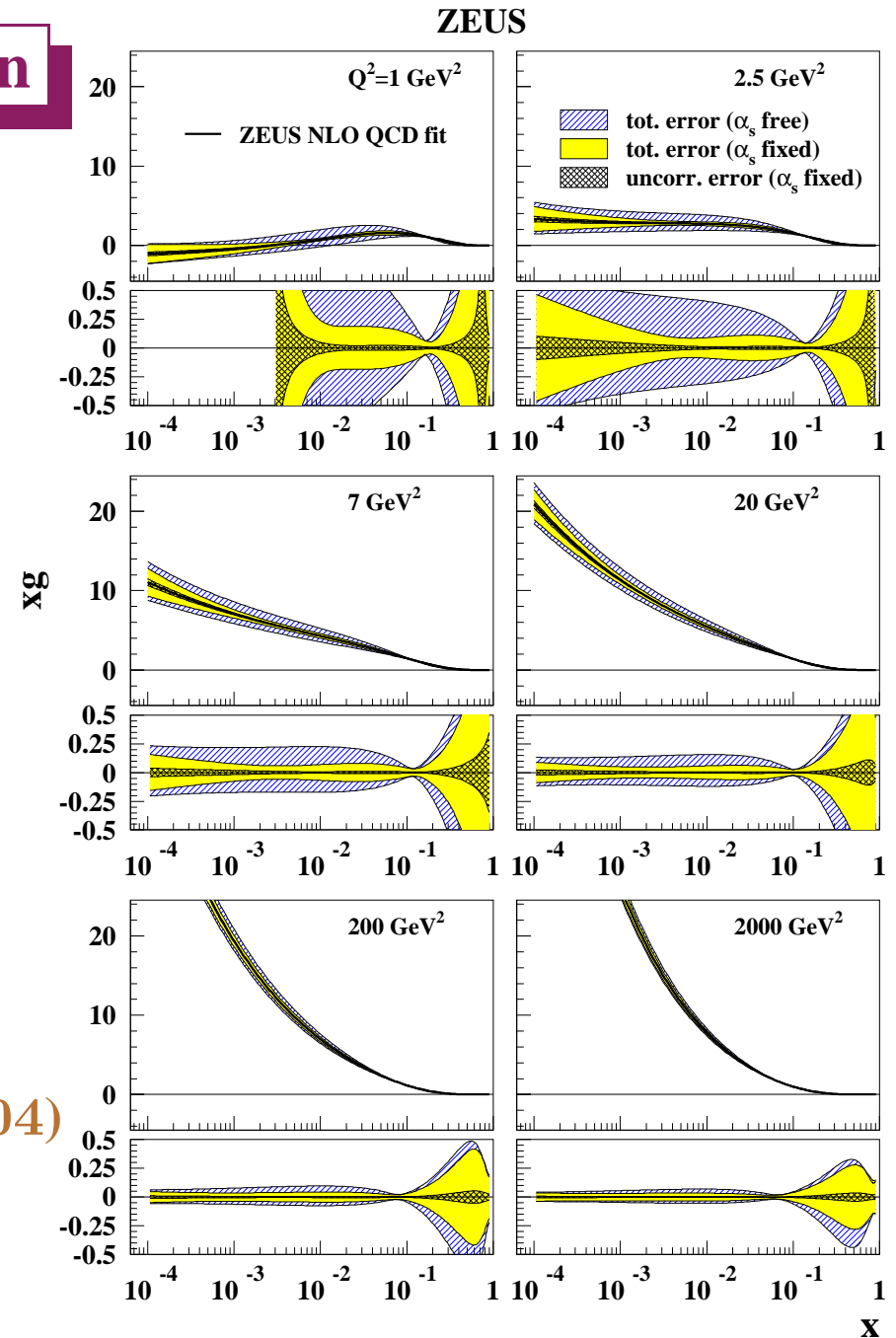
$$\pm 0.0032(\text{corr}) \pm 0.0036(\text{norm})$$

$$\pm 0.0018(\text{model}) \Rightarrow 0.1166 \pm 0.0052$$

(+theor. unc. due to terms beyond NLO $\sim \pm 0.004$)

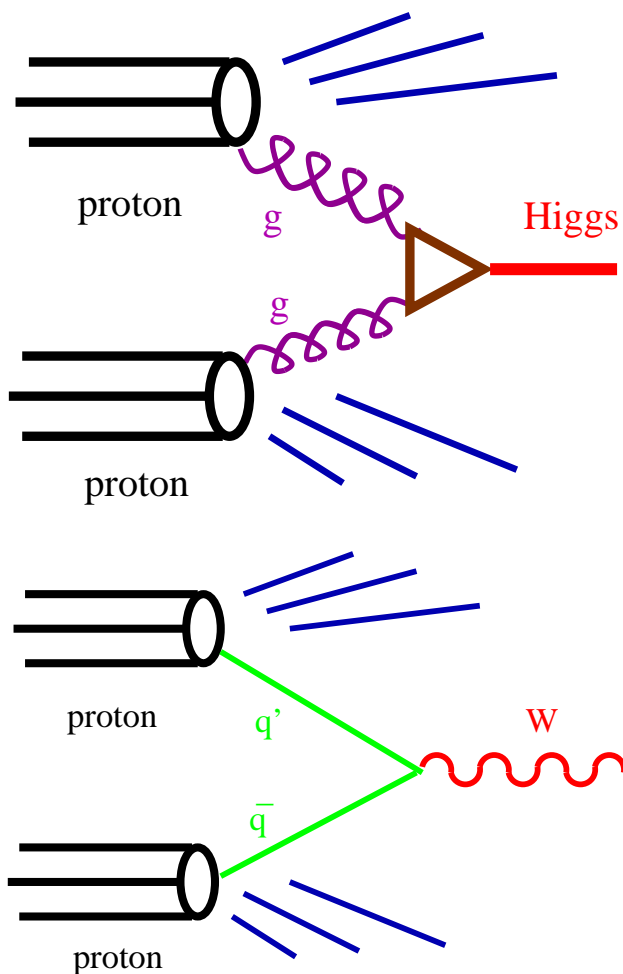
- Consistent with world average (Bethke, 2011):

$$\rightarrow \alpha_s(M_Z) = 0.1184 \pm 0.0007$$



Universality (and usefulness) of Proton PDFs

$$\sigma_{pp \rightarrow H(W,Z,\dots)+X} = \sum_{a,b} \int_0^1 dx_1 f_{a/p}(x_1, \mu_F^2) \int_0^1 dx_2 f_{b/p}(x_2, \mu_F^2) \hat{\sigma}_{ab \rightarrow H(W,Z,\dots)}$$



σ_H sensitive to gluon distribution at

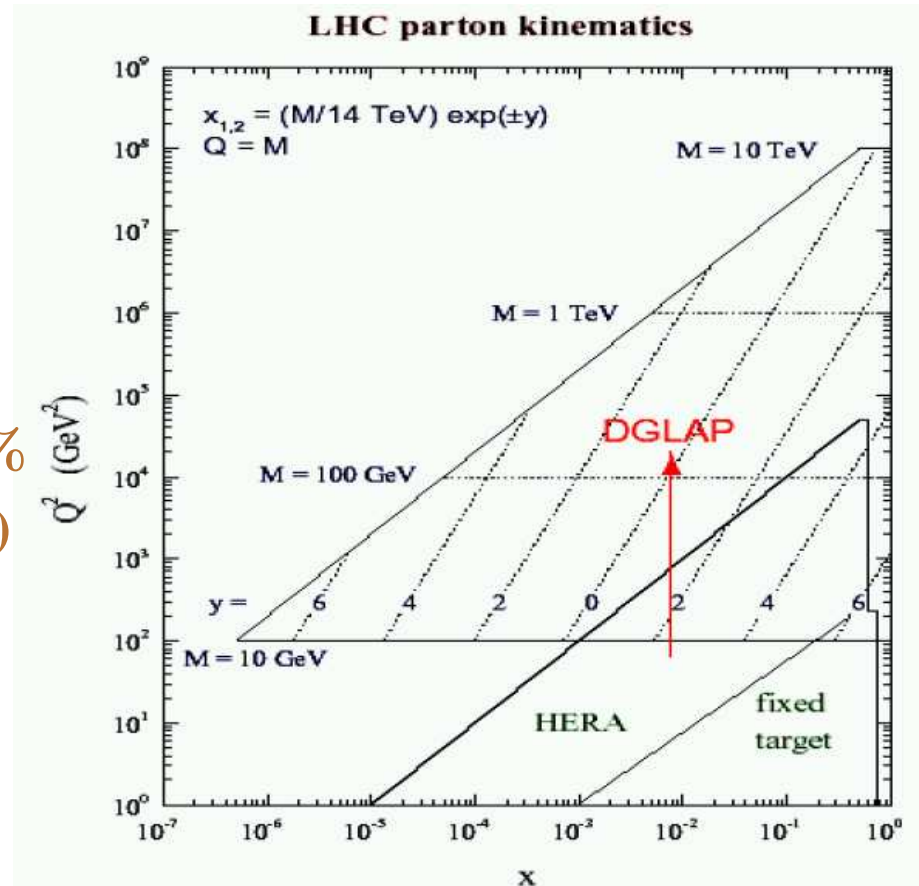
$x \sim \frac{M_H}{\sqrt{s}} \sim 8 \cdot 10^{-3}$
 and $\mu_F^2 \sim M_H^2 \sim 13000 \text{ GeV}^2$;

$\Delta\sigma_H^{PDF} / \sigma_H \sim \pm 3\%$
 (for $M_H = 115 \text{ GeV}$)

σ_W sensitive to sea distribution at

$x \sim \frac{M_W}{\sqrt{s}} \sim 6 \cdot 10^{-3}$
 and $\mu_F^2 \sim M_W^2 \sim 6400 \text{ GeV}^2$;

$\Delta\sigma_W^{PDF} / \sigma_W \sim \pm 3\%$

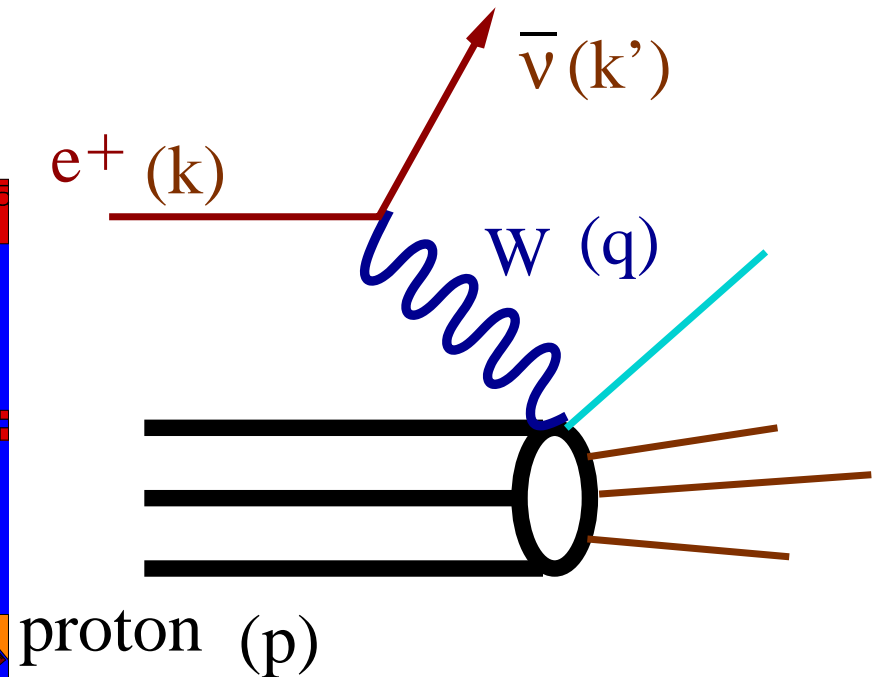
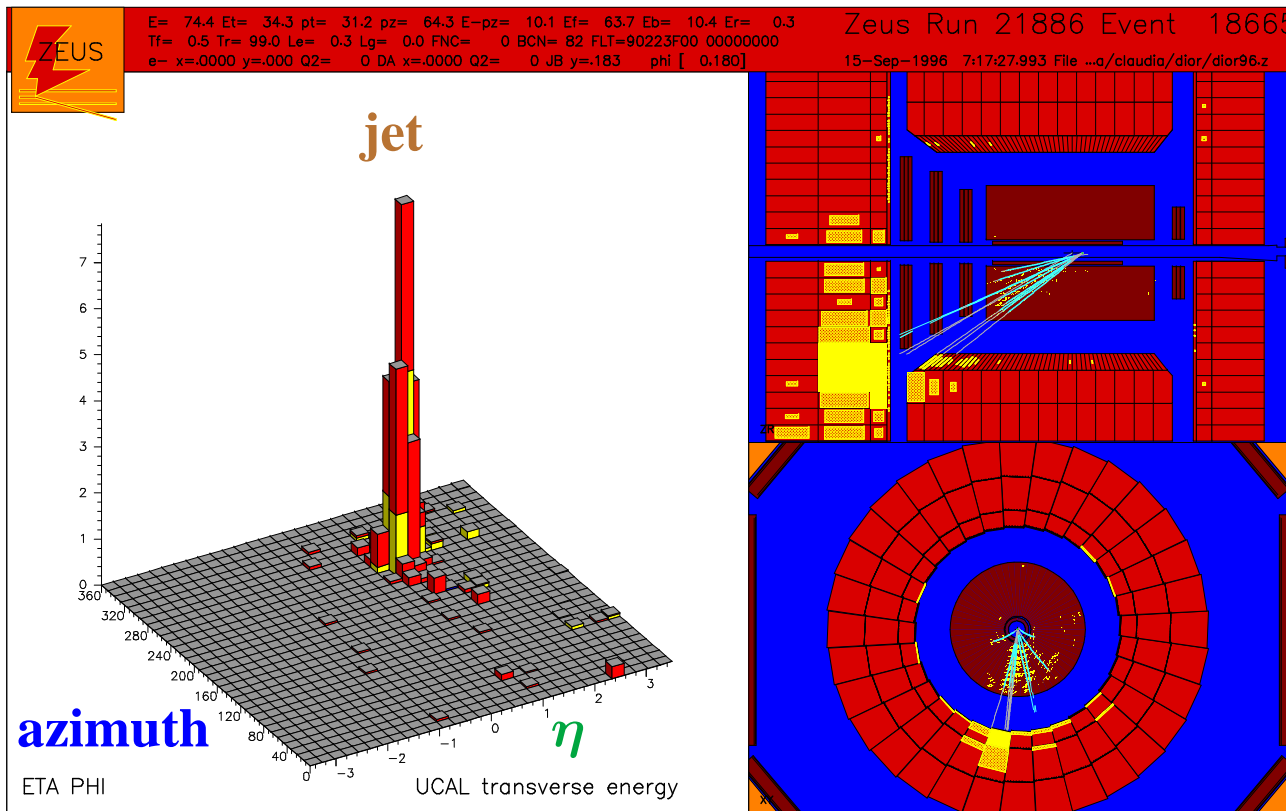


Structure Functions (II)

Charged Current Deep Inelastic Scattering

● Charged Current DIS event candidate

$Q^2 \sim 1200 \text{ GeV}^2$ and $x_{Bj} \sim 0.06$



Charged Current Deep Inelastic Scattering

- Measurements of the differential cross section

$d\sigma/dQ^2$ in Charged Current DIS $e^\pm p$

$$ep \rightarrow \nu + X$$

- Cross-section formulae in LO QCD

$$\frac{d\sigma(e^+p)}{dx dQ^2} = \frac{G_F^2}{2\pi} \eta_W^2 \cdot \sum_i (\bar{u}_i + (1-y)^2 d_i)$$

$$\frac{d\sigma(e^-p)}{dx dQ^2} = \frac{G_F^2}{2\pi} \eta_W^2 \cdot \sum_i (u_i + (1-y)^2 \bar{d}_i)$$

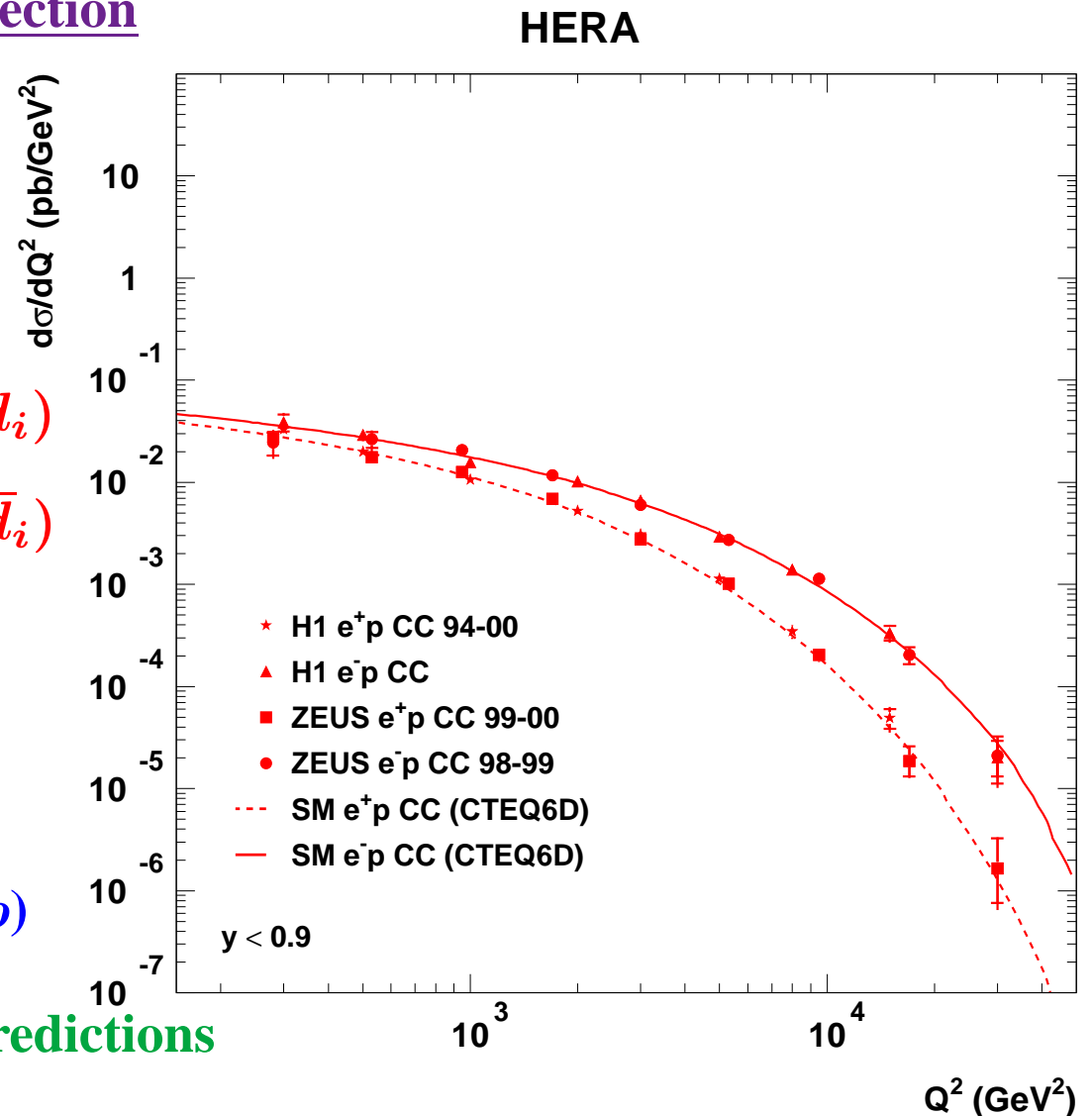
where $\eta_W = M_W^2 / (Q^2 + M_W^2)$

⇒ W -Propagator effects

⇒ flavour selection:

d (u)-quark contributes only to e^+p (e^-p)

- Good description by Standard Model Predictions up to the highest $Q^2 \sim 30000 \text{ GeV}^2$



Neutral Current Deep Inelastic Scattering

- Measurements of the differential cross section

$d\sigma/dQ^2$ in Neutral Current DIS $e^\pm p$

$$ep \rightarrow e + X$$

- Cross-section formulae in LO QCD

$$\frac{d\sigma(e^\pm p)}{dx dQ^2} = \frac{2\pi\alpha^2}{xQ^4} \cdot (Y_+ \cdot F_2(x, Q^2) -$$

$$-y^2 \cdot F_L(x, Q^2) \mp Y_- \cdot xF_3(x, Q^2))$$

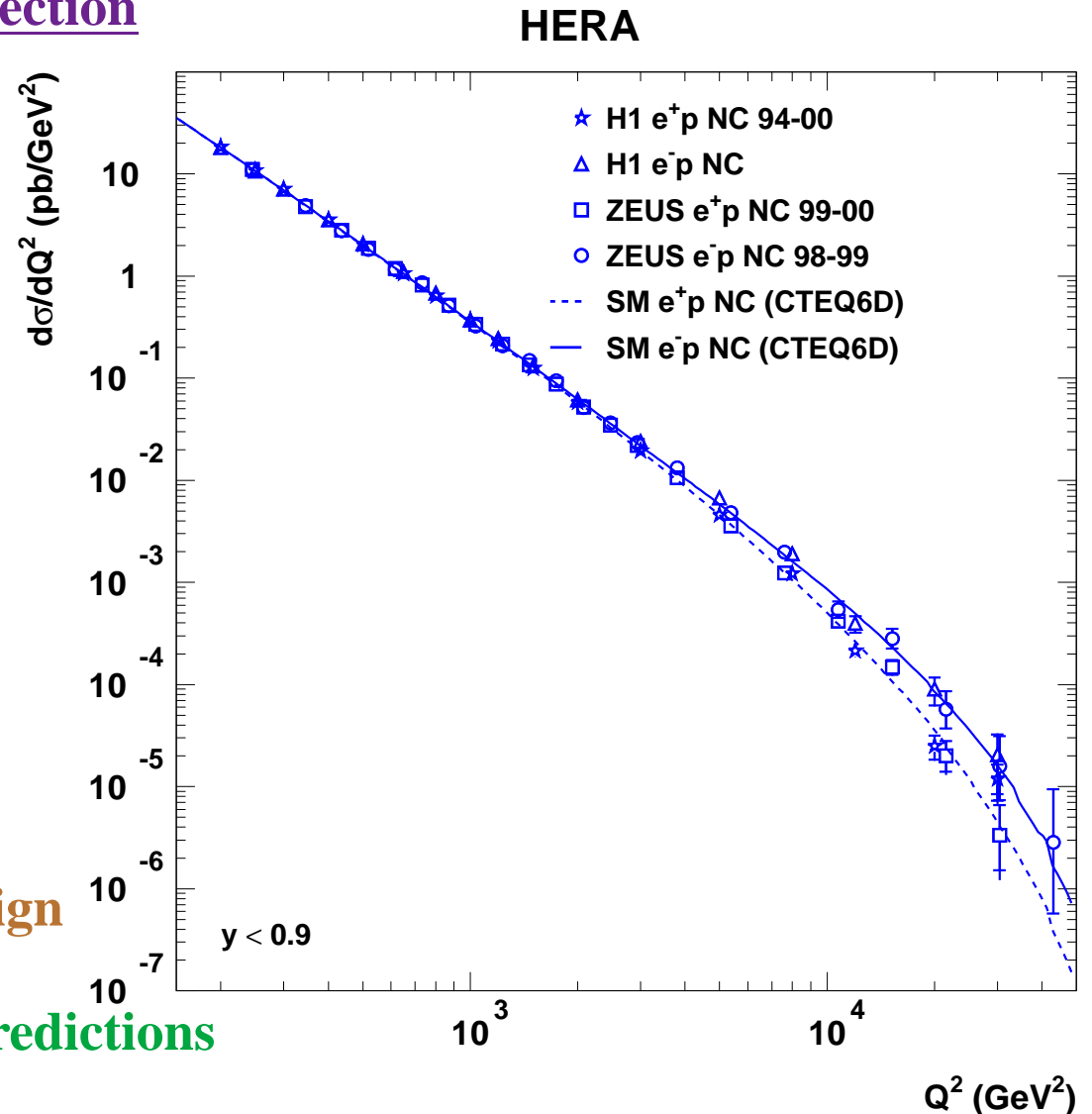
$$F_2 = F_2^{\text{em}} + F_2^{\text{int}} \cdot \eta_{\gamma Z} + F_2^{\text{wk}} \cdot \eta_{\gamma Z}^2$$

$$\text{where } \eta_{\gamma Z} = Q^2 / (Q^2 + M_Z^2)$$

⇒ Z-Propagator effects

⇒ Parity-violating term (F_3) changes sign

- Good description by Standard Model Predictions up to the highest $Q^2 \sim 40000 \text{ GeV}^2$



Neutral vs Charged Current Deep Inelastic Scattering

- Measurements of the differential cross section

$d\sigma/dQ^2$ in Neutral Current DIS $e^\pm p$

$$\frac{d\sigma(e^\pm p)}{dx dQ^2} = \frac{2\pi\alpha^2}{xQ^4} \cdot (Y_+ \cdot F_2(x, Q^2) - y^2 \cdot F_L(x, Q^2) \mp Y_- \cdot xF_3(x, Q^2))$$

$$F_2 = F_2^{\text{em}} + F_2^{\text{int}} \cdot \eta_{\gamma Z} + F_2^{\text{wk}} \cdot \eta_{\gamma Z}$$

where $\eta_{\gamma Z} = Q^2 / (Q^2 + M_Z^2)$

and Charged Current DIS $e^\pm p$

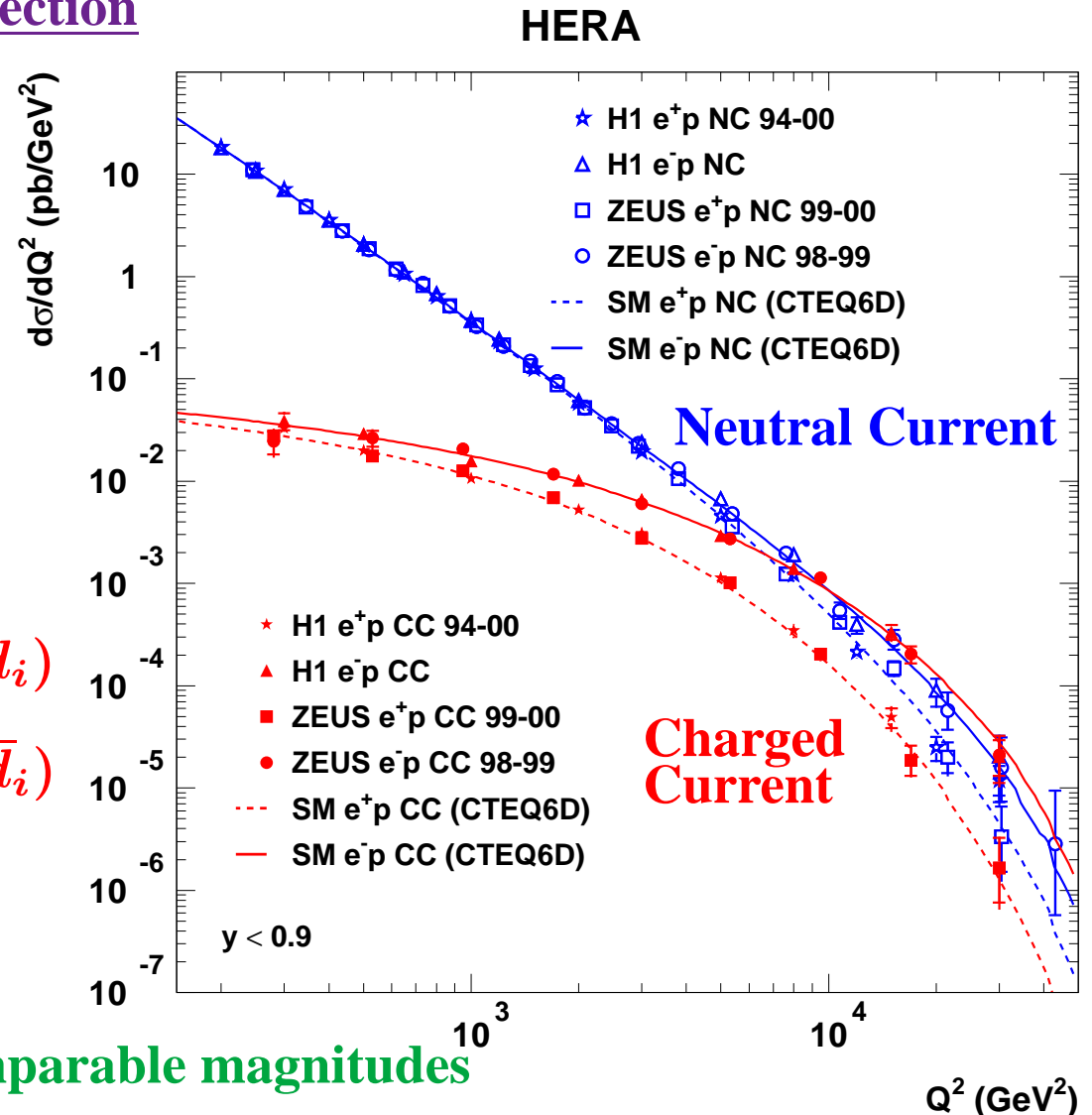
$$\frac{d\sigma(e^+ p)}{dx dQ^2} = \frac{G_F^2}{2\pi} \eta_W^2 \cdot \sum_i (\bar{u}_i + (1-y)^2 d_i)$$

$$\frac{d\sigma(e^- p)}{dx dQ^2} = \frac{G_F^2}{2\pi} \eta_W^2 \cdot \sum_i (u_i + (1-y)^2 \bar{d}_i)$$

where $\eta_W = M_W^2 / (Q^2 + M_W^2)$

- NC and CC DIS cross sections have comparable magnitudes

at $Q^2 \sim M_W^2 \sim M_Z^2 \sim 10^4 \text{ GeV}^2 \Rightarrow$ **Direct observation of electroweak unification**



Charged Current Deep Inelastic e^+p Scattering

- Measurement of the reduced cross section in CC DIS:

$$\tilde{\sigma}(e^+p) = (G_F^2 \eta_W^2 / 2\pi x)^{-1} d\sigma_{\text{Born}} / dx dQ^2$$

→ Sensitivity to flavour composition

$$\tilde{\sigma}(e^+p) = x(\bar{u} + \bar{c} + (1 - y)^2(d + s))$$

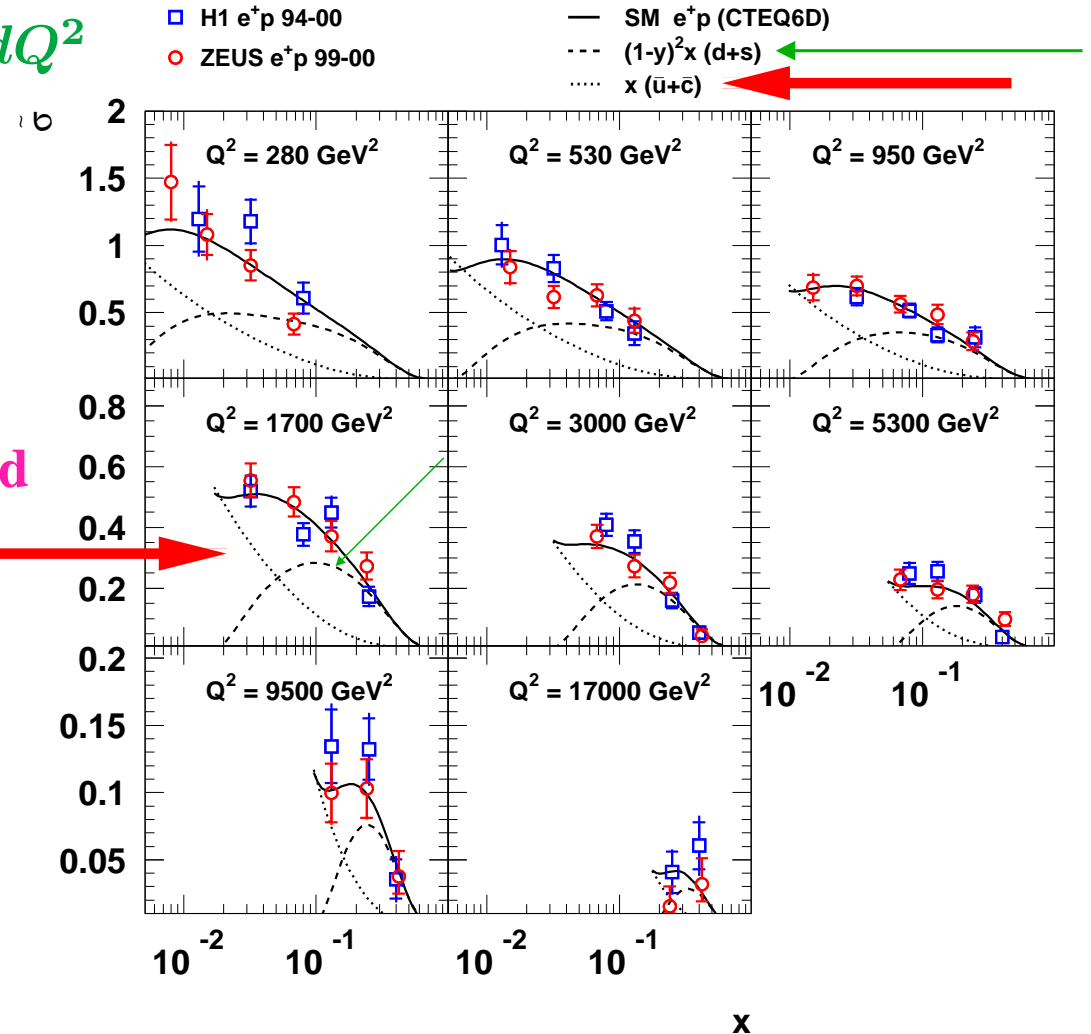
→ Sensitivity to valence quarks

$$\tilde{\sigma}(e^+p) \rightarrow x(1 - y)^2 d_V \text{ (high-}x\text{)}$$

- Good description by SM predictions based on CTEQ6 parametrizations of PDFs

→ valence quarks and flavour composition determined from fixed-target data

HERA e^+p Charged Current



Charged Current Deep Inelastic e^-p Scattering

- Measurement of the reduced cross section in CC DIS:

$$\tilde{\sigma}(e^-p) = (G_F^2 \eta_W^2 / 2\pi x)^{-1} d\sigma_{\text{Born}} / dx dQ^2$$

→ Sensitivity to flavour composition

$$\tilde{\sigma}(e^-p) = x(u + c + (1 - y)^2(\bar{d} + \bar{s}))$$

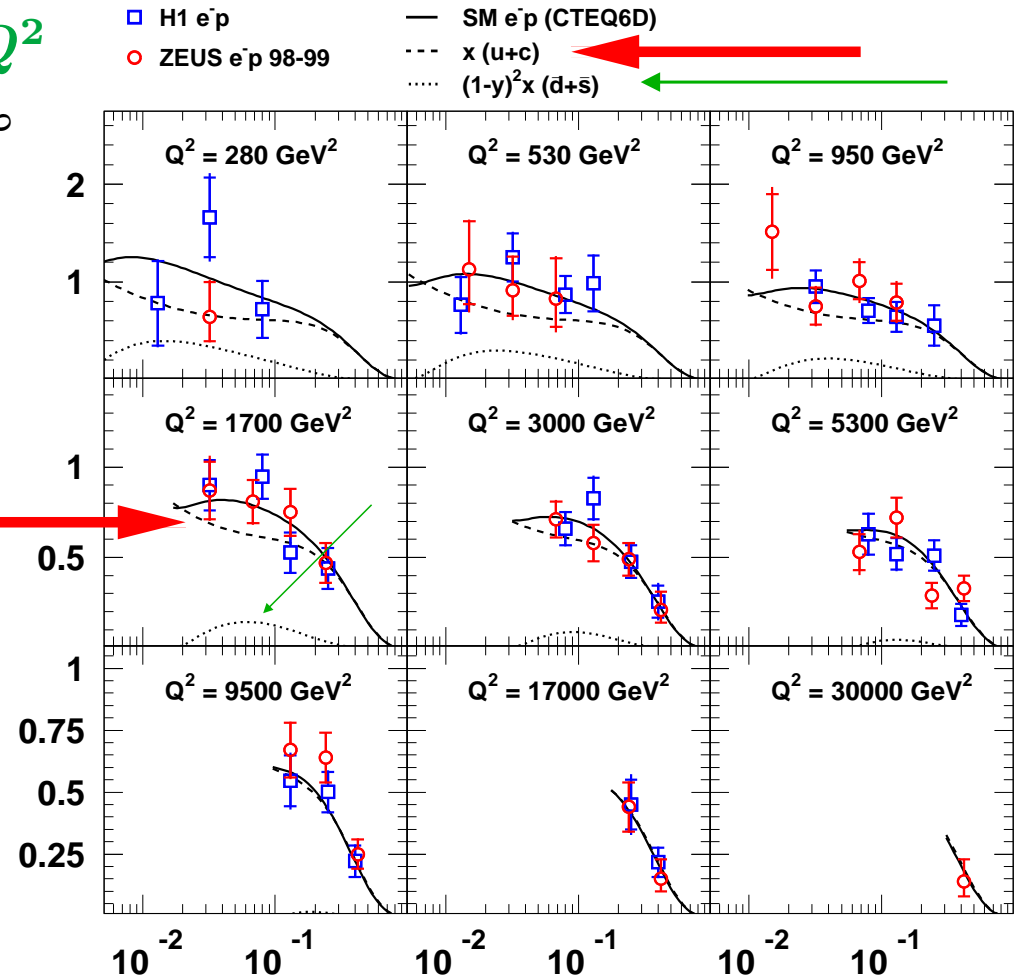
→ Sensitivity to valence quarks

$$\tilde{\sigma}(e^-p) \rightarrow xu_V \text{ (high-}x\text{)}$$

- Good description by SM predictions based on CTEQ6 parametrizations of PDFs

→ valence quarks and flavour composition determined from fixed-target data

HERA e^-p Charged Current



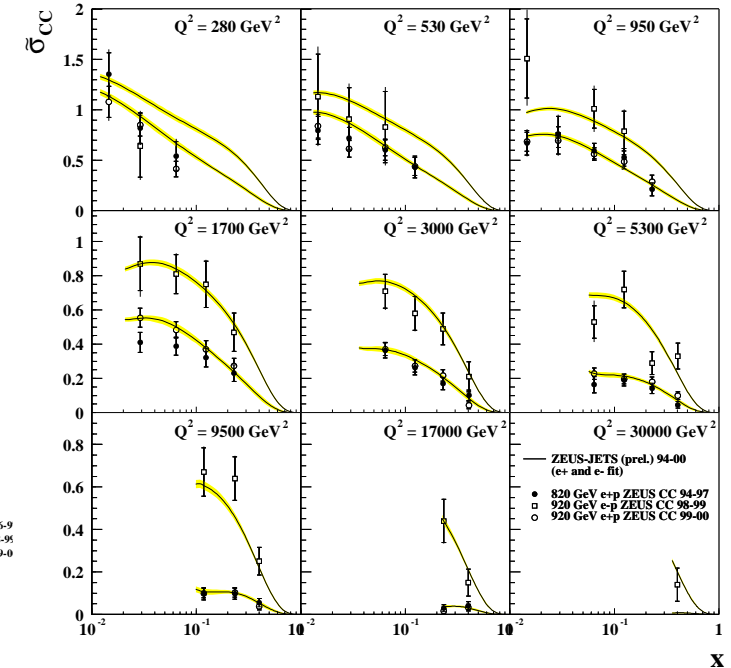
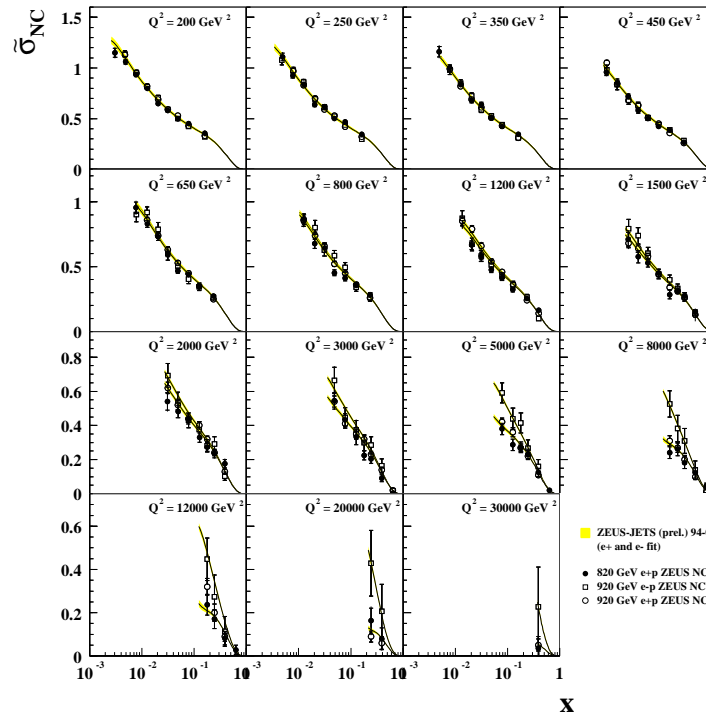
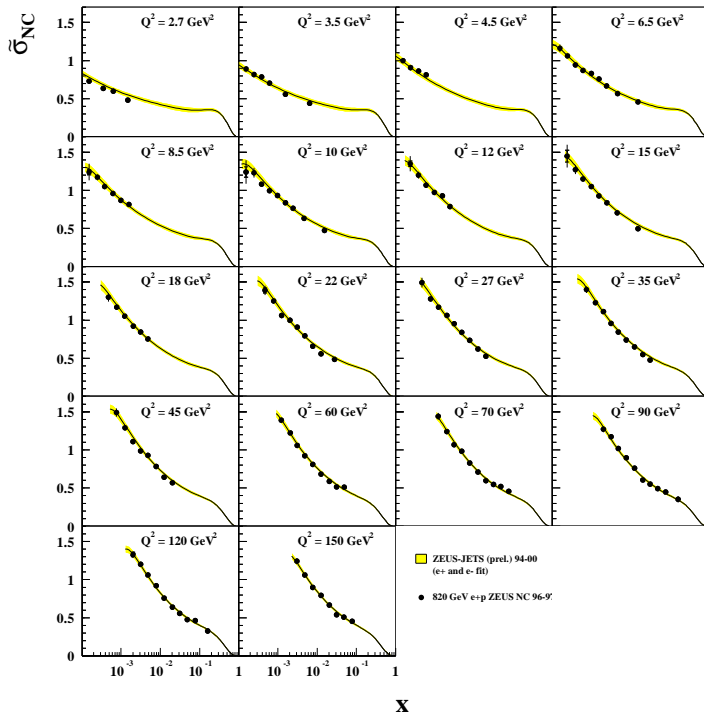
x

Determination of the Proton PDFs with ZEUS data alone

ZEUS NC DIS low Q^2

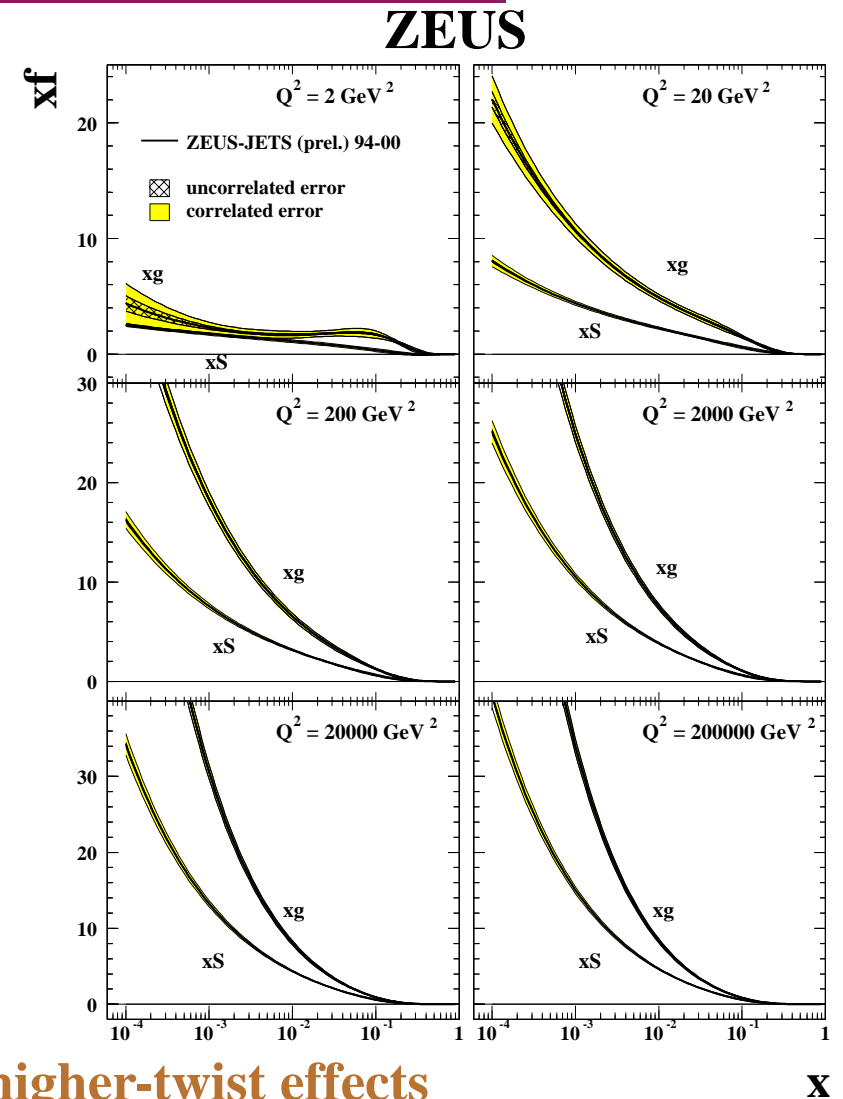
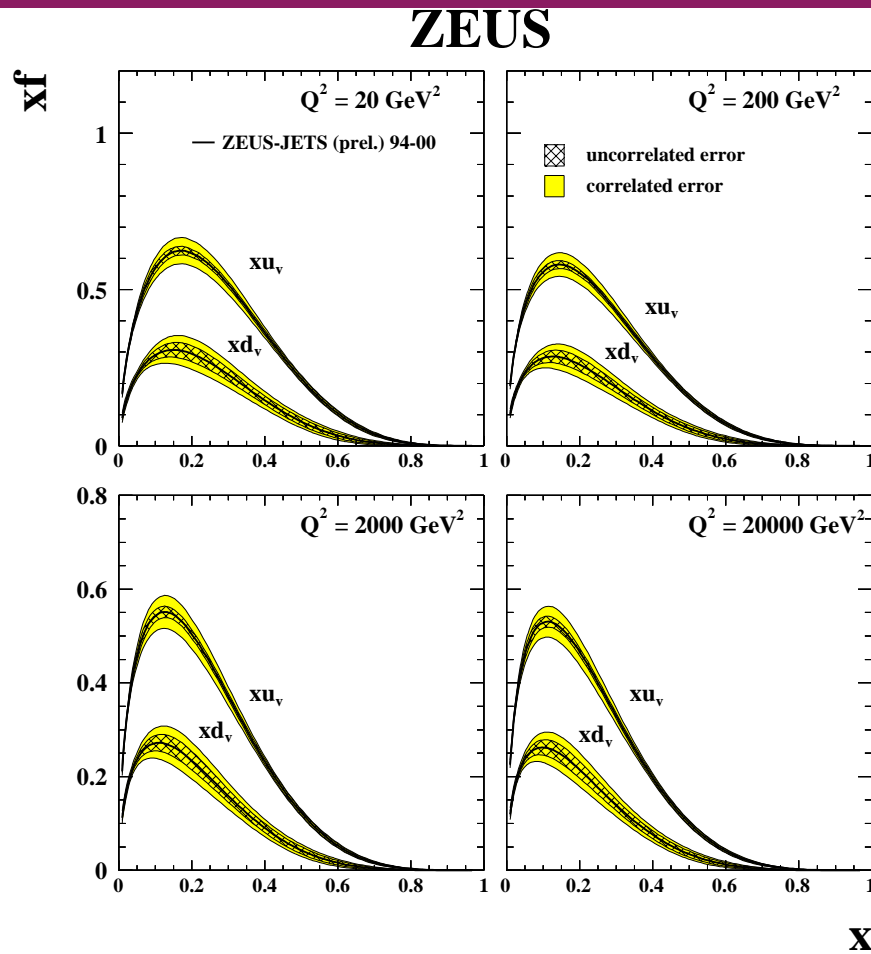
ZEUS NC DIS high Q^2

CC DIS high Q^2
ZEUS



- Fit of **ZEUS-only** data: **NC DIS $e^\pm p$** and **CC DIS $e^\pm p$** in the region $2.5 < Q^2 < 30000 \text{ GeV}^2$, $6.3 \cdot 10^{-5} < x < 0.65$ and $W^2 > 20 \text{ GeV}^2$ using **DGLAP** evolution equations at **NLO**: $\rightarrow xu_V, xd_V, xS, xg$ (no HERA information on flavour composition of the sea: flavour-averaged sea)
 \Rightarrow **Good description of Structure Function data (577 data points)**

Determination of the Proton PDFs with ZEUS data alone



- xu_v, xd_v : precision competitive with global fits

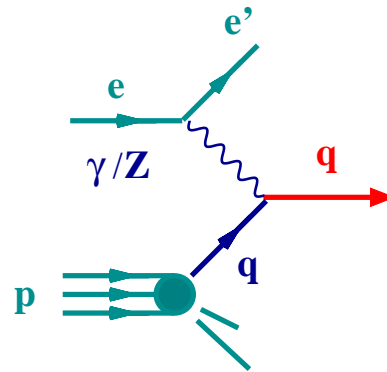
→ free from uncert. due to nuclear corrections and higher-twist effects

- xS, xg : as precise as in global fits (HERA data are crucial)

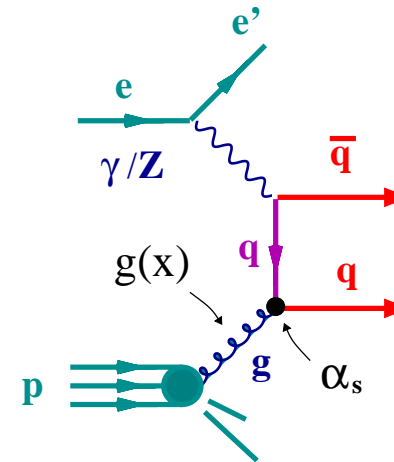
Jets in NC DIS

Jet Production in Neutral Current Deep Inelastic Scattering

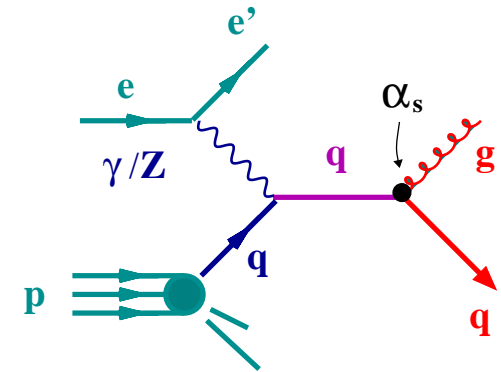
- Jet production in neutral current deep inelastic scattering up to $\mathcal{O}(\alpha_s)$:



Quark-Parton Model



Boson-Gluon Fusion



QCD Compton

- Perturbative QCD calculations of jet cross sections:

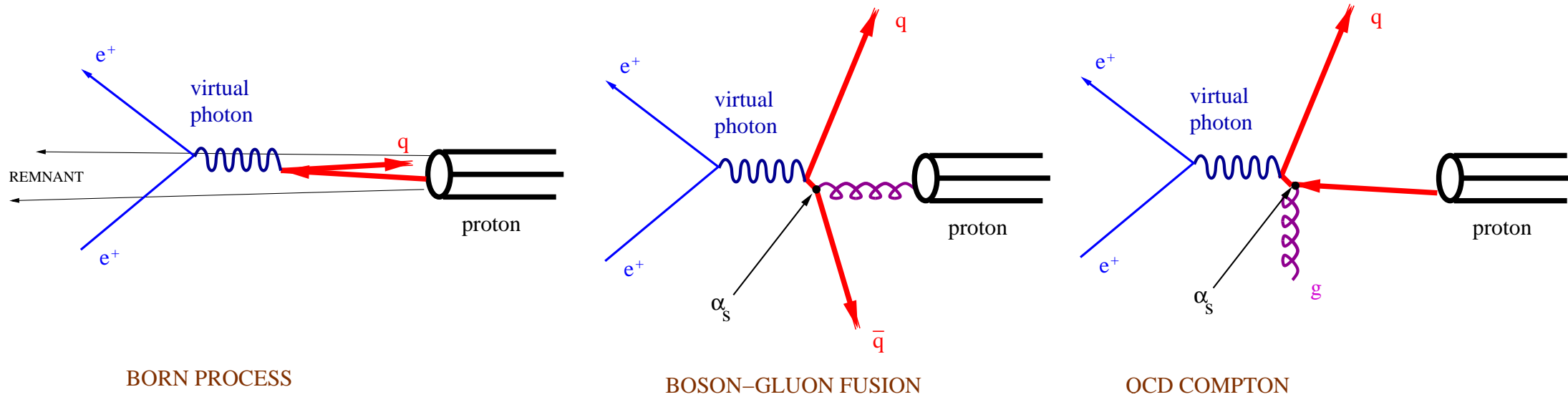
$$\sigma_{jet} = \sum_{a=q,\bar{q},g} \int dx f_a(x, \mu_F^2) \hat{\sigma}_a(x, \alpha_s(\mu_R), \mu_R^2, \mu_F^2)$$

- f_a : parton a density in the proton, determined from experiment; **long-distance structure of the target**
- $\hat{\sigma}_a$: subprocess cross section, calculable in pQCD; **short-distance structure of the interaction**

Jet Production in Neutral Current Deep Inelastic Scattering

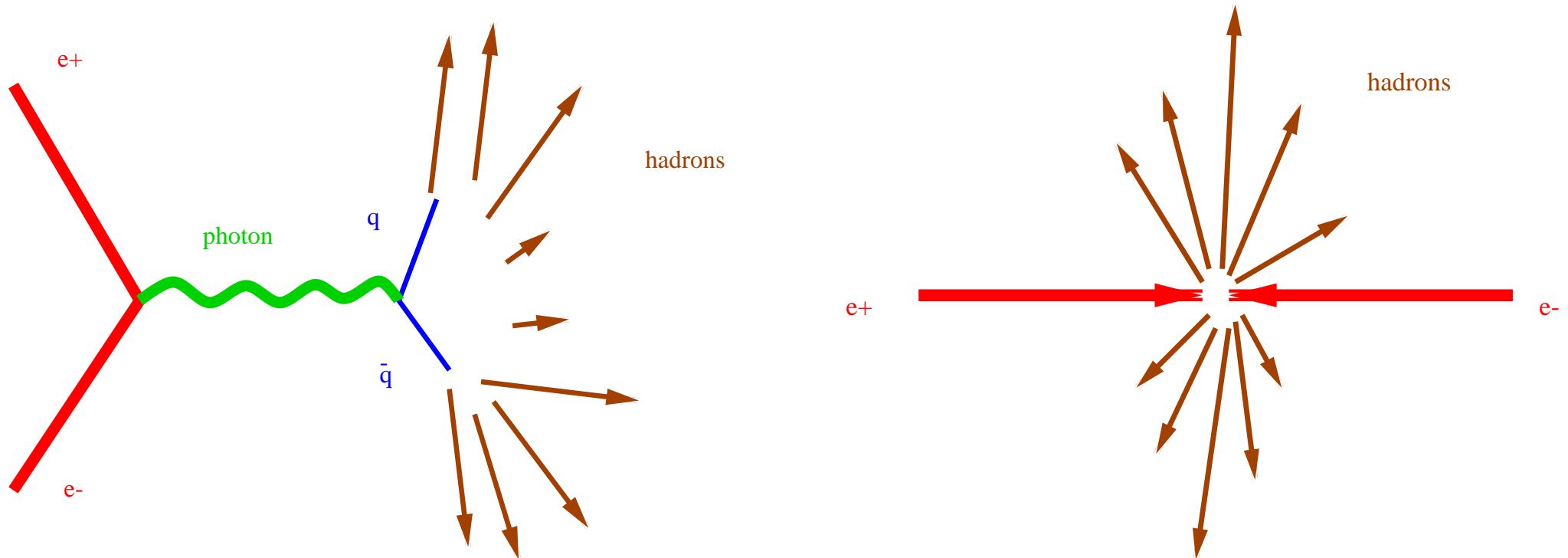
- In the region where the wealth of data from fixed-target and collider experiments has allowed **an accurate determination of the proton PDFs**, **measurements of jet production in NC DIS provide**
 - a sensitive test of the pQCD predictions of the short-distance structure
 - a determination of the strong coupling constant α_s
- To perform a **stringent test of the pQCD predictions** and a **precise determination of α_s** :
 - * **Observables for which the predictions are directly proportional to α_s**
 - Jet cross sections in the Breit frame
 - * **Small experimental uncertainties** → Jets with relatively high transverse energy
 - * **Small theoretical uncertainties** → NLO QCD calculations
 - **Jet algorithm: longitudinally invariant k_T cluster algorithm** (Catani et al)
(small parton-to-hadron effects, infrared safe, suppression of beam-remnant jet)
 - Jet selection criteria

High- E_T Jet Production in the Breit Frame



- In the Breit frame the virtual boson collides head-on with the proton
- High- E_T jet production in the Breit frame
 - suppression of the Born contribution (struck quark has zero E_T)
 - suppression of the beam-remnant jet (zero E_T)
 - lowest-order non-trivial contributions from $\gamma^* g \rightarrow q\bar{q}$ and $\gamma^* q \rightarrow qg$
 - ⇒ directly sensitive to hard QCD processes (α_s)

Variables for Jet Search in e^+e^- annihilations

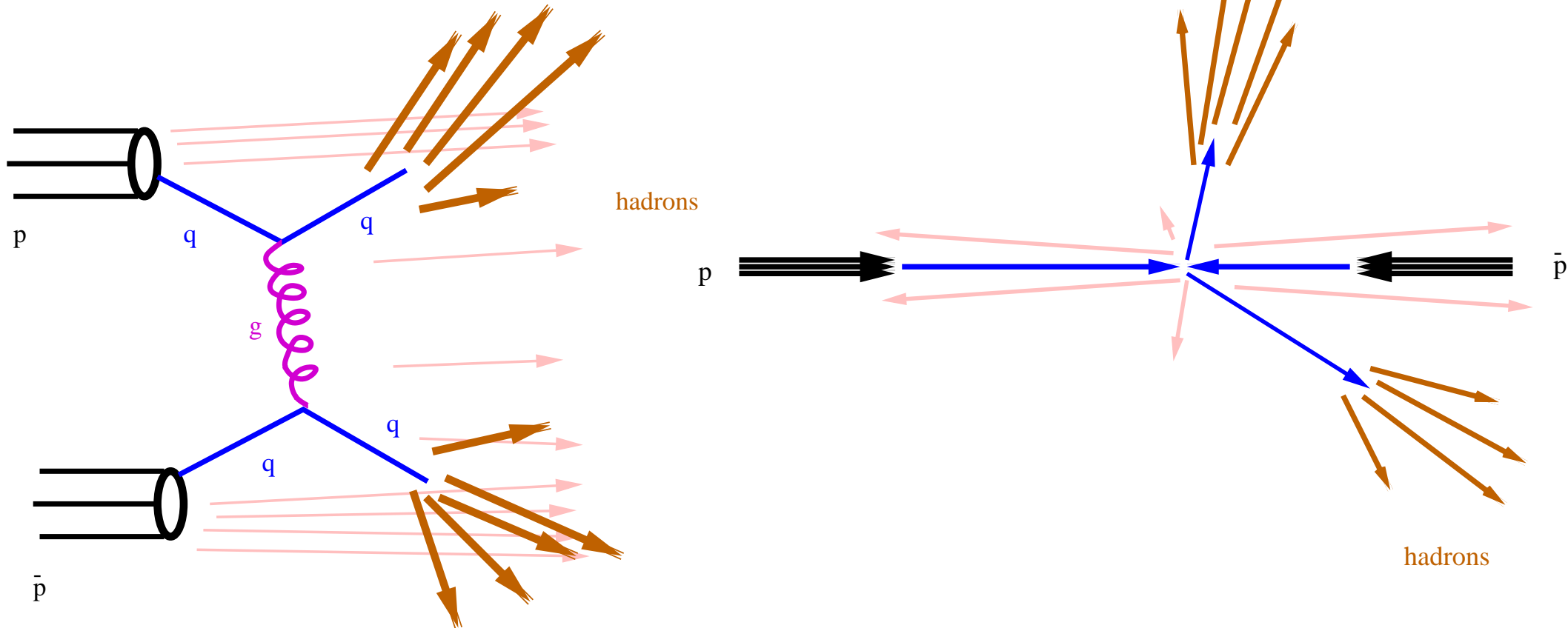


- e^+e^- annihilations in the centre-of-mass system
- Invariance under rotations \Rightarrow Energies and angles

\Rightarrow Input to the jet algorithm: E_i , θ_i and ϕ_i for every hadron i

\Rightarrow “distance” between hadrons i and j : their angular separation θ_{ij}

Variables for Jet Search in $p\bar{p}$ collisions



- $p\bar{p}$ collisions in the centre-of-mass system
- However the initial-state parton-parton system is NOT at rest!
depending upon the momentum fractions, x_p and $x_{\bar{p}}$, wrt the parent hadrons
⇒ the final-state partonic system is **BOOSTED** along the beam axis

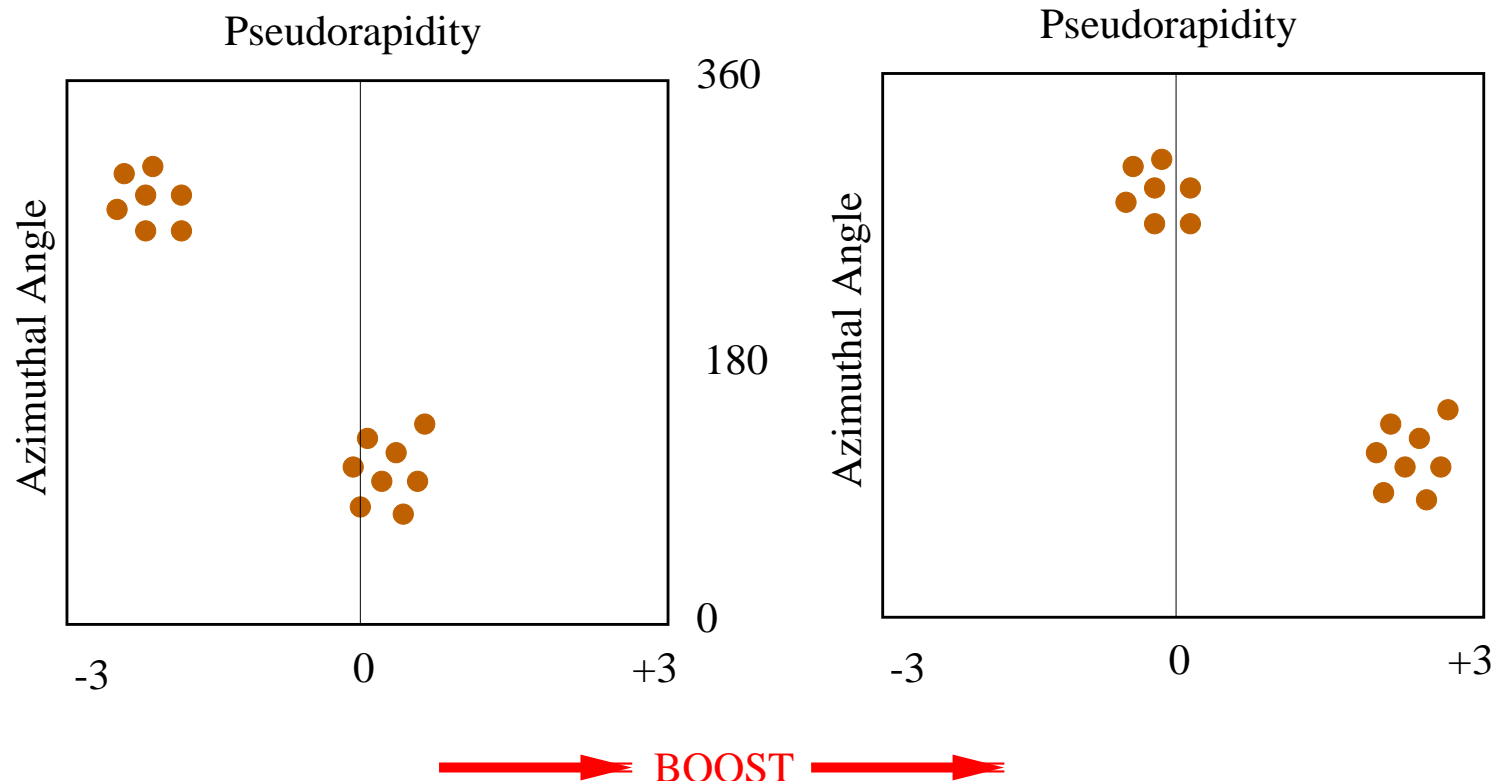
Variables for Jet Search in $p\bar{p}$ collisions (II)

- Angular separations are **NOT** invariant under boosts!

⇒ a given set of hadrons will appear more collimated depending upon the boost

- To treat on equal footing all possible final-state hadronic systems

invariance under longitudinal boosts ⇒ transverse energy, pseudorapidity* and azimuthal angle



Under a boost:

$$\eta' = \eta + f(x_p, x_{\bar{p}})$$

⇒ the difference in η
between hadrons i and j

$\Delta\eta_{ij}$ IS INVARIANT!

The “distance” defined as

$$r \equiv \sqrt{\Delta\eta_{ij}^2 + \Delta\phi_{ij}^2}$$

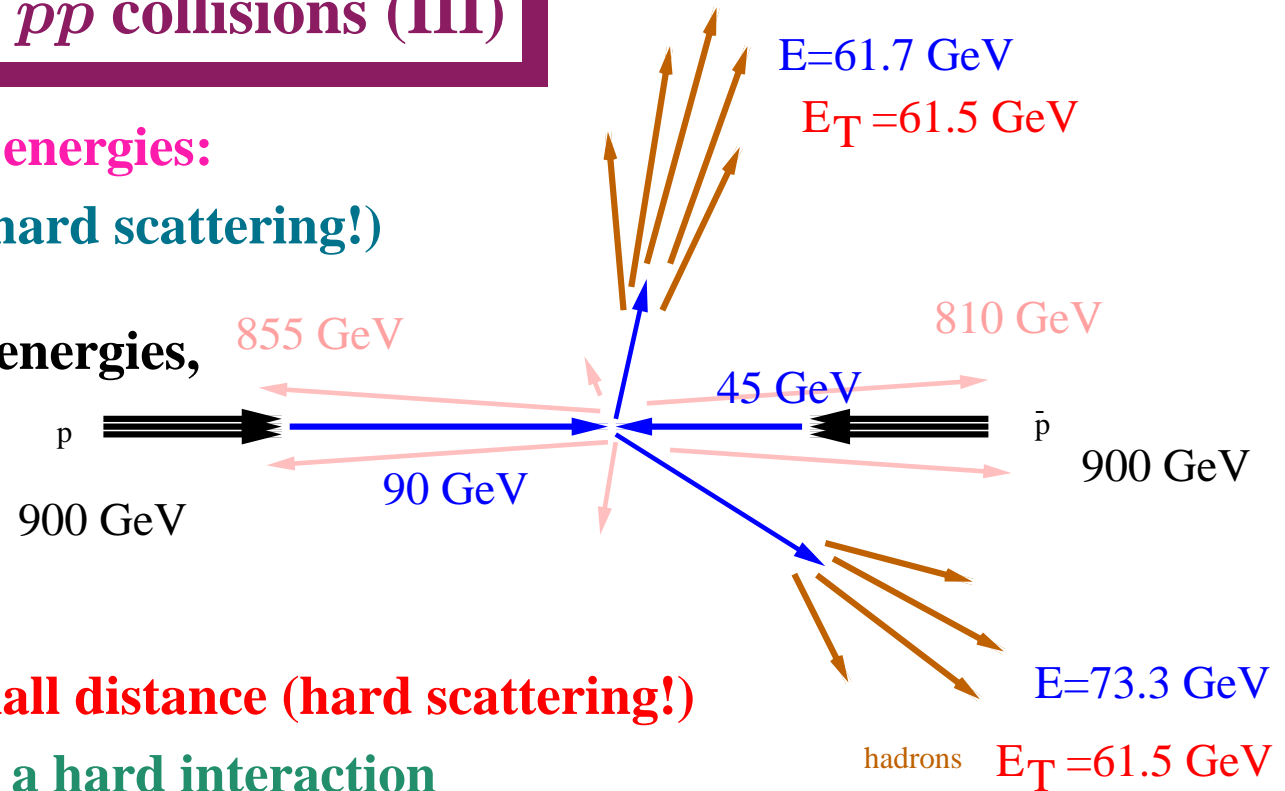
is INVARIANT!

Variables for Jet Search in $p\bar{p}$ collisions (III)

- Advantage of using transverse energies:

Large energy \neq small distance (hard scattering!)

The beam remnant jets have huge energies,
but they **HAVE NOT** undergone
a hard scattering!



- Large momentum transfer \equiv small distance (hard scattering!)

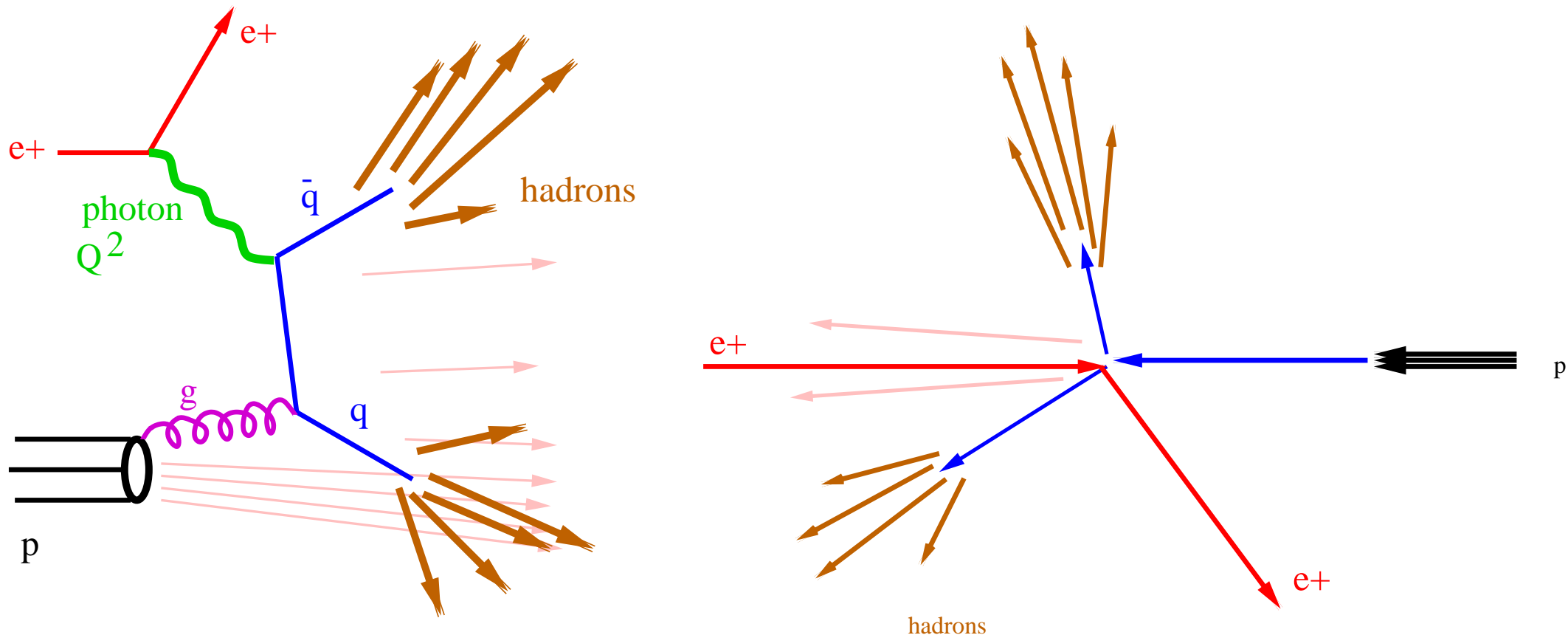
\Rightarrow large transverse energies signal a hard interaction

- The use of transverse energies helps to disentangle between the products of the hard interaction and the beam remnant jets (absent in e^+e^- annihilations)

\Rightarrow Input to the jet algorithm: $E_{T,i}$, η_i and ϕ_i for every hadron i

\Rightarrow “distance” between hadrons i and j : $\sqrt{\Delta\eta_{ij}^2 + \Delta\phi_{ij}^2}$

Variables for Jet Search in ep collisions at high Q^2 (DIS)



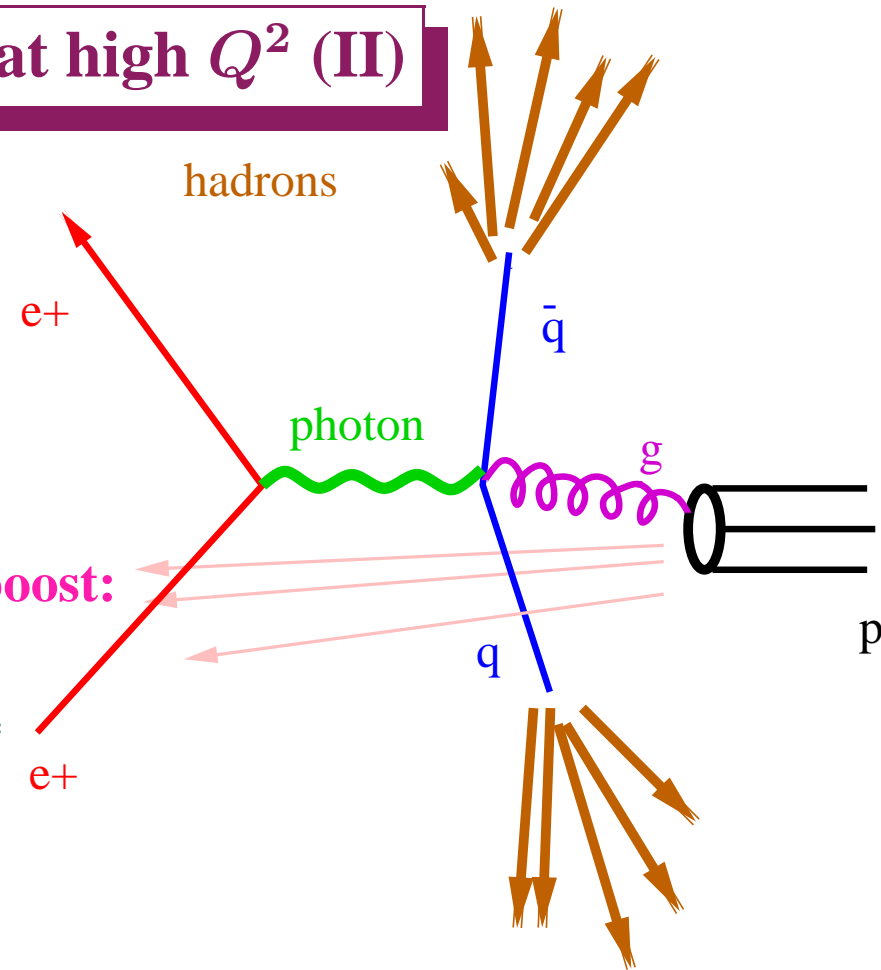
● The kinematics of ep collisions at high Q^2 poses several challenges:

→ Presence of beam remnant jet

→ the initial-state γ^* -parton system is **boosted** (the parton carries a fraction of the proton's momentum) and **rotated** (the γ^* carries P_T)

Variables for Jet Search in ep collisions at high Q^2 (II)

- The effect of the P_T carried by the γ^* is removed
 → by selecting a frame in which
 the γ^* **collides head-on** with the proton
 (the **Breit frame** is one example)
- The γ^* -parton system can still have a longitudinal boost:
 invariance under longitudinal boosts demands
 → the use of transverse energies, pseudorapidities*
 and azimuthal angles
- The use of transverse energies helps to suppress the effects of the beam remnant jet
 ⇒ Input to the jet algorithm: $E_{T,i}^B$, η_i^B and ϕ_i^B in the **Breit frame** for every hadron i
 ⇒ “distance” between hadrons i and j : $\sqrt{(\Delta\eta_{ij}^B)^2 + (\Delta\phi_{ij}^B)^2}$ in the **Breit frame**



The best choice for jet algorithm in ep collisions

- There is no best choice since, at the end, it is a question of having the smallest uncertainty for the given observable:
 - the smallest theoretical uncertainties (higher-order contributions)
 - the smallest hadronisation effects
 - the smallest experimental uncertainties
- At present, the longitudinally invariant k_T algorithm is a good choice for accurate comparisons between data and perturbative QCD at HERA
 - jet cross sections in neutral current DIS
 - jet cross sections in photoproduction
- Performance of the longitudinally invariant k_T algorithm in ZEUS:
 - small higher-order contributions (5%, 10 – 20%; varying μ_R by factors 0.5 and 2)
 - small hadronisation corrections (< 10%, < 10%; comparing hadron/parton levels)
 - small hadronisation uncertainties (1%, 2 – 3%; comparing two MC models)
 - small experimental uncertainties (3%, 4%; comparing two MC models)

The longitudinally invariant k_T algorithm for ep collisions

- The clustering procedure is as follows:

- List of particles (or calorimeter cells, ...)

- For every object k and for every pair of objects i, j the “distances” are evaluated

$$d_k^2 = E_{T,k}^2 \text{ (distance to the beam)}$$

$$d_{ij}^2 = \min(E_{T,i}^2, E_{T,j}^2) \cdot ((\eta_i - \eta_j)^2 + (\phi_i - \phi_j)^2)$$

- If, of all the values $\{d_k^2, d_{ij}^2\}$, d_{mn}^2 is the smallest, then objects m and n are combined into a single new object according to

$$E_{T,ij} = E_{T,i} + E_{T,j}, \quad \eta_{ij} = \frac{E_{T,i} \cdot \eta_i + E_{T,j} \cdot \eta_j}{E_{T,ij}}, \quad \phi_{ij} = \frac{E_{T,i} \cdot \phi_i + E_{T,j} \cdot \phi_j}{E_{T,ij}}$$

- If, however, d_k^2 is the smallest, then object k is considered a “protojet” and is removed from the list

- The procedure is iterated until the list of objects is empty

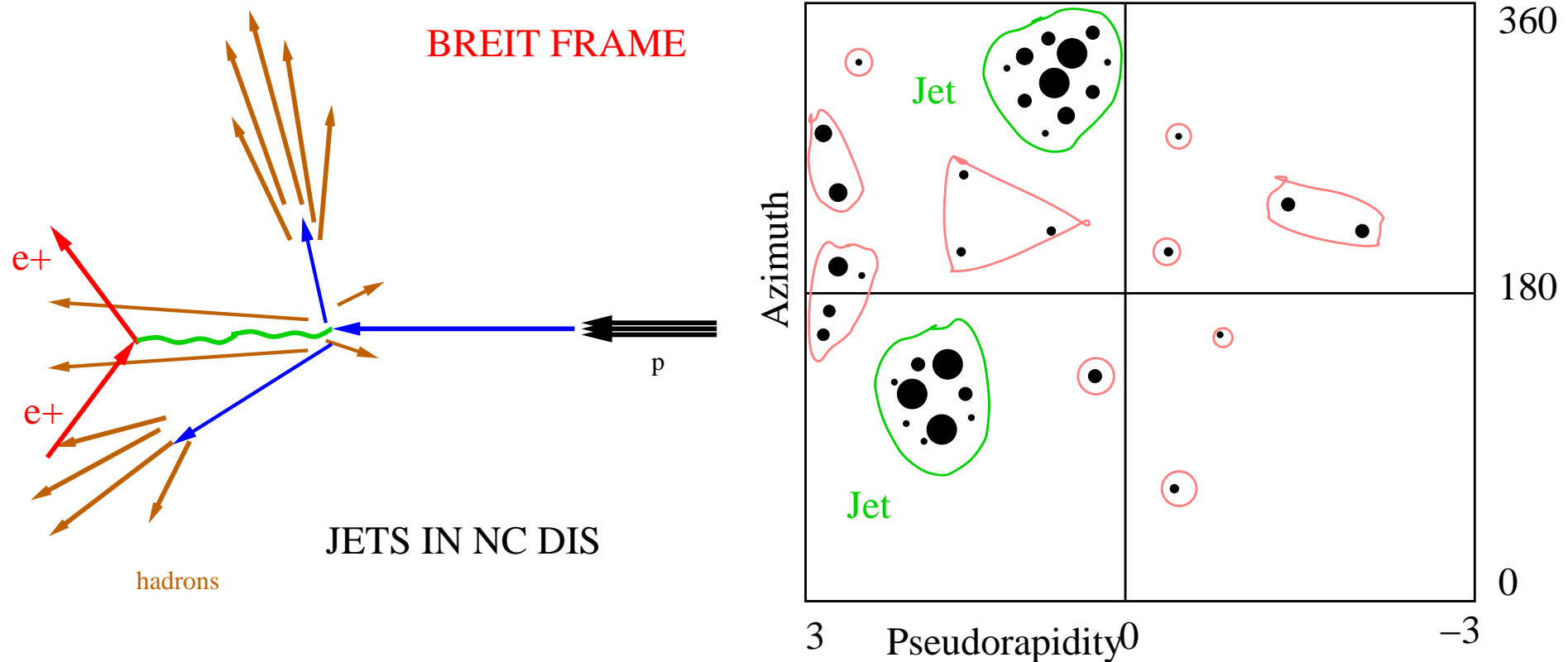
- From the list of “protojets” the jets are selected by imposing certain criteria:

- jet pseudorapidity in the range $C_L < \eta_{\text{jet}} < C_U$

- jet transverse energy in the range $E_{T,\text{jet}} > E_{T,0}$

⇒ the lower the $E_{T,0}$ is the larger the theoretical and experimental uncertainties are!

The longitudinally invariant k_T algorithm for NC DIS



- **Infrared and collinear safe to all orders in perturbative QCD**
- **Invariant under longitudinal boosts (along the γ^* -proton axis)**
- **Suppression of beam remnant jet contributions through the use of transverse energies and by not forcing all the particles to be assigned to jets (nor requiring a certain jet shape)**
- **Small experimental and theoretical uncertainties**

Dijet Cross Sections in NC DIS ($5 < Q^2 < 15000 \text{ GeV}^2$)

- Measurement of differential dijet cross sections over a wide range in $Q^2 \rightarrow 5 < Q^2 < 15000 \text{ GeV}^2$ and $0.2 < y < 0.6$ for dijet production with

$$E_T^{jet,1(2)}(\text{Breit}) > 5 \text{ GeV}$$

$$E_T^{jet,1}(\text{Breit}) + E_T^{jet,2}(\text{Breit}) > 17 \text{ GeV}$$

$$-1 < \eta^{jet,1(2)}(\text{Lab}) < 2.5$$

- Detailed investigation of the jet algorithms:

→ Smallest parton-to-hadron effects: inclusive k_T

- Comparison with NLO QCD calculations:

→ $\mu_R = \bar{E}_T, \mu_F = \sqrt{200} \text{ GeV}$

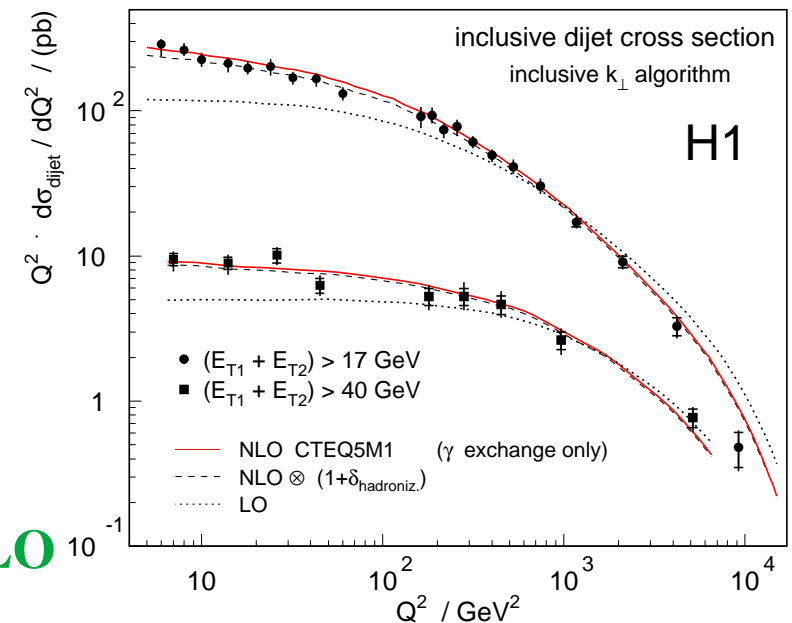
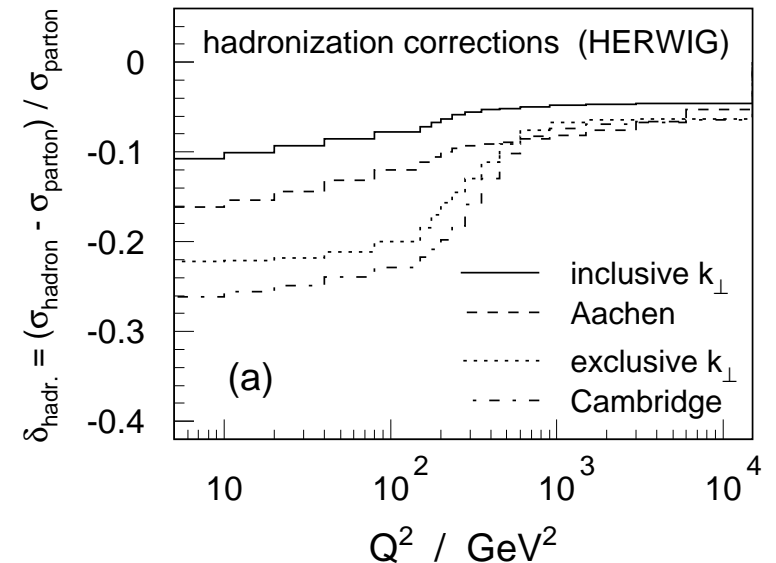
→ CTEQ5M1 parametrisations of proton PDFs

→ parton-to-hadron corrections applied

- NLO QCD gives a good description of the data over

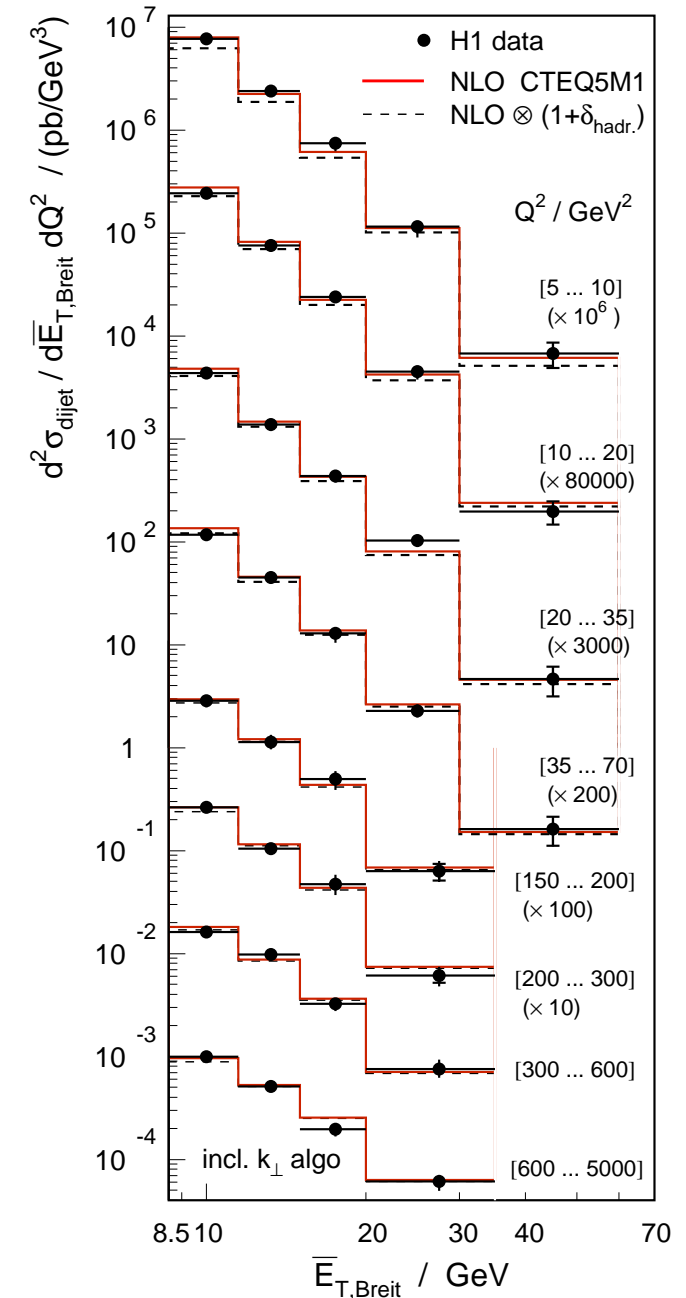
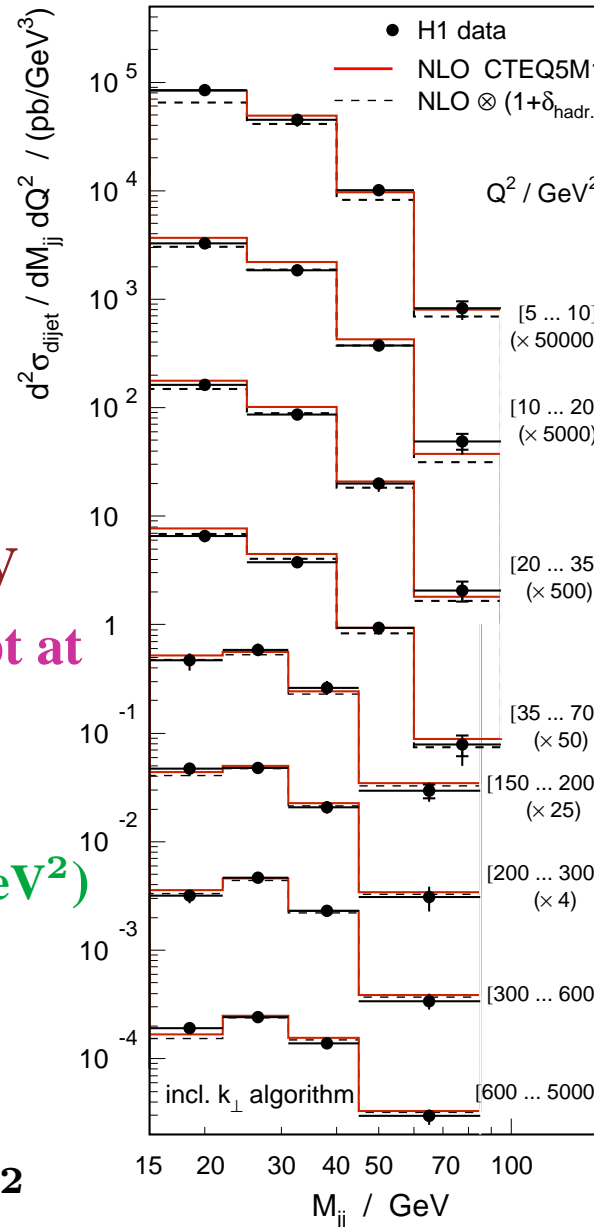
a wide range in Q^2 and E_T ; the Q^2 dependence is

observed to be reduced at high- E_T and described by NLO



Dijet Cross Sections in NC DIS

- **Measurement of double differential cross sections**
 $d\sigma/dM_{JJ}dQ^2$, $d\sigma/d\bar{E}_{T,Breit}dQ^2$
 over $5 < Q^2 < 5000 \text{ GeV}^2$
- It is observed that the spectra get harder as Q^2 increases
- **NLO QCD describes well the data over $15 < M_{JJ} < 95 \text{ GeV}$ and $8.5 < \bar{E}_{T,Breit} < 60 \text{ GeV}$ except at low Q^2 , where the shape is ok but not the normalisation**
- **Overview: at high $Q^2 (> 70 \text{ GeV}^2)$ NLO describes the data well; as Q^2 decreases the theoretical uncertainties become large and NLO fails for $Q^2 < 10 \text{ GeV}^2$**



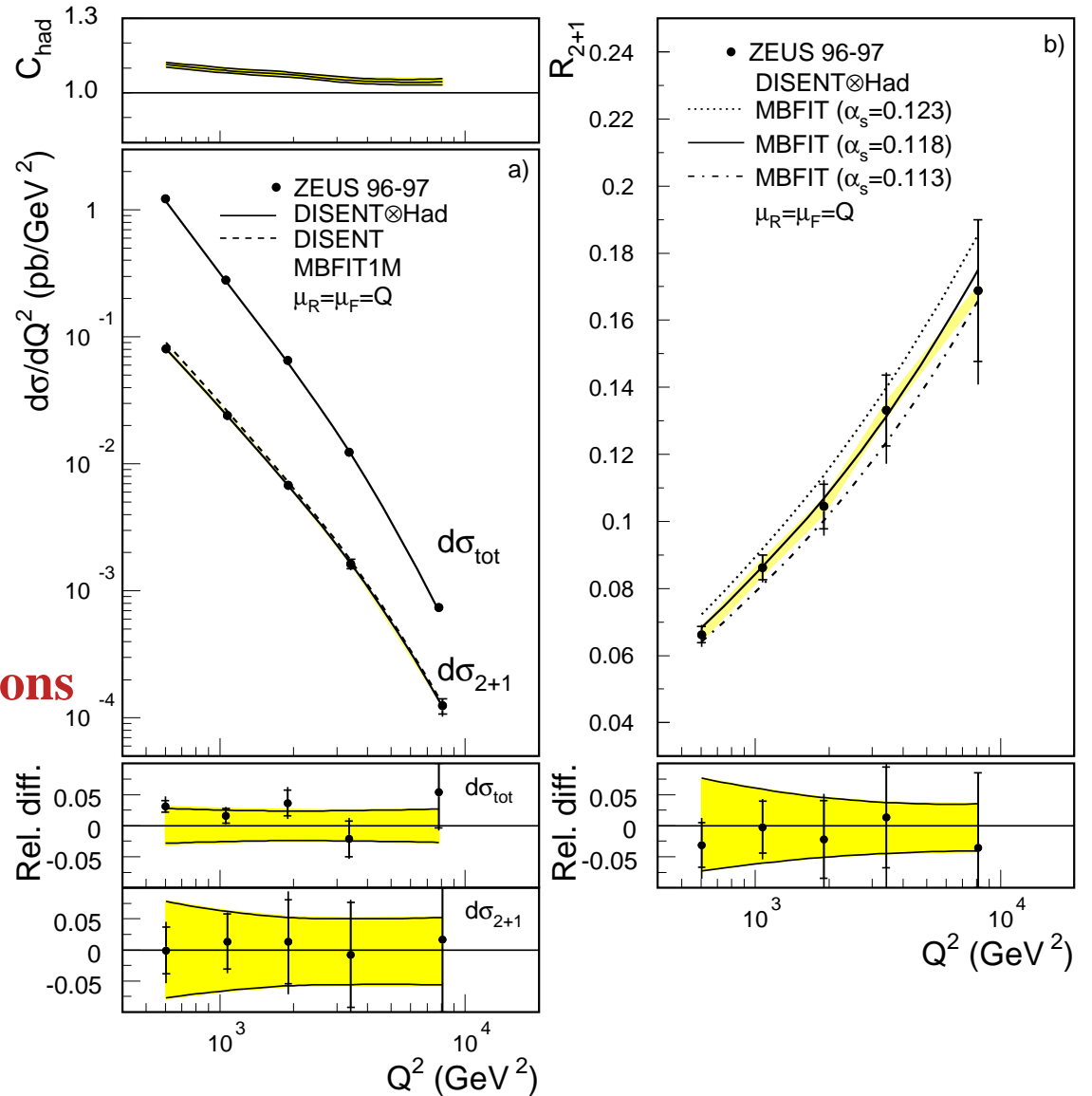
Dijet Cross Sections at $Q^2 > 470 \text{ GeV}^2$ and extraction of α_s

- Dijet cross section $d\sigma_{2+1}/dQ^2$ for $470 < Q^2 < 20000 \text{ GeV}^2$
 $E_T^{jet,1}(\text{Breit}) > 8 \text{ GeV}$
 $E_T^{jet,2}(\text{Breit}) > 5 \text{ GeV}$
 $-1 < \eta^{jet,1(2)}(\text{Lab}) < 2$

→ **Ratio $R_{2+1} \equiv \frac{d\sigma_{2+1}/dQ^2}{d\sigma_{tot}/dQ^2}$**

- Small experimental uncertainties.
- Comparison with NLO QCD calculations
- Small theoretical uncertainties:
 - uncertainties on the proton PDFs
 - hadronisation corrections
 - higher-order terms ($> \text{NLO}$)

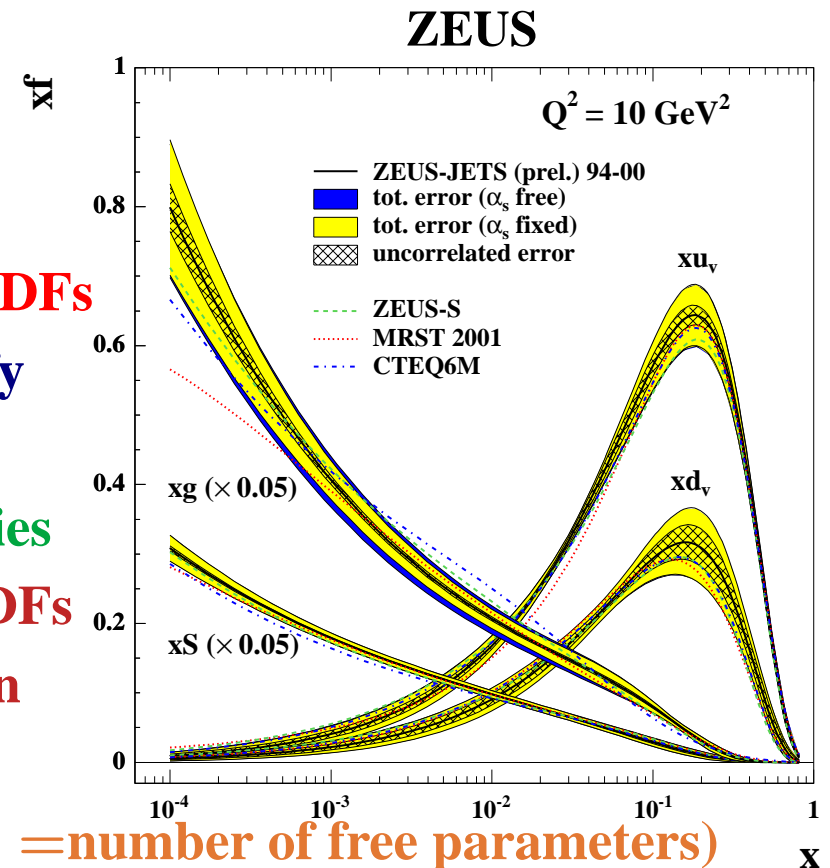
ZEUS



Uncertainties of the Proton PDFs: effects on jet cross sections

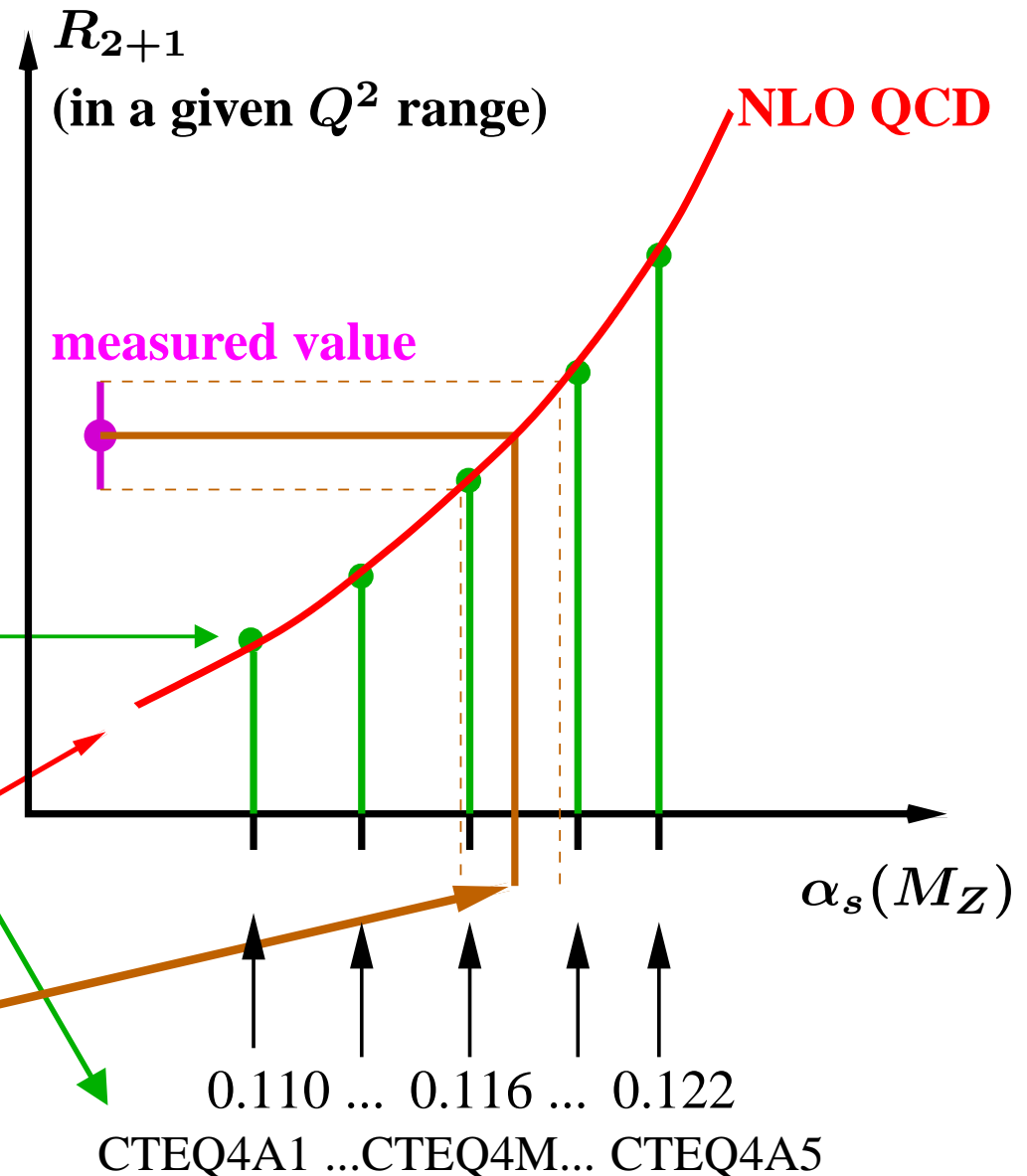
- Comparison of jet cross-section calculations using different parametrisations of the proton PDFs (e.g. MRST vs CTEQ) **DOES NOT give a reliable estimation of the uncertainties due to the proton PDFs**
- Several groups have developed methods to quantify these uncertainties by accounting (properly) for
 - the statistical and correlated systematic uncertainties of each data set used in the determination of the PDFs
 - the theoretical uncertainties affecting the extraction of the PDFs in the DGLAP fits
- CTEQ's analysis provides $2N_p + 1$ PDF sets ($N_p = \text{number of free parameters}$) consisting of the best fit S_0 and eigenvector basis sets in the plus and minus directions along each eigenvector, such that the best estimate and its uncertainty can be calculated
 - ⇒ for any function of the proton PDFs (e.g. σ_{jet})

$$\Delta\sigma_{jet} = \frac{1}{2} \left(\sum_{i=1, N_p} [\sigma_{jet}(S_i^+) - \sigma_{jet}(S_i^-)]^2 \right)^{1/2}$$



Dijet Cross Sections at $Q^2 > 470 \text{ GeV}^2$ and extraction of $\alpha_s(M_Z)$

- **NLO QCD calculations of $d\sigma_{2+1}/dQ^2$ depend on $\alpha_s(M_Z)$ through**
 - **Matrix Elements:** $\hat{\sigma} \sim A \cdot \alpha_s + B \cdot \alpha_s^2$
 - **proton PDFs:** α_s assumed in evolution
- **To take into account the correlation the NLO QCD calculations are performed using various sets of proton PDFs which assume different values of α_s**
- **The resulting NLO QCD calculations are parametrised as a function of $\alpha_s(M_Z)$ in each region of Q^2 of the measurements**
- **From the measured value of R_{2+1} in each region of Q^2 the value of $\alpha_s(M_Z)$ and its uncertainty are extracted**



Dijet Cross Sections at $Q^2 > 470 \text{ GeV}^2$ and extraction of α_s

- Study of the **scale dependence of $\alpha_s(Q)$** :
from the measured $R_{2+1}(Q^2)$ in each Q^2 region
→ $\alpha_s(\langle Q \rangle)$ is extracted
The measurements are consistent with the running of α_s predicted by perturbative QCD
- A combined value of $\alpha_s(M_Z)$ has been extracted:

$$\alpha_s(M_Z) = 0.1166 \pm 0.0019 \text{ (stat.)}$$

$$+0.0024 \text{ (exp.)} +0.0057 \text{ (th.)}$$

$$-0.0033 \text{ (exp.)} -0.0044 \text{ (th.)}$$

- The theoretical uncertainty dominates:

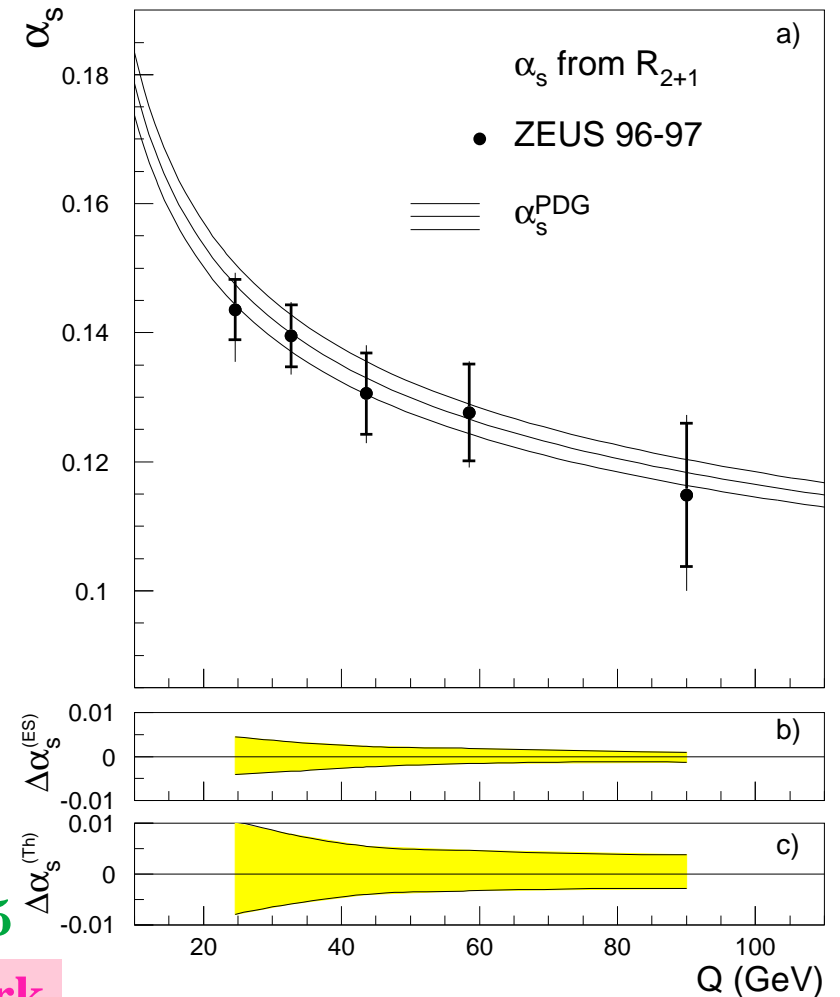
→ terms beyond NLO $\Delta\alpha_s(M_Z) = \begin{matrix} +0.0055 \\ -0.0042 \end{matrix}$

→ uncertainties proton PDFs $\Delta\alpha_s(M_Z) = \begin{matrix} +0.0012 \\ -0.0011 \end{matrix}$

→ hadronisation corrections $\Delta\alpha_s(M_Z) = \pm 0.0005$

Improvements depend upon further Theoretical Work

ZEUS



Inclusive Jet Cross Sections in NC DIS at $Q^2 > 125 \text{ GeV}^2$

$ep \rightarrow e + \text{jet} + X$: inclusive jets at high Q^2

- Jets searched using the k_T cluster algorithm in Breit frame
- Kinematic region: $Q^2 > 125 \text{ GeV}^2$ and $|\cos \gamma_h| < 0.65$
- At least one jet with $E_{T,B}^{\text{jet}} > 8 \text{ GeV}$ and $-2 < \eta_B^{\text{jet}} < 1.5$

• Small experimental uncertainties

- uncorrelated: $\sim \pm 3$ (7)% at low (high) $Q^2/E_{T,B}^{\text{jet}}$
- correlated: $\sim \pm 5$ (2)% at low (high) $Q^2/E_{T,B}^{\text{jet}}$

• Small theoretical uncertainties

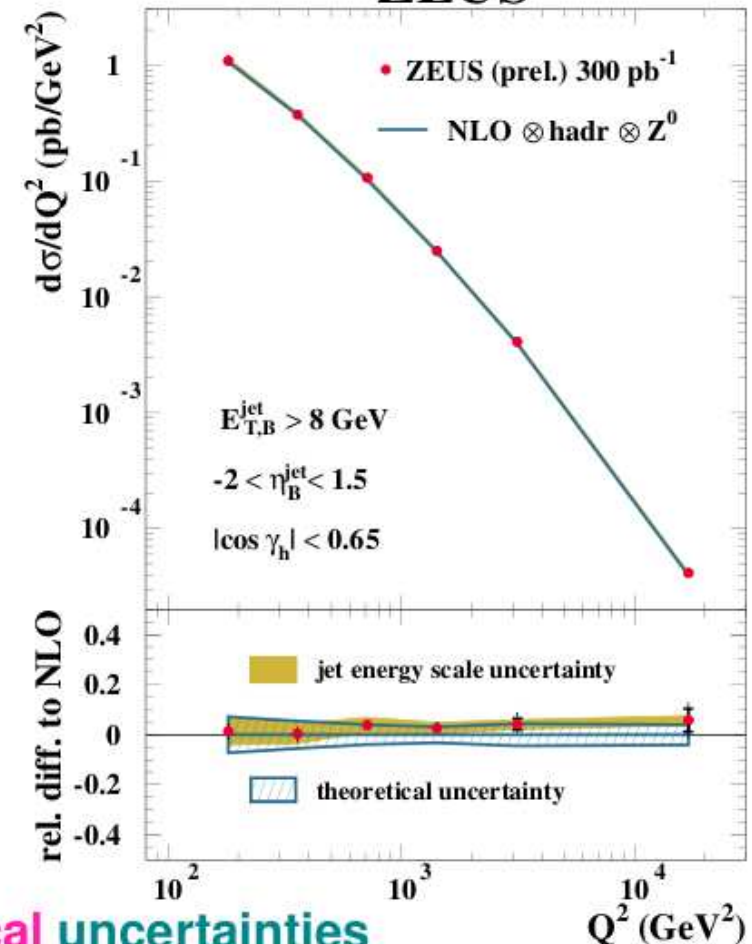
- higher orders (below $\pm 5\%$ for $Q^2 > 250 \text{ GeV}^2$)
- proton PDFs (below $\pm 3\%$)
- $\alpha_s(M_Z)$ (below ± 1 (2)% at low (high) $Q^2/E_{T,B}^{\text{jet}}$)
- parton-to-hadron corrections (below $\pm 2\%$)

→ Good description of data by NLO prediction
 → validity of the description of the dynamics of jet production at $\mathcal{O}(\alpha_s^2)$

→ Measurements provide direct sensitivity to $\alpha_s(M_Z)$ with small experimental and theoretical uncertainties

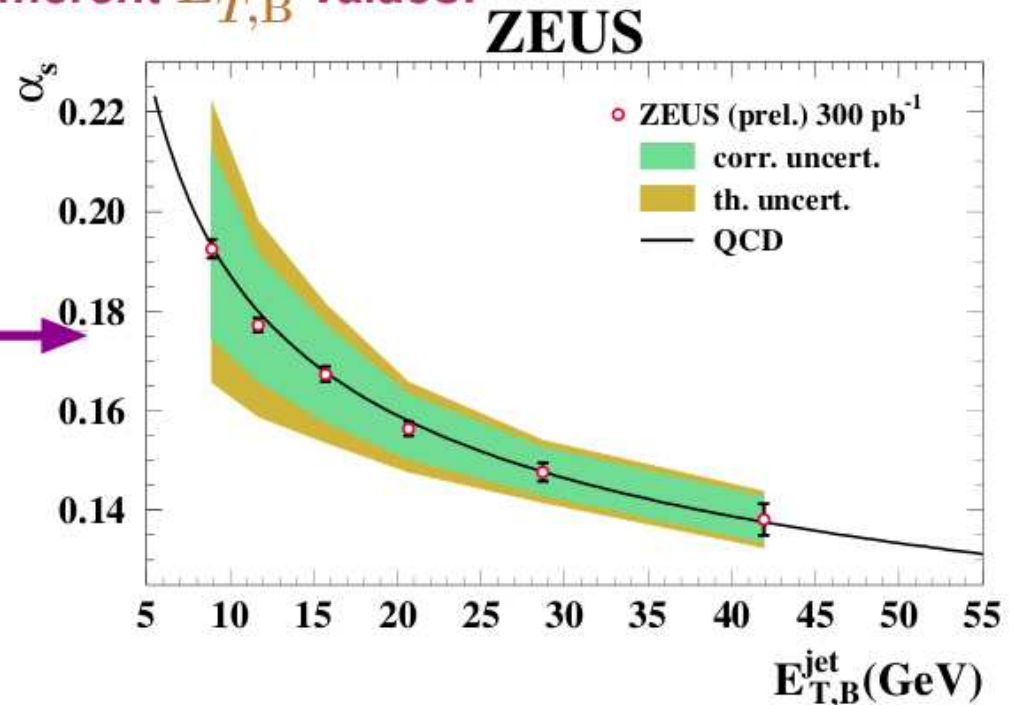
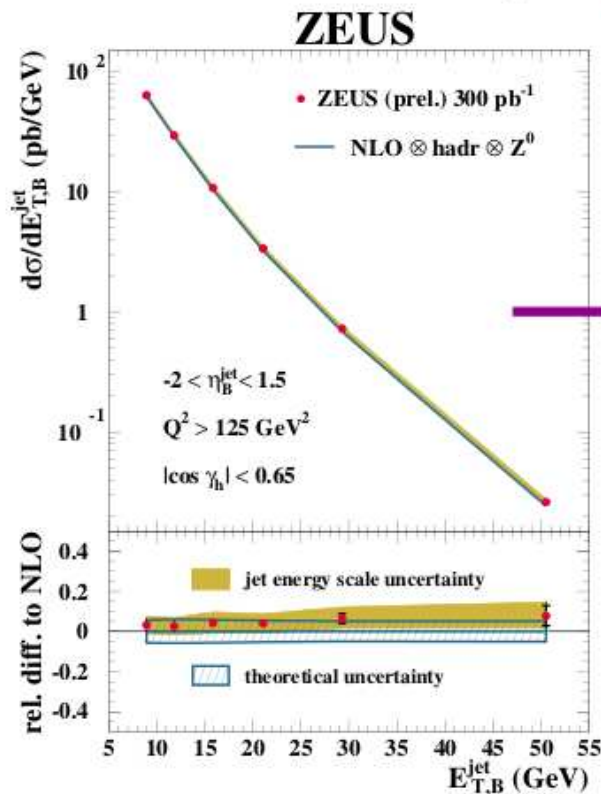
$\mathcal{L} = 300 \text{ pb}^{-1}$

ZEUS



Inclusive Jet Cross Sections and extraction of α_s

- The energy-scale dependence of the coupling was determined by extracting α_s from the measured $d\sigma/dE_{T,B}^{\text{jet}}$ at different $E_{T,B}^{\text{jet}}$ values:



→ Results in good agreement with the predicted running of α_s over a large range in $E_{T,B}^{\text{jet}}$

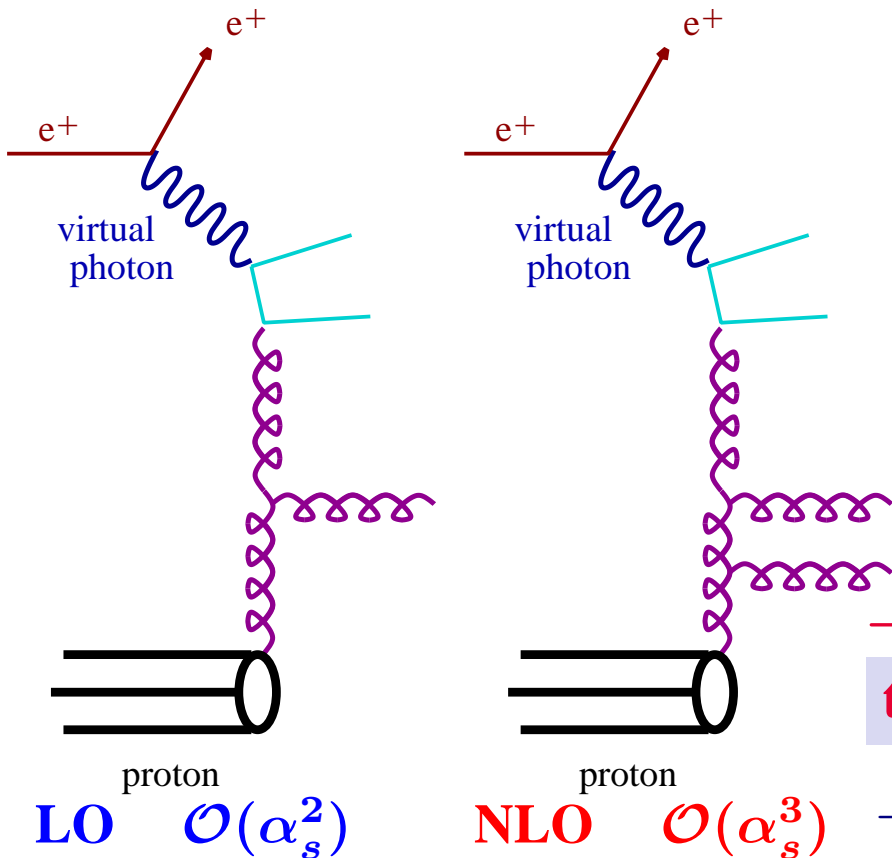
- A value of $\alpha_s(M_Z)$ was determined from $Q^2 > 500 \text{ GeV}^2$:

$$\alpha_s(M_Z) = 0.1208^{+0.0037}_{-0.0032} \text{ (exp.) } ^{+0.0022}_{-0.0022} \text{ (th.)}$$

experimental uncertainty: $+3.1\%$
 -2.6%
theoretical uncertainty: $\pm 1.9\%$

Three-jet cross sections in NC DIS

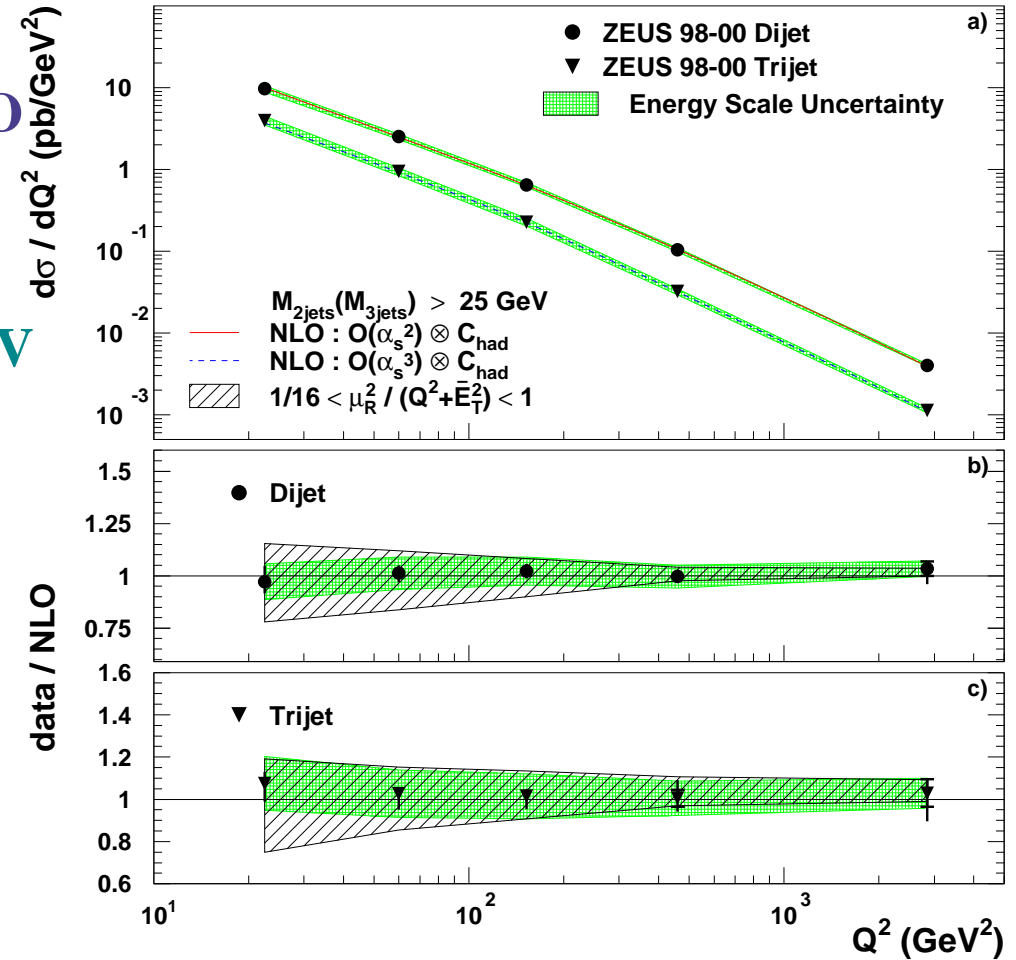
- Three-jet cross sections test QCD beyond LO directly $\rightarrow \sigma_{3jet} \propto \alpha_s^2$
- At least three jets with $E_T^{jet}(\text{Breit}) > 5 \text{ GeV}$ and $-1 < \eta^{jet}(\text{Lab}) < 2.5, M_{3jets} > 25 \text{ GeV}$



\rightarrow NLO calculations ($\mathcal{O}(\alpha_s^3)$): good description of the data over the whole range $10 < Q^2 < 5000 \text{ GeV}^2$

$\rightarrow \alpha_s(M_Z) = 0.1179 \pm 0.0013 \text{ (stat.)}_{-0.0046}^{+0.0028} \text{ (exp.)}_{-0.0046}^{+0.0064} \text{ (th.)}$

ZEUS



Jet Substructure in NC DIS

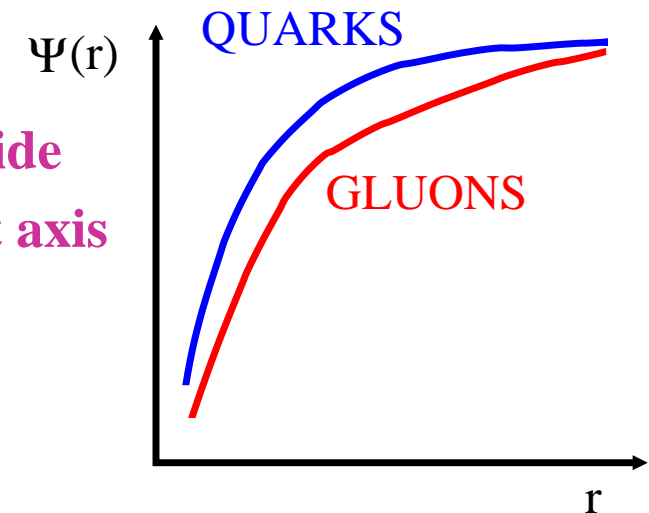
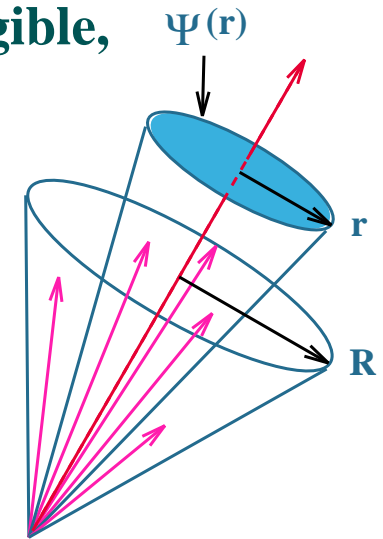
Jet Substructure in Neutral Current Deep Inelastic Scattering

- At sufficiently **high** E_T^{jet} , where fragmentation effects become negligible, the jet substructure is expected to be calculable by pQCD
- **Measurements of jet substructure allow investigations on**
 - the differences between quark- and gluon-initiated jets and
 - the dynamics of the different partonic final states,
 - as well as determinations of α_s

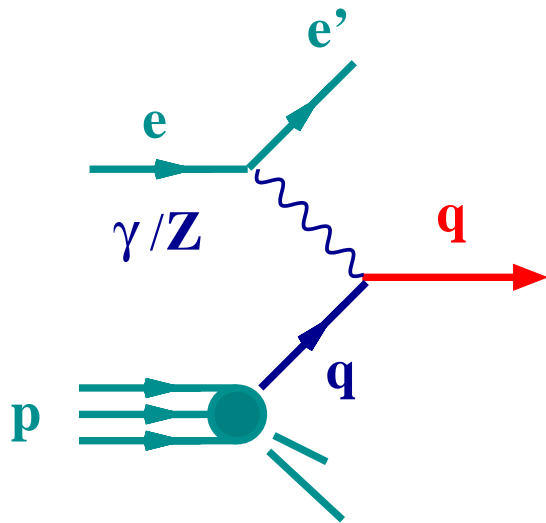
- **Integrated jet shape:**
$$\langle \Psi(r) \rangle = \frac{1}{N_{jets}} \sum_{jets} \frac{E_T(r)}{E_T^{jet}}$$

Average fraction of the jet's transverse energy that lies inside a circle in the η - ϕ plane of radius r concentric with the jet axis

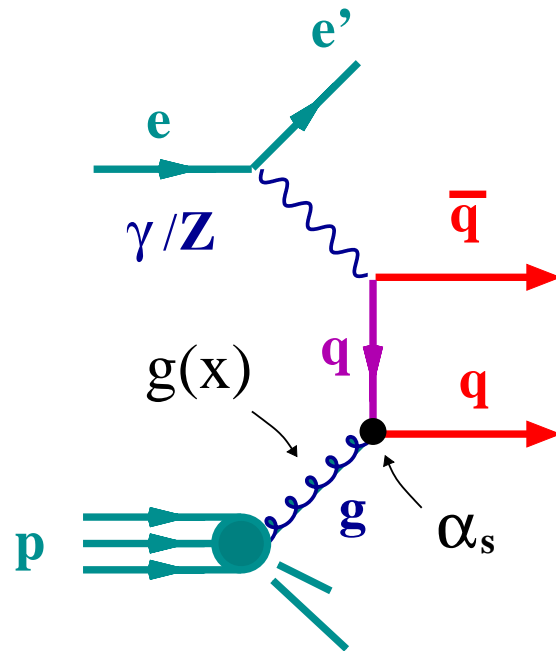
- QCD predicts that gluon jets are broader than quark jets
 $\Rightarrow \Psi_{QUARKS}(r) > \Psi_{GLUONS}(r)$



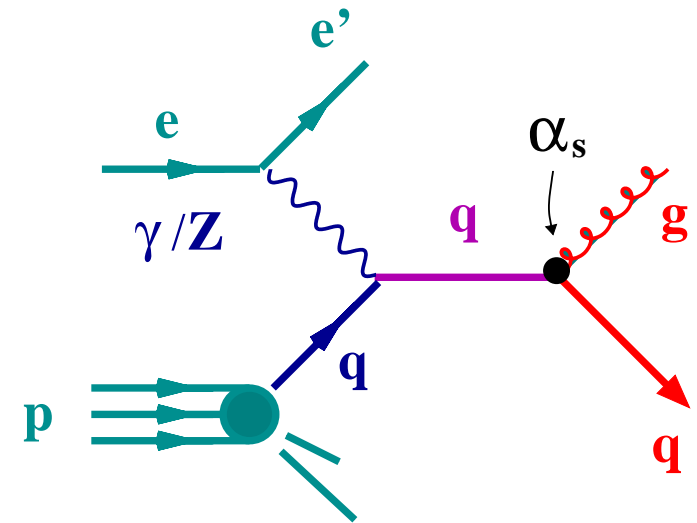
Jet Substructure in Neutral Current Deep Inelastic Scattering



Quark-Parton Model



Boson-Gluon Fusion



QCD Compton

One-jet events

Enriched in quark jets

Two-jet events

Higher content of gluon jets

Jet Substructure in Neutral Current Deep Inelastic Scattering

- Comparison with calculations:

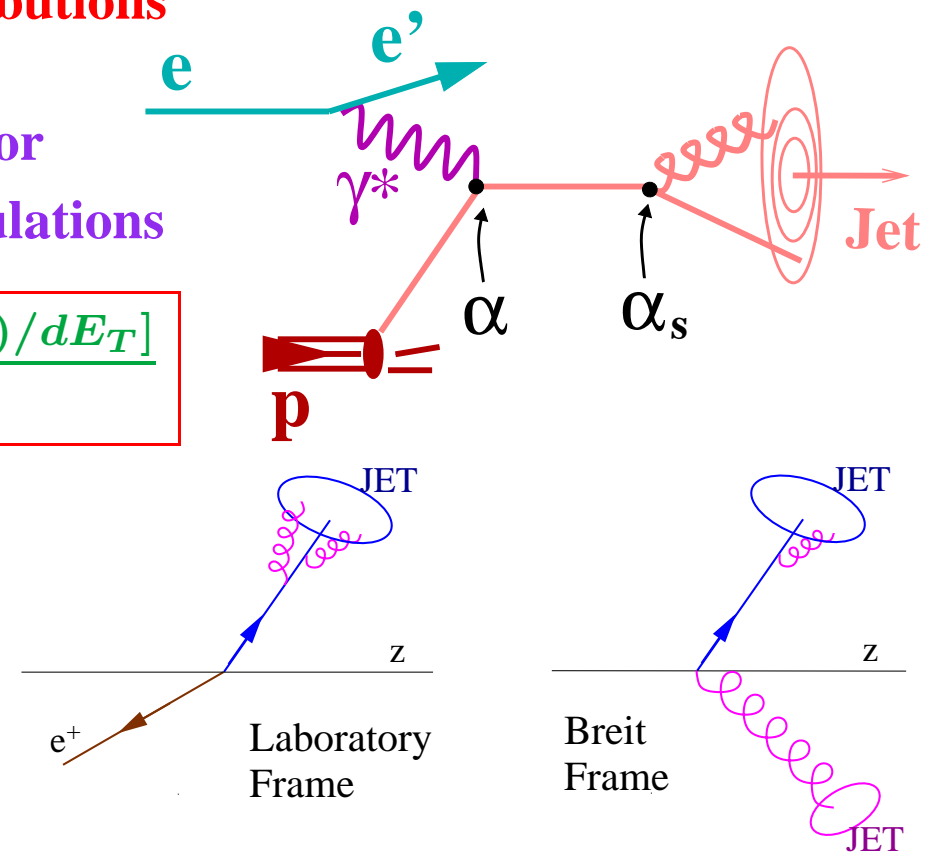
→ Monte Carlo generators (ARIADNE-CDM, LEPTO-MEPS) approximate the substructure of jets with parton showers

→ Fixed-order QCD calculations: at lowest order a jet consists of one parton (no structure); higher-order terms give the non-trivial contributions

- E.g. the lowest non-trivial-order contribution for one-jet events is given by $\mathcal{O}(\alpha\alpha_s)$ pQCD calculations

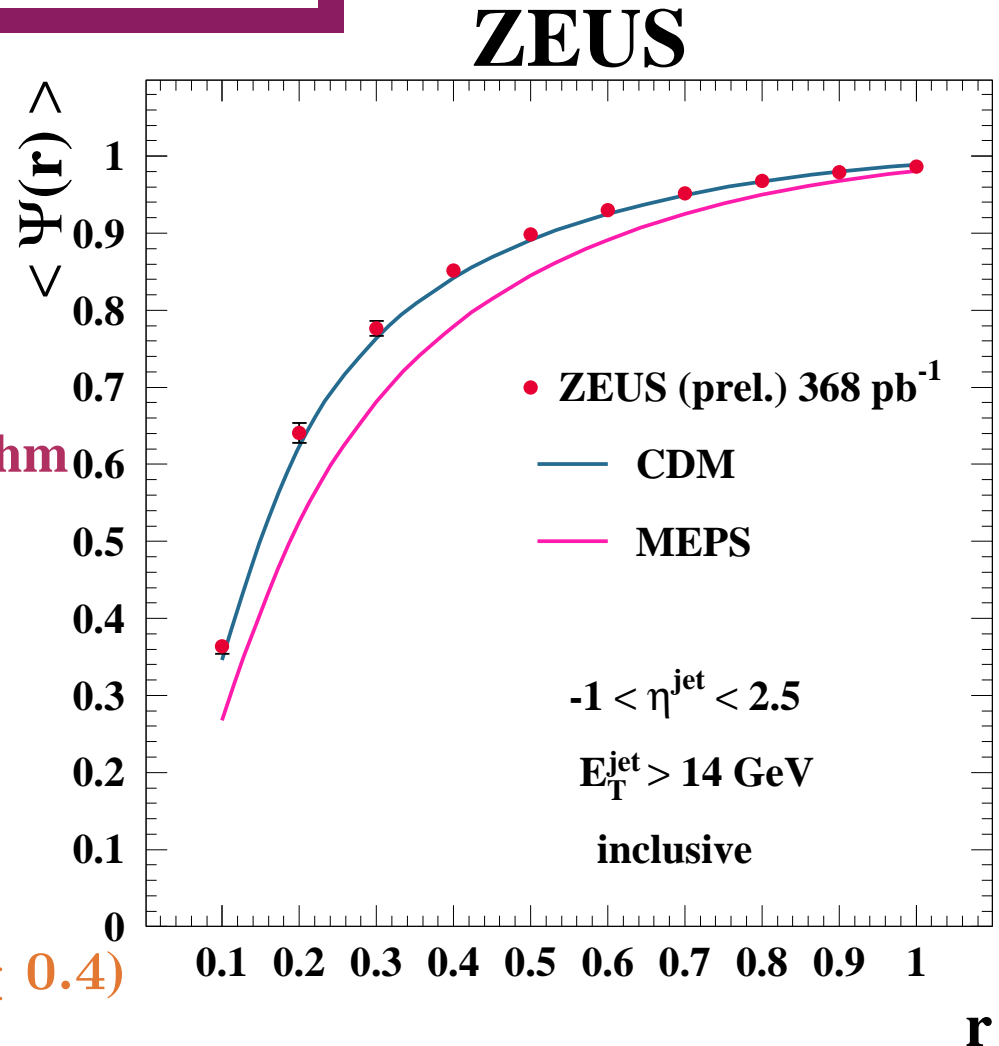
$$\langle 1 - \Psi(r) \rangle = \frac{\int dE_T E_T [d\sigma(ep \rightarrow 2\text{partons})/dE_T]}{E_T^{jet} \sigma_{jet}(E_T^{jet})}$$

- NLO QCD calculations of jet substructure can be made in the laboratory frame since it is possible to have 3 partons in the same jet (not possible in the Breit frame)



Measurements of Jet Substructure in NC DIS

- Measurement of $\langle \Psi(r) \rangle$ for an **inclusive sample of jets** in NC DIS with $Q^2 > 125 \text{ GeV}^2$ using HERA II data: $\mathcal{L} = 368 \text{ pb}^{-1}$
- Jets are defined using the k_T -cluster algorithm (longitudinally invariant mode) in the laboratory frame and required to have $E_T^{\text{jet}}(\text{Lab}) > 14 \text{ GeV}$ and $-1 < \eta^{\text{jet}}(\text{Lab}) < 2.5$
- The measurements of $\langle \Psi(r) \rangle$ have been corrected for detector effects ($< 10\%$ for $r \geq 0.4$)
- Comparison to QCD-inspired Monte models:
 - the colour-dipole model (CDM, ARIADNE) reproduces the data well
 - matrix-elements plus parton-showers (MEPS, LEPTO) predict too-broad jets



Measurements of Jet Substructure in NC DIS

- Measurement of $\langle \Psi(r) \rangle$ in NC DIS with $Q^2 > 125 \text{ GeV}^2$ using $\mathcal{L} = 368 \text{ pb}^{-1}$ for two samples of jets:

One-jet events

$$E_T^{\text{jet}} > 14 \text{ GeV}, -1 < \eta^{\text{jet}} < 2.5$$

Two-jet events

both jets are required to have

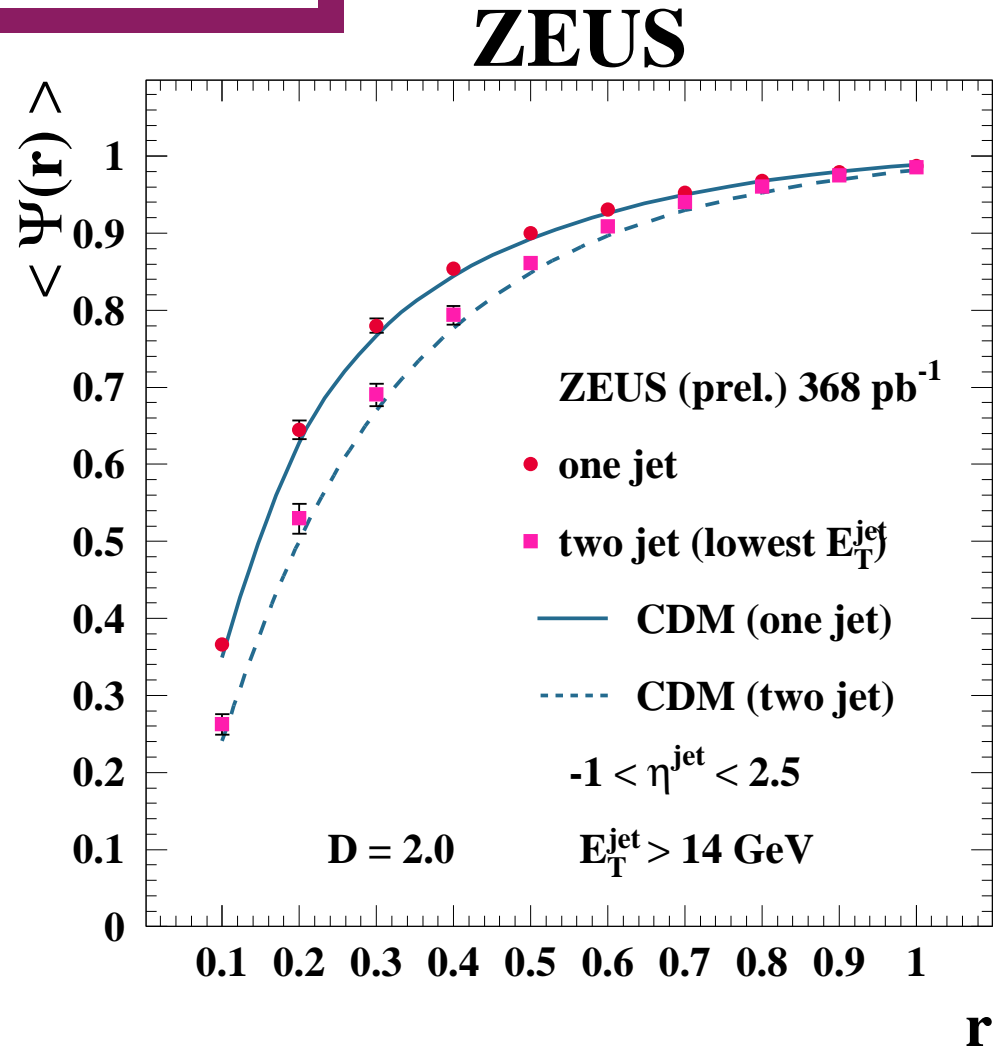
$$E_T^{\text{jet}} > 14 \text{ GeV}, -1 < \eta^{\text{jet}} < 2.5$$

and to be close to each other in the η - ϕ plane

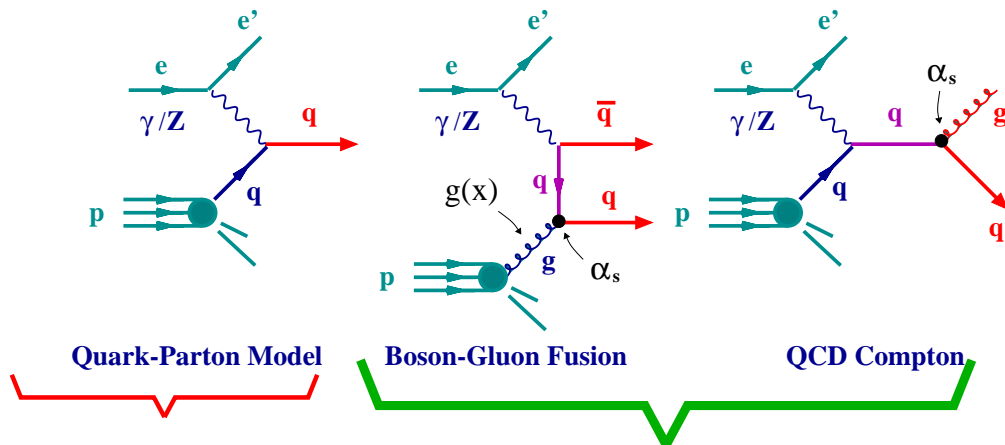
$$\text{distance jet-jet} = \sqrt{\Delta\eta^2 + \Delta\phi^2} \leq D = 2$$

→ the jet with lowest E_T^{jet} is considered

- The lowest- E_T^{jet} jet in the two-jet event sample is **BROADER**



Measurements of Jet Substructure in NC DIS



One-jet events

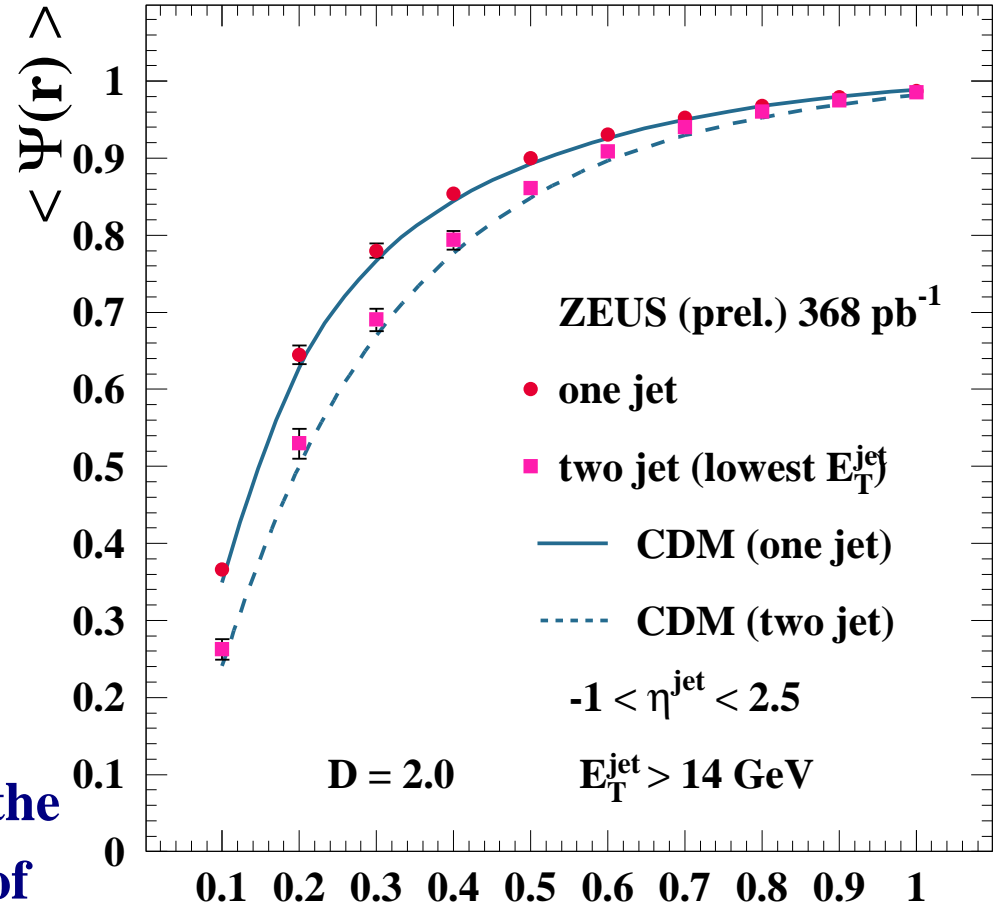
- Enriched in quark jets

Two-jet events

- Higher content of gluon jets

- The observation that the lowest- E_T^{jet} jet in the two-jet event sample is **BROADER** than that of the one-jet sample is consistent with a **higher gluon content in two-jet events**

ZEUS



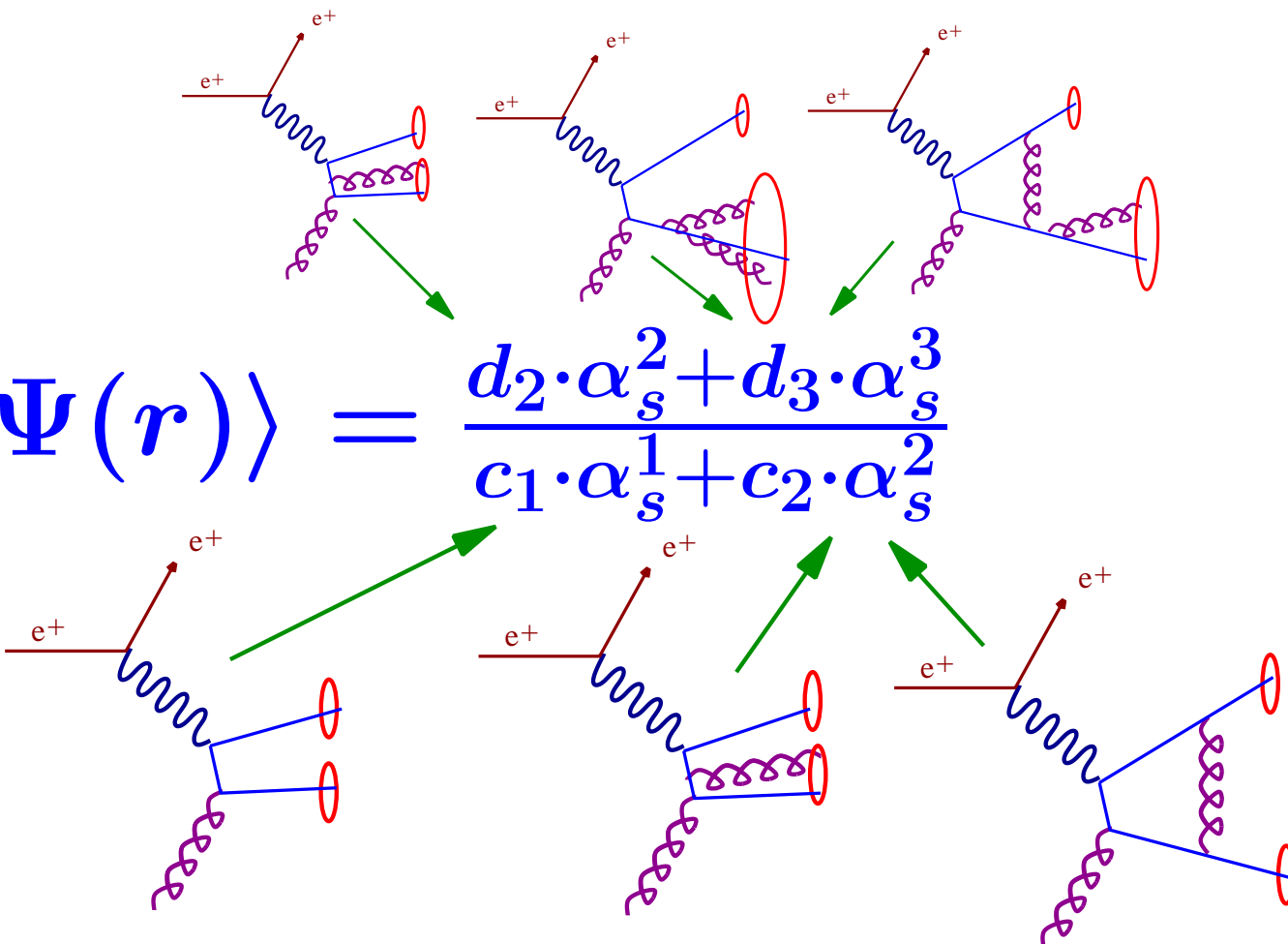
→ The colour-dipole model (CDM, ARIADNE) reproduces the data reasonably well; in particular, the difference in jet shape between the two samples

NLO QCD calculations for **inclusive/one-jet production**

$$\langle 1 - \Psi(r) \rangle = \frac{b_1 \cdot \alpha_s^1 + b_2 \cdot \alpha_s^2}{a_0 \cdot \alpha_s^0 + a_1 \cdot \alpha_s^1}$$

- **DISENT program:** $\alpha_s(M_Z) = 0.118$; $\mu_R = \mu_F = Q$; CTEQ6 proton PDFs
 → **Dominant theoretical uncertainty: terms beyond NLO, < 5% for $r \geq 0.2$**

NLO QCD calculations for **two-jet production**



$$\langle 1 - \Psi(r) \rangle = \frac{d_2 \cdot \alpha_s^2 + d_3 \cdot \alpha_s^3}{c_1 \cdot \alpha_s^1 + c_2 \cdot \alpha_s^2}$$

- **NLOJET++ program:** $\alpha_s(M_Z) = 0.118$; $\mu_R = \mu_F = Q$; CTEQ6 proton PDFs

Measurements of Jet Substructure in NC DIS vs NLO QCD

- Measurement of $\langle \Psi(r) \rangle$ in NC DIS with $Q^2 > 125 \text{ GeV}^2$ using $\mathcal{L} = 368 \text{ pb}^{-1}$ for two samples of jets:

One-jet events

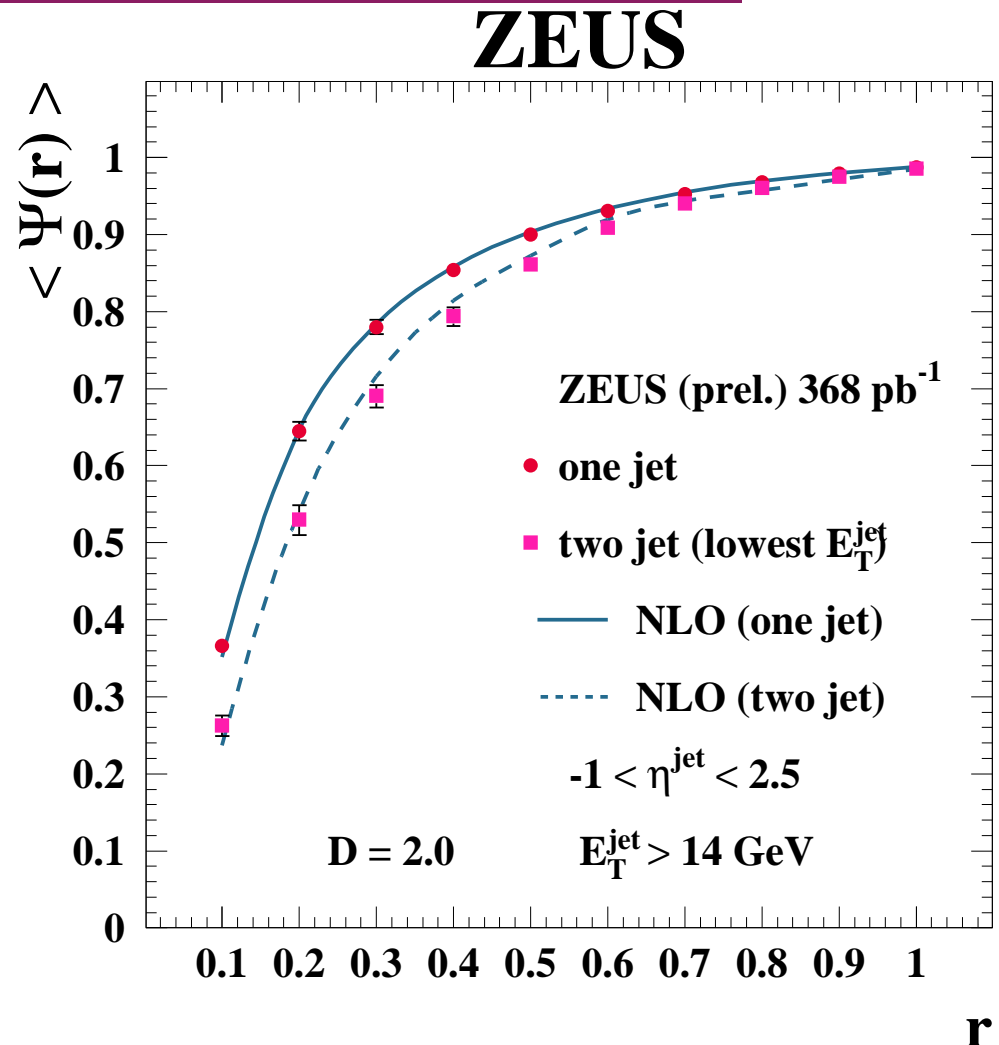
$$E_T^{jet} > 14 \text{ GeV}, -1 < \eta^{jet} < 2.5$$

Two-jet events

$$E_T^{jet} > 14 \text{ GeV}, -1 < \eta^{jet} < 2.5$$

$$\text{distance jet-jet} = \sqrt{\Delta\eta^2 + \Delta\phi^2} \leq D = 2$$

→ the jet with lowest E_T^{jet} is considered



NLO QCD calculations corrected for hadronisation effects ($< 10\%$ for $r \geq 0.4$) reproduce the data reasonably well; in particular, the difference in jet shape between the two samples

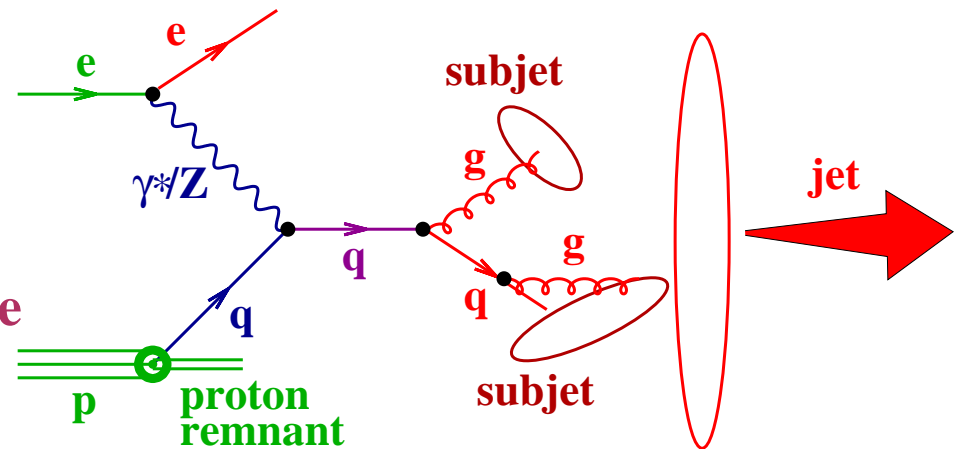
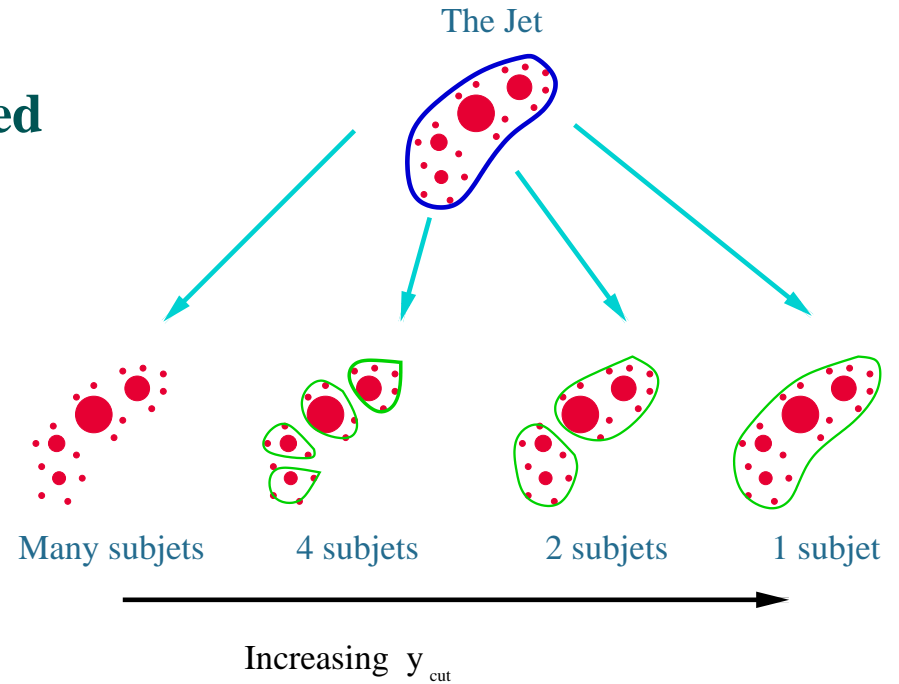
Jet Substructure in NC DIS: subjets

- The internal structure of jets has also been studied using **the subjet topology**
- Subjets are resolved within a jet by reapplying the k_T -cluster algorithm on all the particles belonging to the jet until for every pair of particles the distance between clusters is above

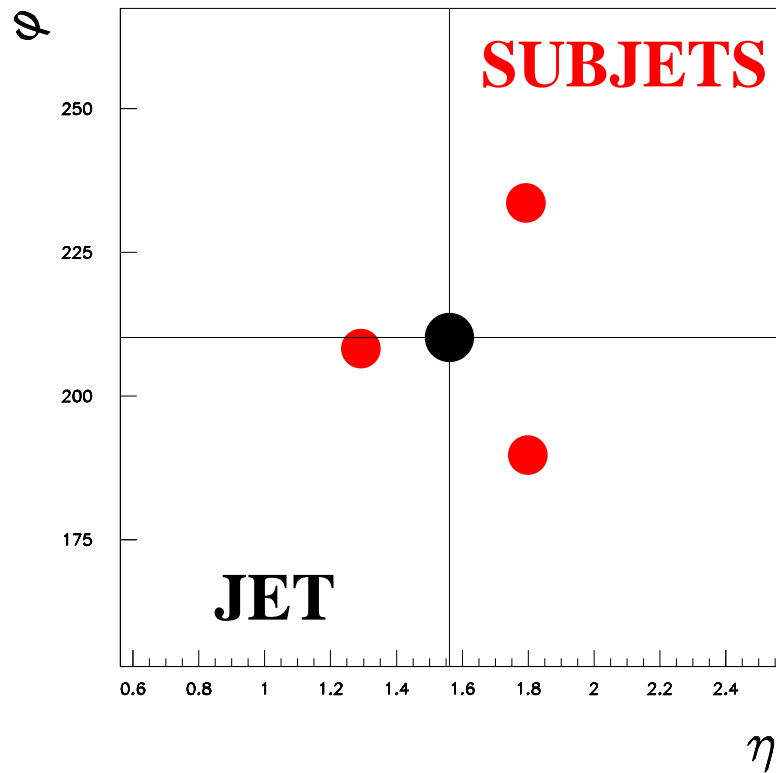
$$d_{cut} = y_{cut} \cdot (E_T^{jet})^2$$

- all remaining clusters are called **subjets**
- the **subjet multiplicity** depends upon the resolution parameter y_{cut}

- The distributions of subjets are sensitive to the pattern of parton radiation

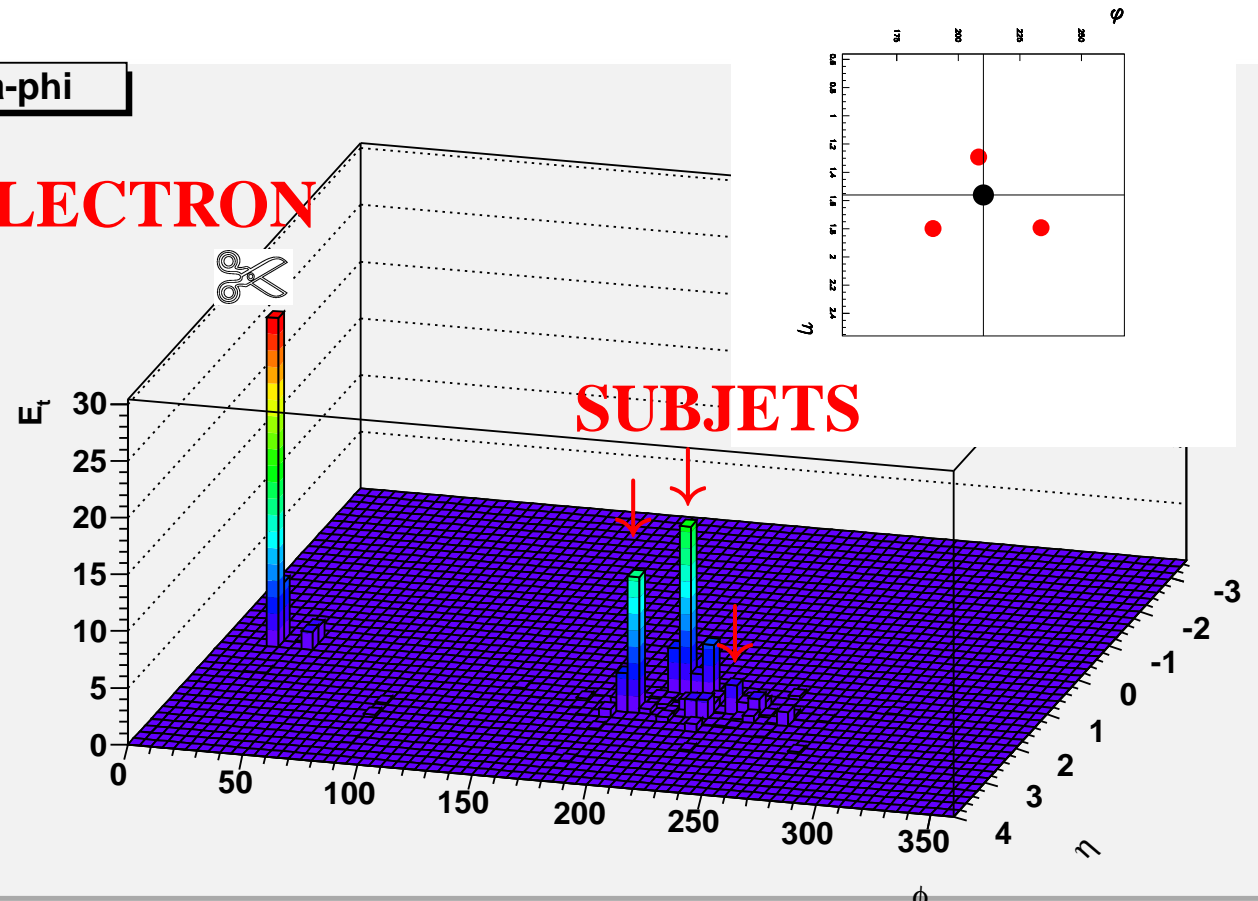


NC DIS event with three subjects at $y_{cut} = 0.01$



Eta-phi

ELECTRON



Measurements of Subjet Distributions in NC DIS

- The pattern of QCD radiation from a primary parton has been studied by measuring normalised cross sections as functions of subjet variables

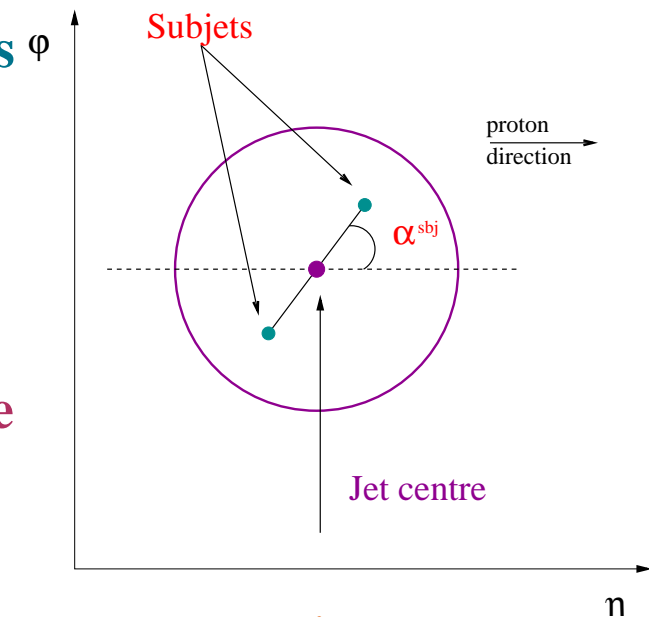
$$E_T^{sbj} / E_T^{jet}, \eta^{sbj} - \eta^{jet}, \phi^{sbj} - \phi^{jet} \text{ and } \alpha^{sbj}$$

- Measurements of the normalised cross sections were done in NC DIS for $Q^2 > 125 \text{ GeV}^2$:

- Jets are defined using the k_T -cluster algorithm in the laboratory frame; at least one jet with $E_T^{jet} > 14 \text{ GeV}$ and $-1 < \eta^{jet} < 2.5$
- Selected sample of jets: jets with exactly **TWO** subjets at $y_{cut} = 0.05$

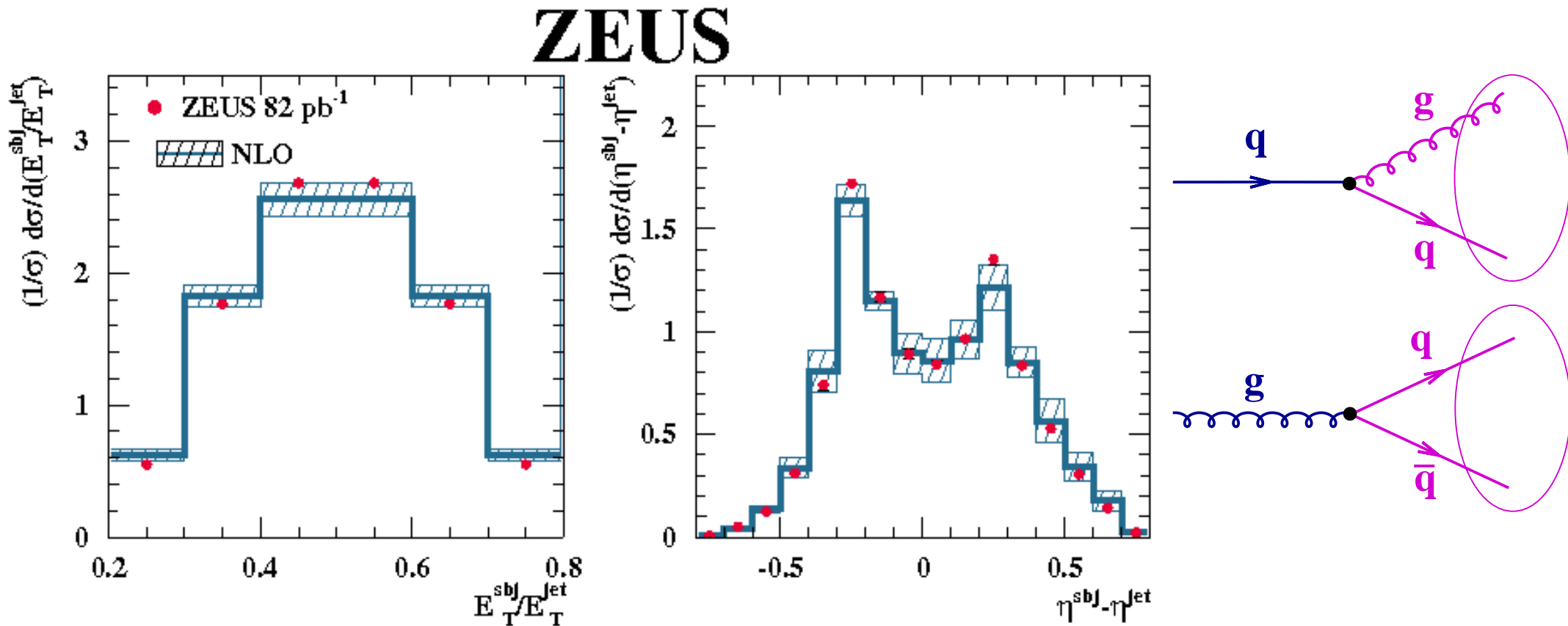
- Comparison to NLO ($\mathcal{O}(\alpha_s^2)$) QCD calculations using DISENT:

- MRST99 set of proton PDFs
- $\alpha_s(M_Z) = 0.1175$
- renormalisation and factorisation scales, $\mu_R = \mu_F = Q$
- corrected for hadronisation effects



Measurements of Subjet Distributions in NC DIS vs NLO

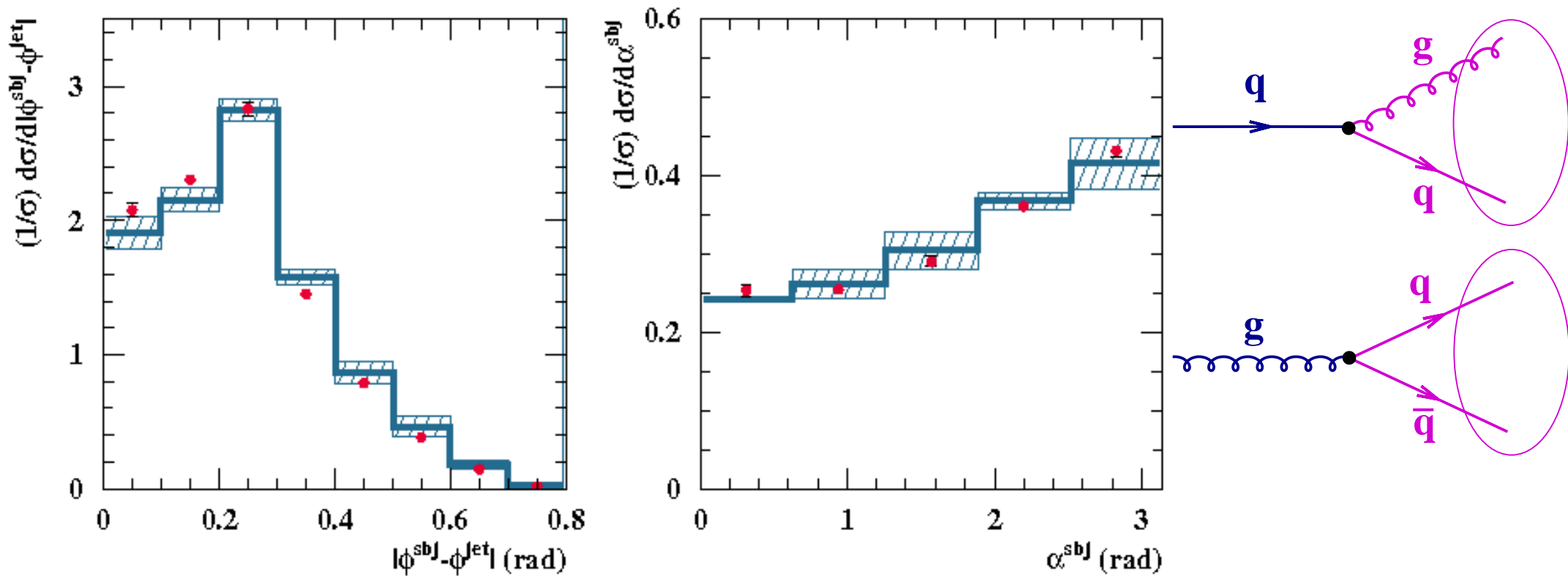
- Measurements of the normalised cross sections for subjet production as functions of E_T^{sbj} / E_T^{jet} and $\eta^{sbj} - \eta^{jet}$ vs NLO QCD calculations



→ NLO QCD calculations describe the data within $\pm 10\%$

Measurements of Subjet Distributions in NC DIS vs NLO

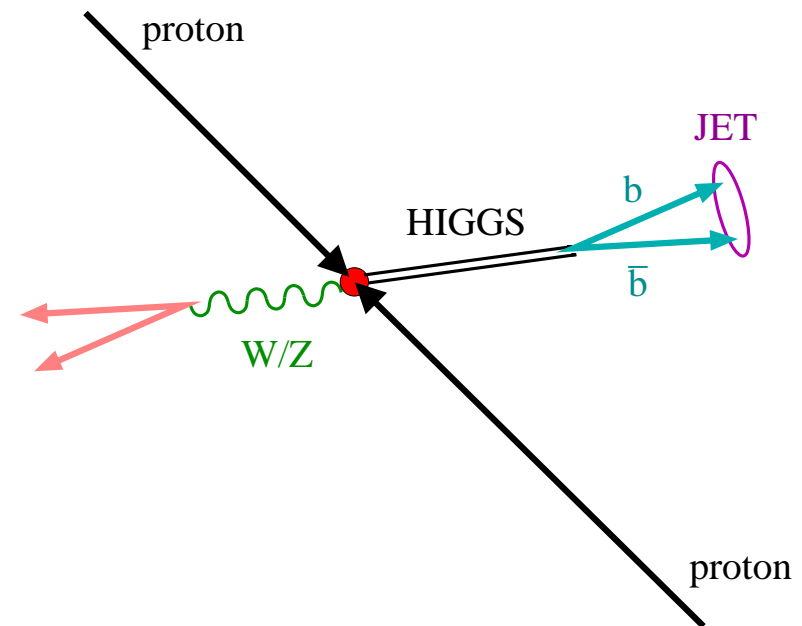
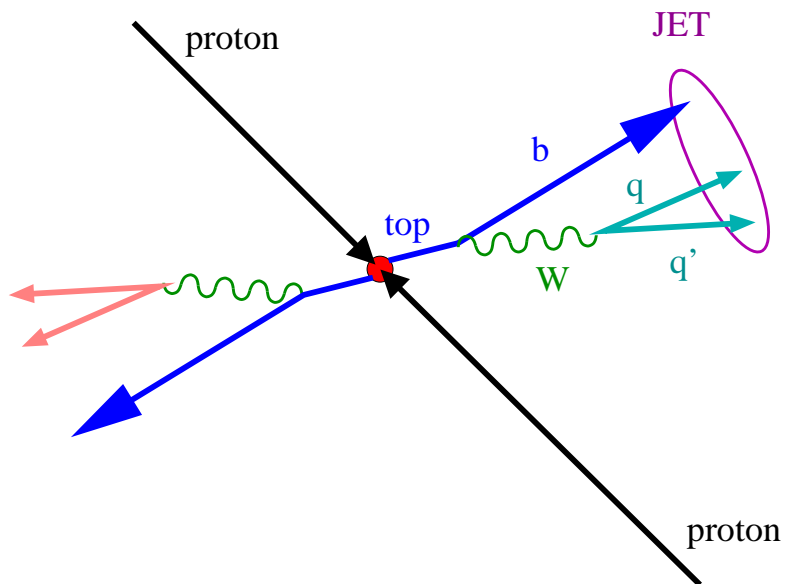
- Measurements of the normalised cross sections for subjet production as functions of $\phi^{sbj} - \phi^{jet}$ and α^{sbj} vs NLO QCD calculations



→ NLO QCD calculations describe the data within $\pm 10\%$

Jet substructure as a tool in hadron-hadron colliders

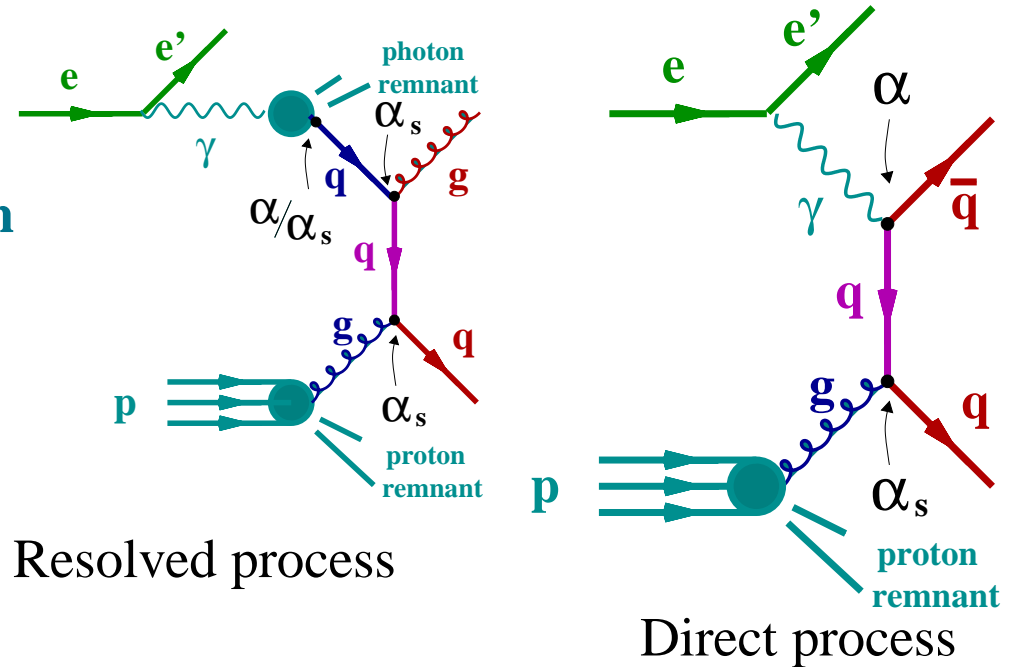
- **Subjects and jet shapes: useful tool to tag quark and gluon initiated jets**
→ with the aim of improving searches of new particles
- **Subjects: new strategies being developed for boosted systems at LHC**
 - studies of hadronic top decays
 - searches for the Higgs boson or supersymmetric particles



Jets in photoproduction

Photoproduction of Jets

- Production of jets in γp collisions has been measured via ep scattering at $Q^2 \approx 0$
- At lowest order QCD, two hard scattering processes contribute to jet production \Rightarrow
- pQCD calculations of jet cross sections



$$\sigma_{jet} = \sum_{a,b} \int_0^1 dy f_{\gamma/e}(y) \int_0^1 dx_\gamma f_{a/\gamma}(x_\gamma, \mu_{F\gamma}^2) \int_0^1 dx_p f_{b/p}(x_p, \mu_{Fp}^2) \hat{\sigma}_{ab \rightarrow jj}$$

longitudinal momentum fraction of γ/e^+ (y), **parton a/γ** (x_γ), **parton b/proton** (x_p)

$\rightarrow f_{\gamma/e}(y)$ = flux of photons in the positron (WW approximation)

$\rightarrow f_{a/\gamma}(x_\gamma, \mu_{F\gamma}^2)$ = **parton densities in the photon** (for direct processes $\delta(1 - x_\gamma)$)

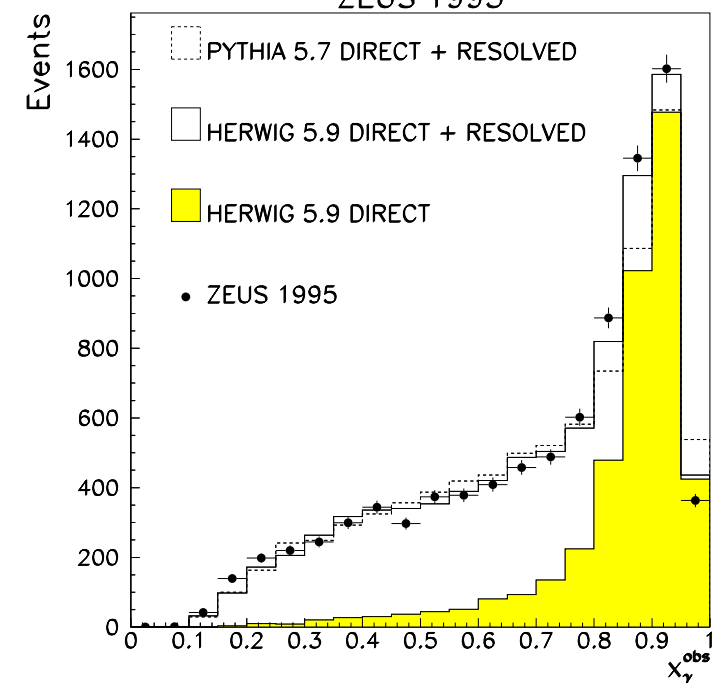
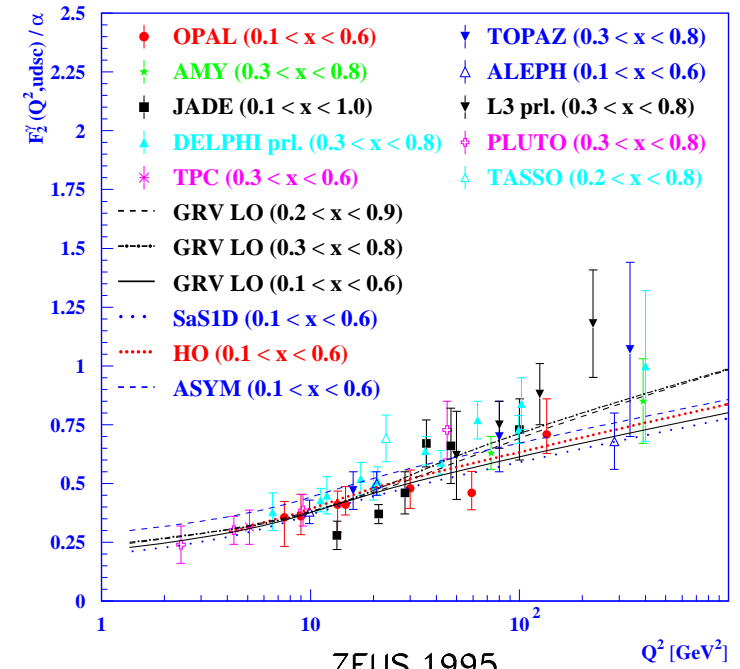
$\rightarrow f_{b/p}(x_p, \mu_{Fp}^2)$ = **parton densities in the proton**

$\rightarrow \sigma_{ab \rightarrow jj}$ **subprocess cross section; short-distance structure of the interaction**

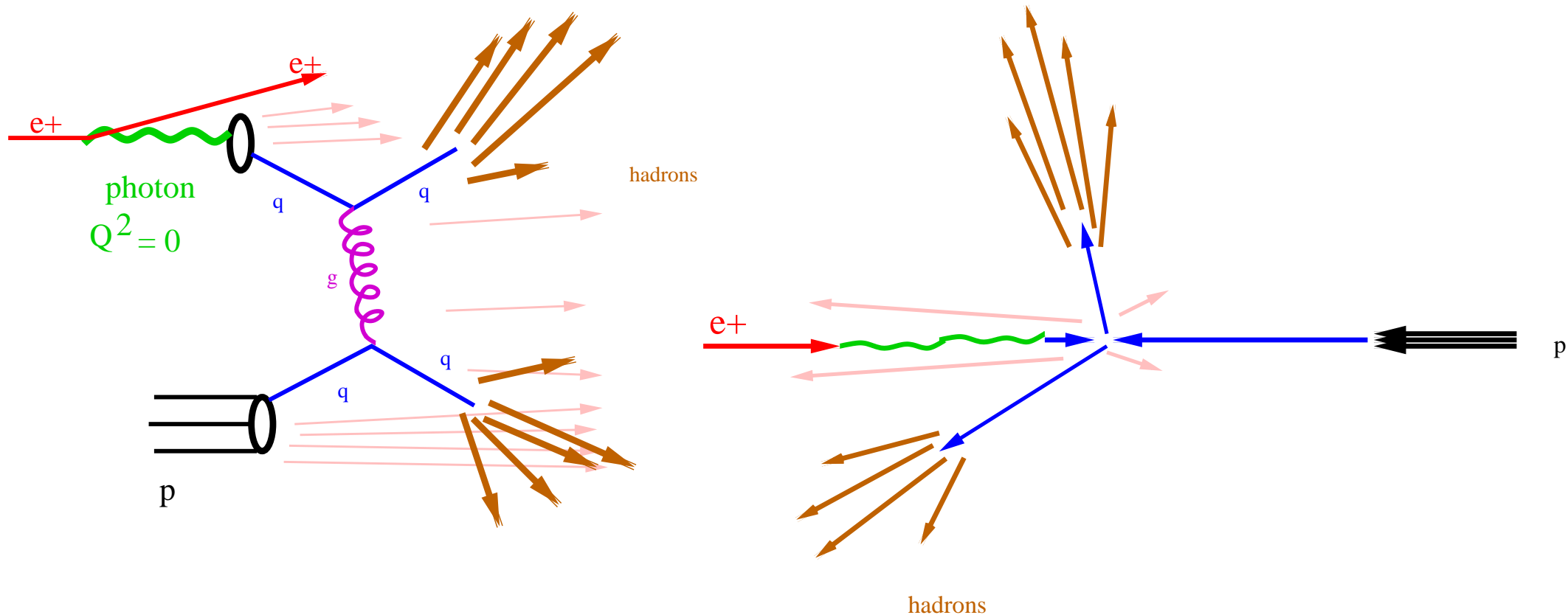
Photoproduction of Jets

- **Measurements of jet photoproduction provide**
 - **Test of NLO QCD predictions based on current parametrisations of the proton and photon PDFs**
 - **Dynamics of resolved and direct processes**
 - **Photon structure: information on quark densities from F_2^γ in e^+e^- ; gluon density poorly constrained.**
- **Jet cross sections in photoproduction are sensitive to both the quark and gluon densities in the photon at larger scales $\mu_{F\gamma}^2 \sim E_{T,jet}^2$ ($200 - 10^4 \text{ GeV}^2$)**
- **Proton structure: well constrained by DIS except for the gluon density at high x . Jet cross sections in γp are sensitive to parton densities at x_p up to ~ 0.6**
- **Observable to separate the contributions: the fraction of the photon's energy participating in the production of the dijet system**

$$x_\gamma^{OBS} = \frac{1}{2E_\gamma} \sum_{i=1}^2 E_T^{jet_i} e^{-\eta^{jet_i}}$$



Variables for Jet Search in ep collisions at low Q^2 (Photoproduction)

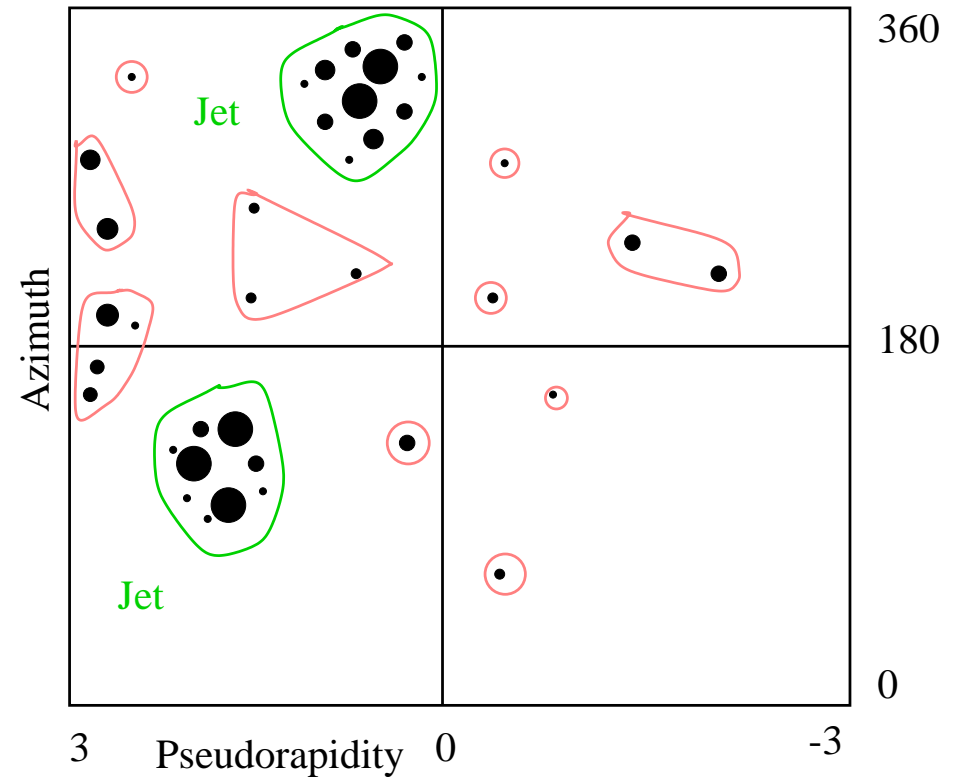
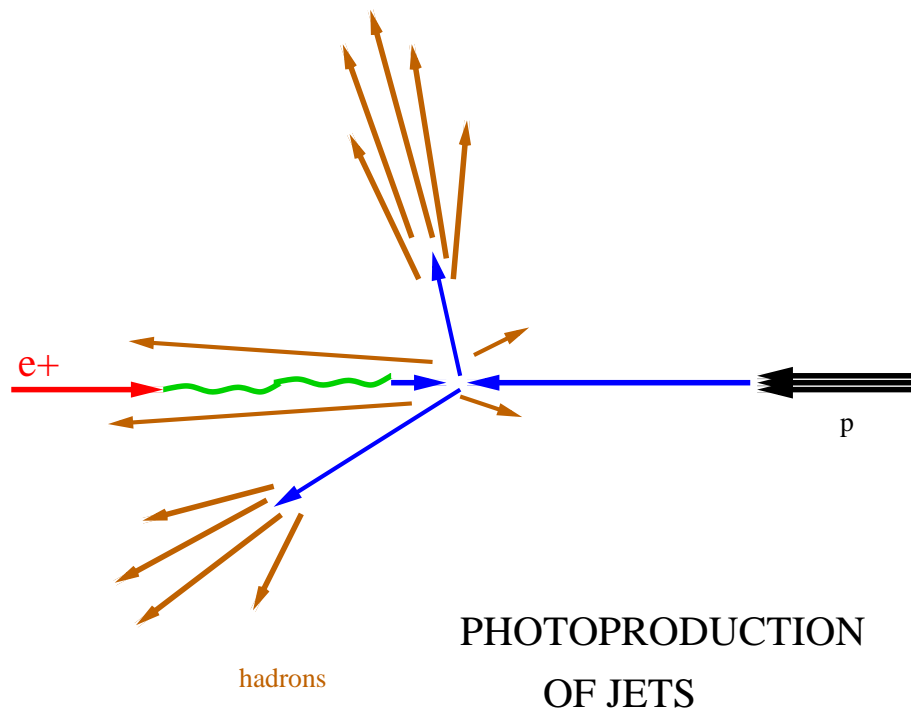


- The kinematics of ep collisions at low Q^2 is similar to that of $p\bar{p}$ collisions

⇒ Input to the jet algorithm: $E_{T,i}$, η_i and ϕ_i for every hadron i

⇒ “distance” between hadrons i and j : $\sqrt{\Delta\eta_{ij}^2 + \Delta\phi_{ij}^2}$

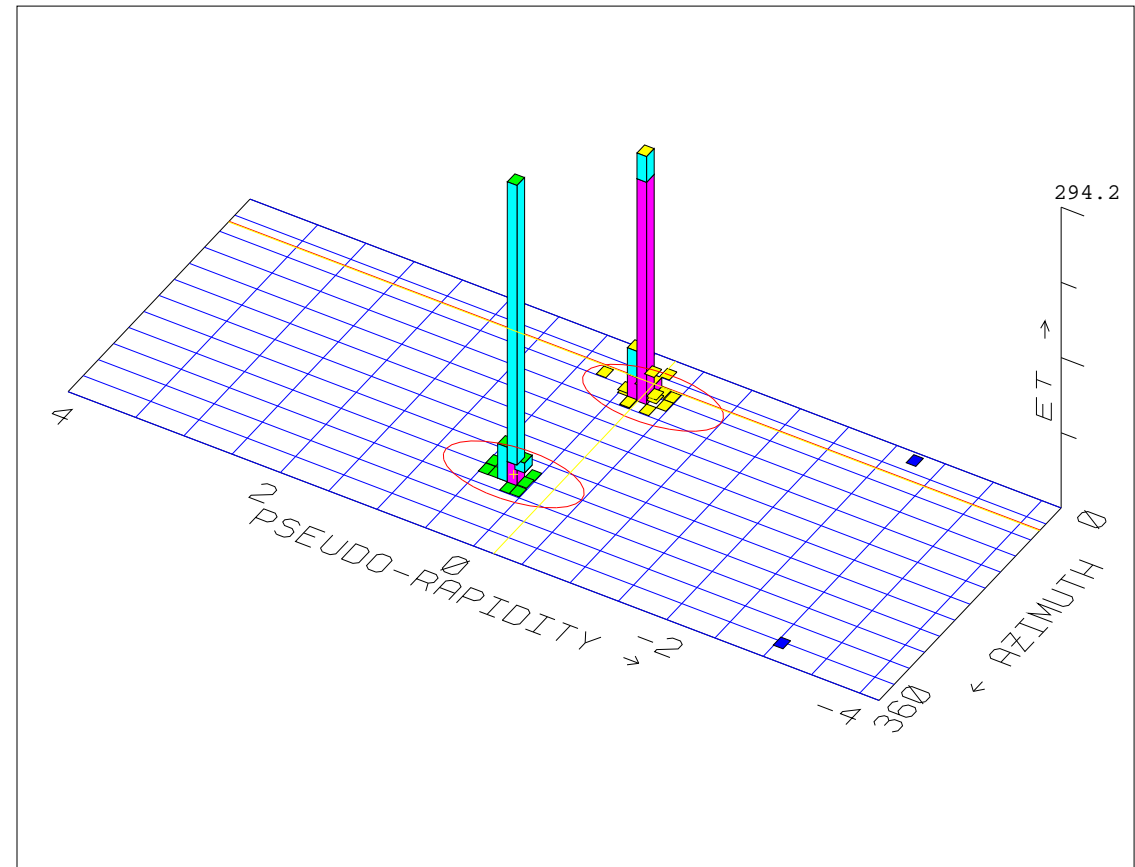
The longitudinally invariant k_T algorithm for photoproduction



- **Infrared and collinear safe to all orders in perturbative QCD**
- **Invariant under longitudinal boosts (along the beam axis)**
- **Suppression of beam remnant jet contributions through the use of transverse energies and by not forcing all the particles to be assigned to jets (nor requiring a certain jet shape)**
- **Small experimental and theoretical uncertainties**

Combining the hadrons to build up jets: cone algorithms

- Maximizing the total transverse energy of the hadrons within a cone of fixed size
- Three-step procedure:
 - constructing the seeds (starting positions for the cone)
 - moving the cone around until a stable position is found
 - dealing with overlapping cones (to merge or not to merge)



- They have been applied mainly to $p\bar{p}$ collisions

- The iterative cone algorithm has been the standard

→ distance definition: $d_{iJ} \equiv \sqrt{(\eta_i - \eta_J)^2 + (\phi_i - \phi_J)^2}$

→ cone axis: $\eta_J \equiv \frac{1}{E_T} \sum_i E_{T,i} \cdot \eta_i$, $\phi_J \equiv \frac{1}{E_T} \sum_i E_{T,i} \cdot \phi_i$, $E_T = \sum_i E_{t,i}$

Fulfilling the requirements (II)

- **The cone algorithm is infrared and collinear safe at NLO**

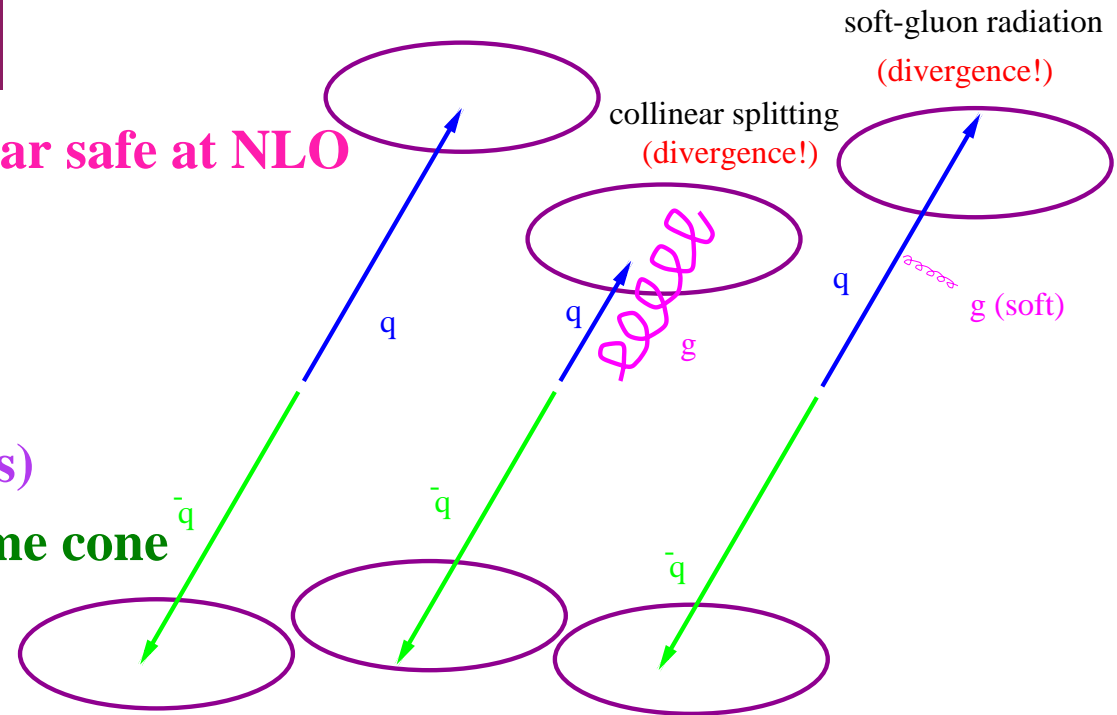
→ **First situation: two particles (partons) with equal and opposite momenta**

Each of them defines a cone \Rightarrow Two jets

→ **Second situation: three particles (partons)**

the two collinear partons will lie in the same cone

\Rightarrow Two jets



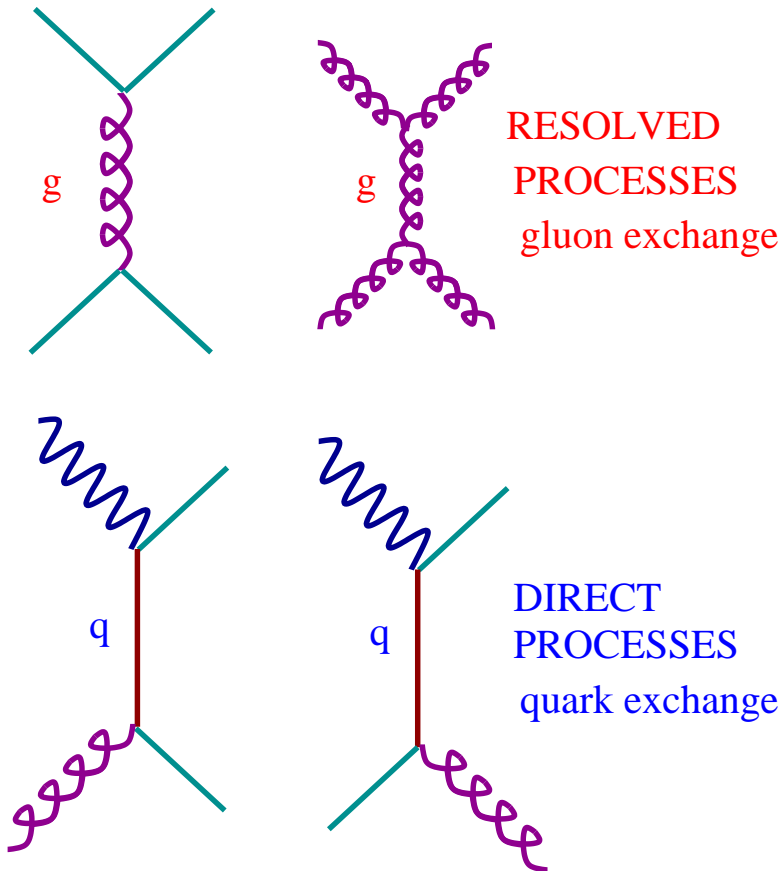
→ **Third situation: if the soft gluon is far from the other partons ($\sqrt{\Delta\eta^2 + \Delta\phi^2} > R$) it won't be lumped with any of them**

\Rightarrow Two jets

The jet axes and transverse energies will differ from the the values found in the 1st or 2nd situation by a quantity that $\rightarrow 0$ as $E(g) \rightarrow 0$!

- **The final result is the same in each configuration!**

Dijet Photoproduction: the dynamics of resolved and direct processes



- The dynamics of dijet production has been investigated by studying the variable:

$$\cos \theta^* \equiv \tanh\left(\frac{1}{2}(\eta^{jet,1} - \eta^{jet,2})\right)$$

→ for two-to-two parton scattering θ^* coincides with the scattering angle in the dijet CMS

- QCD predicts different dijet angular distributions for resolved and direct:

→ **Resolved (gluon-exchange dominated)**

$$d\sigma/d|\cos \theta^*| \sim \frac{1}{(1-|\cos \theta^*|)^2}$$

→ **Direct (quark-exchange only)**

$$d\sigma/d|\cos \theta^*| \sim \frac{1}{(1-|\cos \theta^*|)^1}$$

- The dijet angular distribution $d\sigma/d|\cos \theta^*|$ for $x_\gamma^{OBS} < 0.75$ (“resolved”) should be steeper than that of $x_\gamma^{OBS} > 0.75$ (“direct”) as $|\cos \theta^*| \rightarrow 1$

Dijet Photoproduction: the dynamics of resolved and direct processes

- Measurement of the dijet differential cross section $d\sigma/d|\cos\theta^*|$ for dijet events with

$$E_T^{jet,1} > 14 \text{ GeV}, E_T^{jet,2} > 11 \text{ GeV}$$

$$-1 < \eta^{jet} < 2.4 \text{ (both jets)}$$

in the kinematic region

$$Q^2 < 1 \text{ GeV}^2 \text{ and } 134 < W_{\gamma p} < 277 \text{ GeV}$$

- Phase-space region:

$$|\cos\theta^*| < 0.8, M_{JJ} > 42 \text{ GeV}$$

$$0.1 < \frac{1}{2}(\eta^{jet,1} + \eta^{jet,2}) < 1.3$$

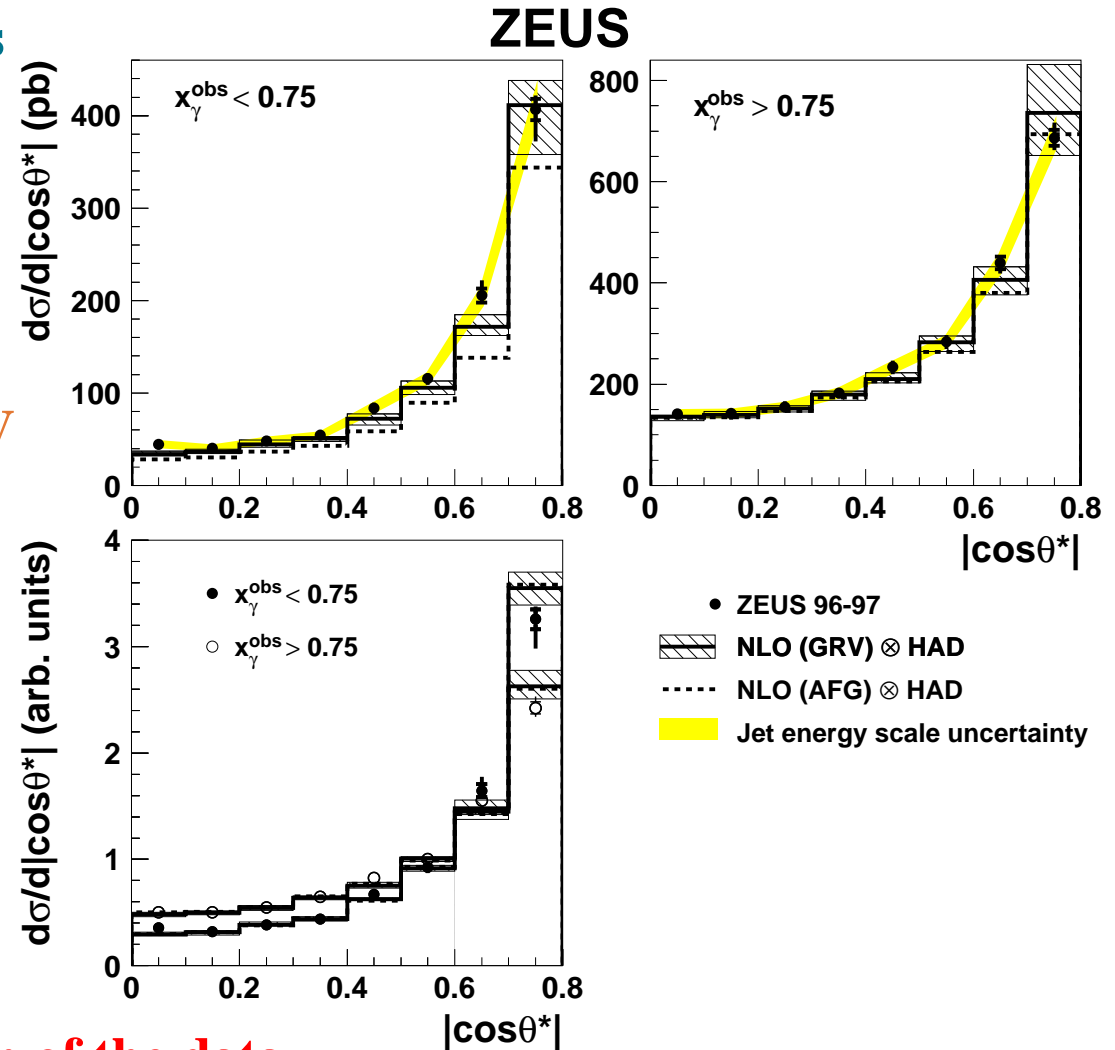
- Comparison with NLO QCD calculations:

→ High- x_γ^{OBS} (“direct”): NLO describes the shape and normalisation of the data

→ Low- x_γ^{OBS} (“resolved”): NLO describes

the shape and (reasonably) the normalisation of the data

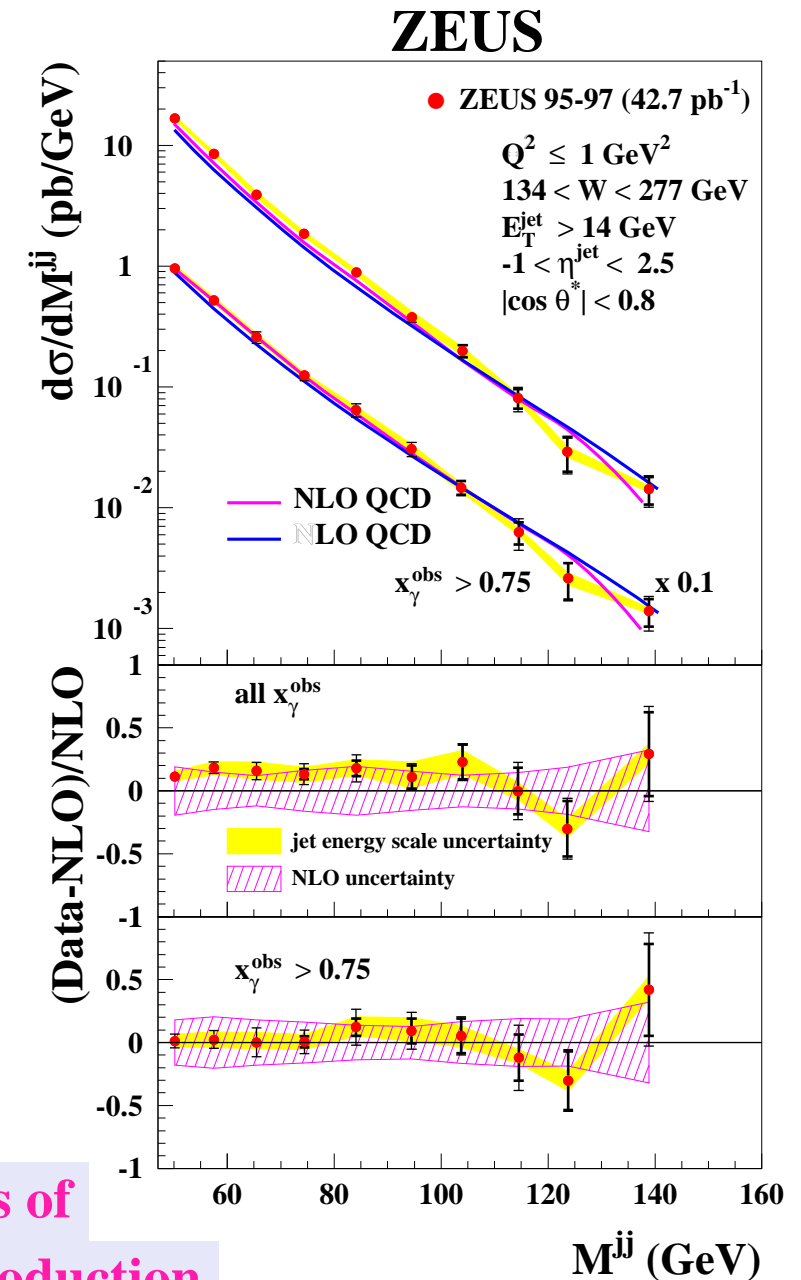
- The dijet angular distribution of the “resolved” sample is steeper than that of “direct”



High- M_{JJ} Dijet Photoproduction

- Measurement of the dijet differential cross section $d\sigma/dM_{JJ}$ in the range $47 < M_{JJ} < 160$ GeV for dijet events with $E_T^{jet} > 14$ GeV, $-1 < \eta^{jet} < 2.5$ and $|\cos \theta^*| < 0.8$
- Small experimental uncertainties:
 - jet energy scale known to 1% \Rightarrow 5% on $d\sigma/dM_{JJ}$
- Small theoretical uncertainties:
 - higher-order terms (varying μ_R) below 15%
 - γ PDFs (GRV-HO, AFG-HO) below 10%
 - resolved processes suppressed at high M_{JJ}
 - small hadronisation corrections, below 5%
- NLO QCD calculations describe the shape and normalisation of the measurements well

→ Validity of the pQCD description of the dynamics of parton-parton and γ -parton interactions in photoproduction

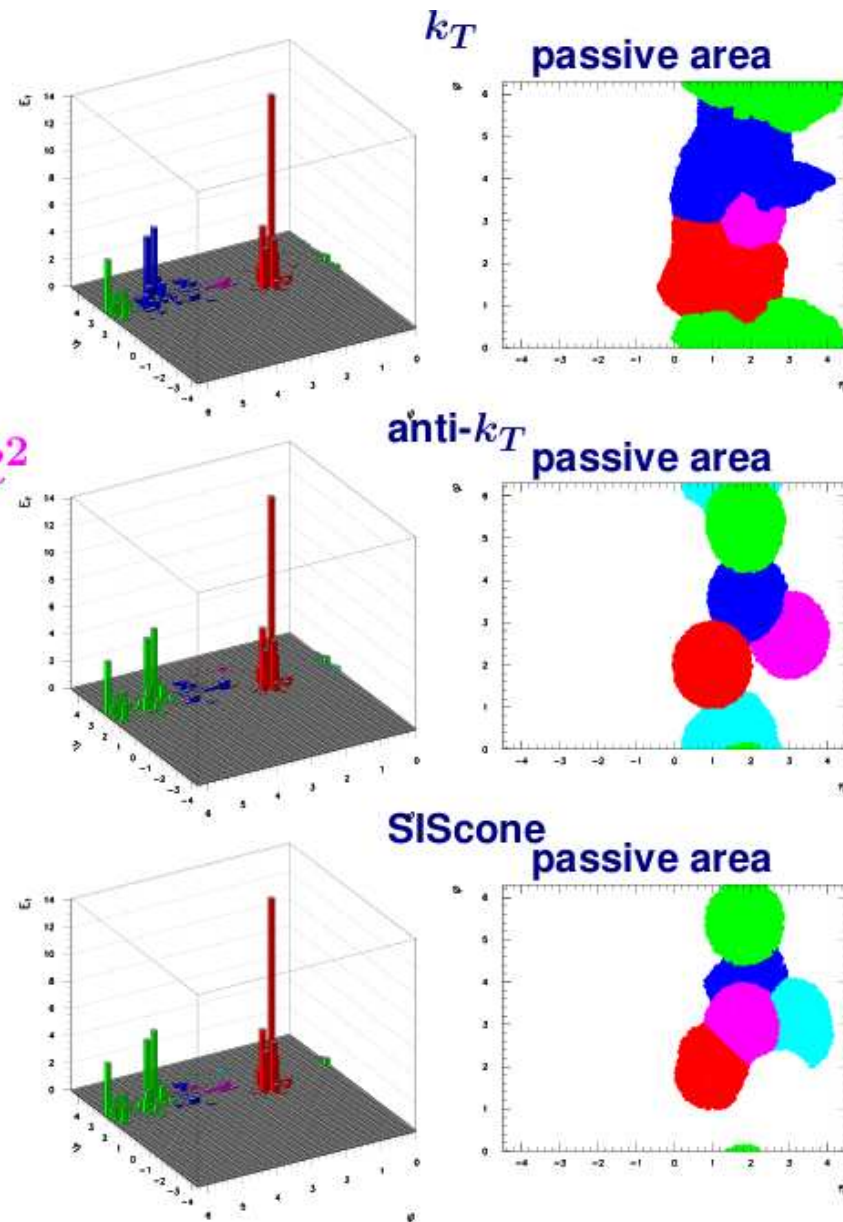


New jet algorithms

- Tests of pQCD with jets require infrared- and collinear-safe jet algorithms:
 - performance of k_T cluster algorithm in longitudinally invariant inclusive mode (S Catani, S Ellis & D Soper) tested extensively at HERA:
 - stringent tests of pQCD: good description of data for different jet radii
 - good performance of algorithm: small theoretical uncertainties / hadronisation corrections
 - new measurements in photoproduction presented here
- New infrared- and collinear-safe jet algorithms:
 - anti- k_T (M Cacciari, G Salam & G Soyez) provides \approx circular jets
 - ★ experimentally desirable
 - SIScone (G Salam & G Soyez) seedless cone algorithm provides infrared- and collinear-safe calculations
 - ★ theoretically necessary
- New studies at HERA:
 - test performance of anti- k_T and SIScone in well-understood hadron-induced reaction:
 - * comparison to measurements based on k_T
 - * comparison of measurements and NLO QCD calculations
 - * study of theoretical uncertainties and hadronisation corrections

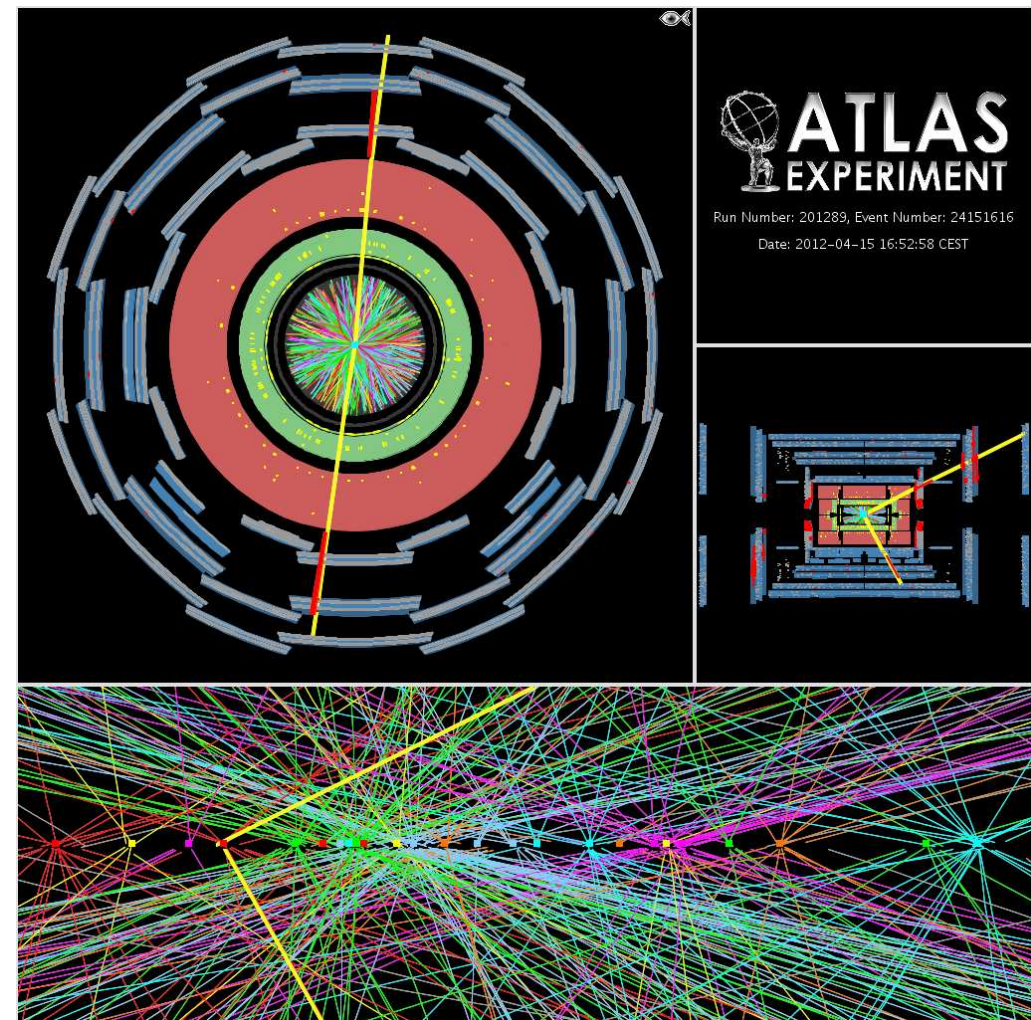
New jet algorithms

- **New infrared- and collinear-safe jet algorithms:**
 - **anti- k_T** (M Cacciari, G Salam & G Soyez)
 - and **SIScone** (G Salam & G Soyez)
- **Cluster algorithms:**
 - $d_{ij} = \min[(E_{T,B}^i)^{2p}, (E_{T,B}^j)^{2p}] \cdot \Delta R^2 / R^2$
 - with $p = 1$ (-1) for k_T (**anti- k_T**)
 - **anti- k_T keeps infrared and collinear safety and provides \approx circular jets (experimentally desirable)**
- **Cone algorithms:**
 - **seedless cone algorithm produces also jets with well-defined area and is infrared and collinear safe (theoretically necessary)**



Benefits of the new jet algorithms

- **Anti- k_t and SISCONe jet algorithms provide jets with better control on the shape (\approx circular) and area (dictated by the jet radius R) than with the k_t jet algorithm**
- **Essential to control and suppress the energy contributions from particles that fall into the jet but originate from**
 - **the “underlying event” (hadrons from the same proton-proton collision but unrelated to the hard interaction (a proton is an extended object))**
 - **additional soft proton-proton interactions overlaid with the interesting one (pile-up)**



$Z \rightarrow \mu^+ \mu^-$ event candidate
with 25 (!!) reconstructed vertices
High pile-up environment in 2012

Inclusive Jet Photoproduction

$ep \rightarrow e + \text{jet} + X$: **inclusive-jet cross sections**

- **Kinematic region:** $Q^2 < 1 \text{ GeV}^2$ and $0.2 < y < 0.85$
- **Jet search:** k_T , anti- k_T and SIScone in laboratory frame
- **At least one jet with** $E_T^{\text{jet}} > 17 \text{ GeV}$ and $-1 < \eta^{\text{jet}} < 2.5$

- **Experimental uncertainties:**

- **systematic:** typically below $\pm 5\%$
- **energy scale** $\pm 1\%$ (!): $\sim \pm 5$ (10)% at low (high) E_T^{jet}

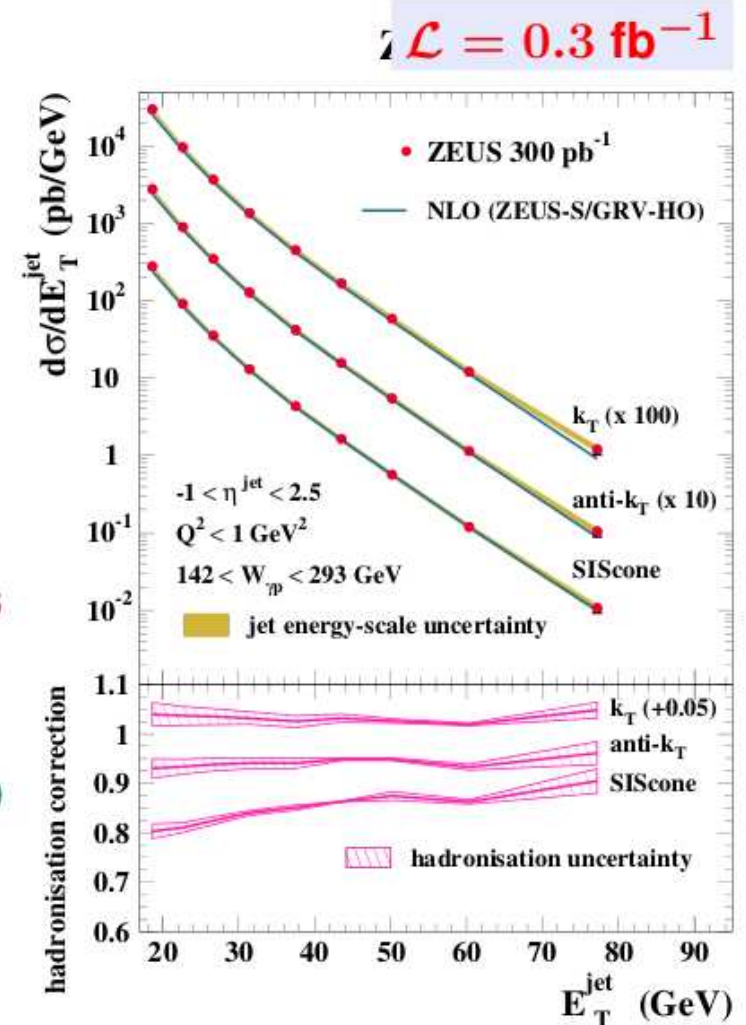
- **Comparison to NLO predictions (Klasen et al):**

- **good description of data by NLO prediction**
- **validity of the description of the dynamics of jet photoproduction at $\mathcal{O}(\alpha_s^2)$**

- **Theoretical uncertainties:**

- **higher orders:** ± 10 (4)% at low (high) E_T^{jet} (k_T /anti- k_T)
 ± 14 (7)% at low (high) E_T^{jet} (SIScone)
- **proton PDFs:** ± 1 (5)% at low (high) E_T^{jet}
- **hadronisation:** $< \pm 3\%$; $\alpha_s(M_Z)$: $< \pm 2\%$
- **photon PDFs:** $\pm 9 - 10$ ($1 - 3$)% at low (high) E_T^{jet}

→ **Measurements provide direct sensitivity to α_s and gluon density with small experimental and theoretical uncertainties**



ZEUS Collab, DESY-12-045

Inclusive Jet Photoproduction and Determination of α_s

- The energy-scale dependence of the coupling was determined from the data → results in good agreement with predicted running of α_s over a wide range in E_T^{jet}
- Values of $\alpha_s(M_Z)$ were extracted from the measured cross sections for $21 < E_T^{\text{jet}} < 71$ GeV:

anti- k_T :

$$\alpha_s(M_Z) = 0.1198^{+0.0023}_{-0.0022} \text{ (exp)}^{+0.0041}_{-0.0034} \text{ (th)}$$

uncert: $+1.9\%$ (exp), $\pm 1.0\%$ (pPDFs), $\pm 0.4\%$ (hadr),
 $+2.3\%$ (HO), $+2.2\%$ (γ PDFs), $+3.9\%$ (total)
 -1.8% , -2.4%

SIScone:

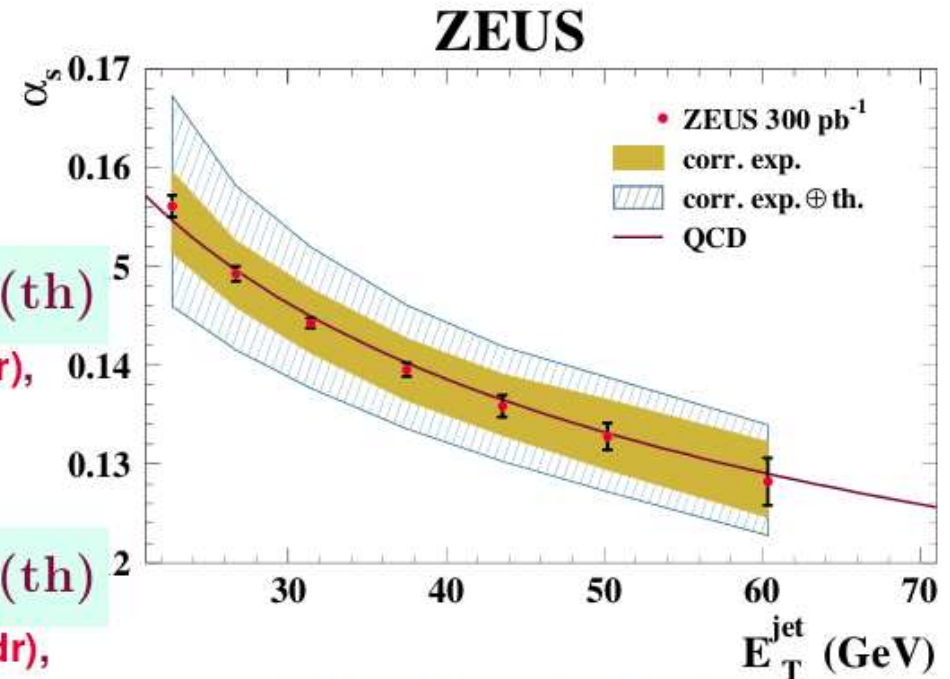
$$\alpha_s(M_Z) = 0.1196^{+0.0022}_{-0.0021} \text{ (exp)}^{+0.0046}_{-0.0043} \text{ (th)}$$

uncert: $\pm 1.8\%$ (exp), $\pm 1.0\%$ (pPDFs), $\pm 0.2\%$ (hadr),
 $+3.2\%$ (HO), $+1.9\%$ (γ PDFs), $+4.3\%$ (total)
 -3.3% , -0.9% , -4.0%

k_T :

$$\alpha_s(M_Z) = 0.1206^{+0.0023}_{-0.0022} \text{ (exp)}^{+0.0042}_{-0.0035} \text{ (th)}$$

uncert: $+1.9\%$ (exp), $\pm 1.0\%$ (pPDFs), $\pm 0.4\%$ (hadr),
 $+2.4\%$ (HO), $+2.3\%$ (γ PDFs), $+4.0\%$ (total)
 -1.8% , -2.5% , -0.9% , -3.4%



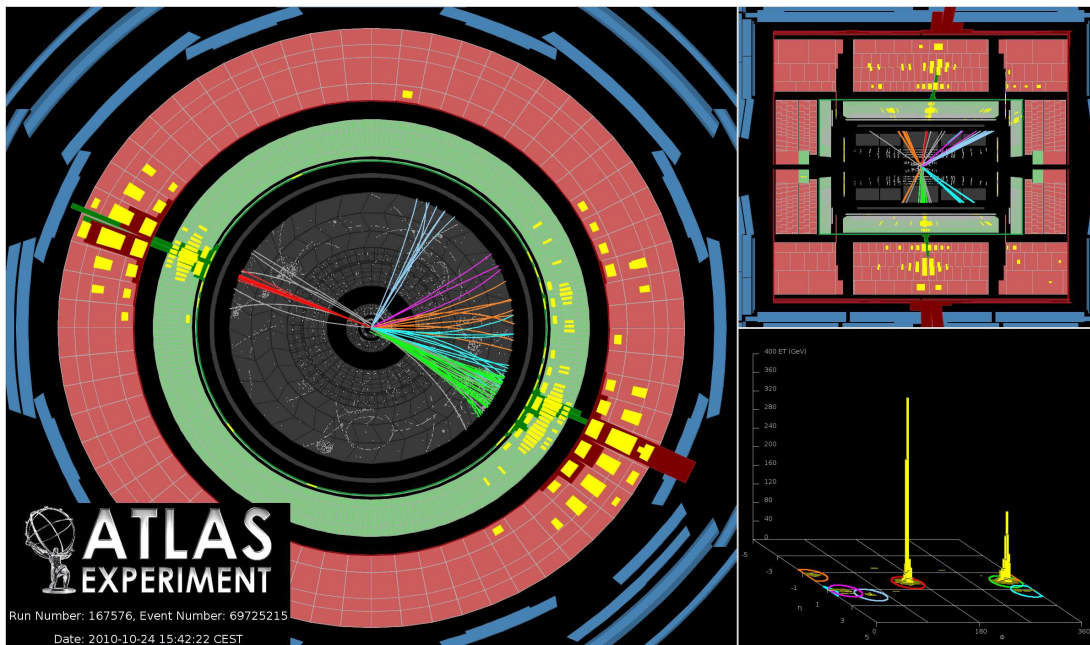
→ $\alpha_s(M_Z)$ from inclusive-jet cross sections in PHP with different jet algorithms are consistent with each other and have similar precision

ZEUS Collab, DESY-12-045

Not yet the end

- The “jet” saga continues this afternoon

→ jets in hadron-hadron colliders → by Aidan Robson



CMS
CMS Experiment at LHC, CERN
Run 133450 Event 16358963
Lumi section: 285
Sat Apr 17 2010, 12:25:05 CEST

